The Ion Transport Basis of
***Clostridium difficile* Associated Diarrhea**

BY

HAYLEY COFFING
B.S., University of Notre Dame, 2012

THESIS

Submitted as partial fulfillment of the requirements
necessary for the degree of Doctor of Philosophy in
Microbiology and Immunology in the Graduate College
of the University of Illinois at Chicago, 2018
Chicago, Illinois

Defense Committee:

      Pradeep Dudeja, Advisor and Chair
      Waddah Alrefai, Medicine
      Ravinder Gill, Medicine
      Alan McLachlan, Microbiology and Immunology
      Nancy Freitag, Microbiology and Immunology

This thesis is dedicated to my parents, siblings, and grandmother who have shown me unconditional love and support throughout my life and academic career. I would not have made it without their constant guidance, encouragement, and support. I am eternally grateful to you all.

ACKNOWLEDGMENTS

I would first like to acknowledge my thesis advisor, Dr. Pradeep Dudeja, for his guidance, mentorship, and leadership during my scientific training. I have learned so much during my time in the lab and I am grateful for the opportunity to receive my training in Dr. Dudeja's lab. I also owe a debt of gratitude to the members of my thesis committee for all their input and guidance including Dr. Waddah Alrefai, Dr. Ravinder Gill, Dr. Alan McLachlan, and Dr. Nancy Freitag. I would also like to thank all the members of the Dudeja, Alrefai, and Gill labs for their friendship and scientific discussions all these years. Finally, a special thank you to Dr. Shubha Priyamvada and Dr. Arivarasu Natarajan –I am immeasurably grateful to you both, for all that you do.

HPC

TABLE OF CONTENTS

TABLE OF CONTENTS (continued)

TABLE OF CONTENTS (continued)

LIST OF TABLES

LIST OF FIGURES

LIST OF ABBREVIATIONS

ADP	Adenosine Diphosphate
AMPK	AMP-activated Protein Kinase
ATGs	Autophagy Related Genes
ATP	Adenosine Triphosphate
CaCC	Ca^{2+}-dependent Calcium Channel
cAMP	cyclic Adenosine Monophosphate
CA	Carbonic Anyhdrase
CD	Crohn's Disease
CDI	*Clostridium difficile* infection
CDT	Clostridium Difficile Transferase (binary toxin)
CF	Cystic fibrosis
CFTR	Cystic Fibrosis Transmembrane Conductance Regulator
CLD	Congenital Chloride Diarrhea
CMA	Chaperone Mediated Autophagy
COX2	Cyclooxygenase 2
CROPs	Combined Repetitive Oligopeptide structures
CSD	Congenital Sodium Diarrhea
CSPG4	Chondroitin Sulfate Proteoglycan 4
DRA	Down Regulated in Adenoma (SLC26A3)
DSS	Dextran sulfate sodium
ENaC	Epithelial Sodium Channel
EPEC	Enteropathogenic *E. coli*

GAPDH	Glyceraldehyde 3-phosphate dehydrogenase
Gp96	Glycoprotein 96
GTD	Glucosyltransferase Domain
GTP	Guanosine Triphosphate
FZD	Wnt receptor Frizzled
HIO	Human Intestinal Organoid
IBD	Inflammatory Bowel Disease
IFNγ	Interferon Gamma
IL-1β	Interleukin 1 Beta
IL-6	Interleukin 6
IL-8	Interleukin 8
IL-10	Interleukin 10
LAMP2A	Lysosomal Associated Membrane Protein 2A
LC3	Microtubule-associated Protein Light Chain 3
LDH	Lactate Dehydrogenase
LSR	Lipolysis Stimulated Lipoprotein Receptor
MCT-1	Monocarboxylate transporter 1
MDR1	Multi-Drug Resistance Gene 1
MPO	Myeloperoxidase
mTOR	Mammalian Target of Rapamycin
MVID	Microvillus Inclusion Disease
MYO5B	Myosin 5B

NFκB   Nuclear Factor Kappa B

NHE1   Na$^+$/H$^+$ exchanger 1 (SLC9A1)

NHE2   Na$^+$/H$^+$ exchanger 2 (SLC9A2)

NHE3   Na$^+$/H$^+$ exchanger 3 (SLC9A3)

NHE8   Na$^+$/H$^+$ exchanger 8 (SLC9A8)

NKCC1   Na$^+$/K$^+$/Cl$^-$ co-transporter 1

PAT-1   Putatitive Anion Transporter 1 (SLC26A6)

PE   Phosphatidylethanolamine

PVRL3   Poliovirus Receptor-Like 3

qRT-PCR   quantitative Real Time PCR

SERT   Serotonin Transporter

SLC9   Solute Carrier 9 family of Na$^+$/H$^+$ exchangers (NHEs)

SLC26   Solute Carrier 26 family of Cl$^-$/HCO$_3^-$ exchangers

TcdA   *C. difficile* Toxin A

TcdB   *C. difficile* Toxin B

TNFα Tumor Necrosis Factor Alpha

Ub   Ubiquitin

UC   Ulcerative colitis

ULK-1/2   Unc-Like Kinases 1/2

UPS   Ubiquitin Proteasome System

SUMMARY

Although *Clostridium difficile* infection is the primary cause of nosocomial diarrhea and hospital acquired infection in the United States, the pathophysiology underlying CDI-associated diarrhea is poorly understood. These studies were conducted to examine the effects of *Clostridium difficile* toxins on intestinal luminal ion exchangers *in vitro*, *in vivo,* and in human CDI. Specifically, we investigated the effects of *C. difficile* toxins TcdA and TcdB on Cl^-/HCO_3^- exchanger Down Regulated in Adenoma (DRA) using cell culture and a toxigenic mouse model. Our studies showed that purified TcdA and TcdB significantly decreased DRA protein, but not mRNA, levels both *in vitro* and *in vivo*. Importantly, the effects of both toxins on DRA appeared to be dependent on the glucosyltransferase activity of each toxin.

These toxin-mediated effects appeared to be specific to DRA as PAT-1 and NHE3 protein and mRNA levels remained unchanged *in vitro* and *in vivo.* We also examined the effects of TcdA and TcdB on various key intestinal ion transporters. We found that mRNA levels of MCT1, NHE2, PAT-1, CFTR, and SERT also remained unchanged in the presence of purified *C. difficile* toxins.

Given that DRA mRNA levels were not changed by *C. difficile* toxins, we hypothesized that TcdA and TcdB were causing downregulation of DRA at the post-transcriptional level, possibly through increased protein degradation. To that end, we found that co-treatment of Caco2 monolayers with purified toxins and Bafilomycin A1, a known inhibitor of lysosomal and autophagic degradation, abrogated the effects of the toxins on DRA protein expression. These results indicated that *C. difficile* toxins may have induced the increased degradation of DRA protein.

SUMMARY (continued)

Utilizing a toxigenic mouse model of CDI, we also found that TcdA alone and TcdA + TcdB administration significantly reduced colonic DRA protein expression in mice without altering mRNA levels. Furthermore, mice administered TcdA and TcdA+TcdB also had reduced colonic expression of NHE3 without significant alterations in mRNA levels. Administration of purified TcdA also resulted increased mRNA levels of inflammatory cytokines and significant release of myeloperoxidase (MPO) in the murine colonic mucosa. Finally, our toxigenic mouse model also identified a possible role for autophagy in toxin-mediated CDI as TcdA-treated mice had decreased levels of autophagy related proteins ATG16L1 and Beclin-1. Likewise, LC3B, a necessary component in autophagosomal maturation and fusion with lysosomeas, was increased in mice administered TcdA.

Lastly, we obtained colonic biopsies from healthy and recurrent CDI patients. We found that patients with recurrent CDI exhibited a drastic loss of colonic DRA protein compared to healthy controls. In total, these studies show, for the first time, that toxin-mediated downregulation of Cl^- transporter DRA may play a key role in decreasing intestinal epithelial electrolyte absorption in CDI and hence may contribute to CDI associated diarrhea.

1. Introduction

The human intestine possesses a large capacity for fluid absorption. Of the 8 to 10 L of fluid presented to the intestine each day, the small intestine absorbs the majority (7L) (50, 73). Under normal physiological conditions, the remaining intestinal fluid content, approximately 100-200 mL, is then excreted in the stool **(Figure 1).** While the large intestine is capable of absorbing up to 5 L per day, it typically only receives 1.5-2 L (46, 73). Importantly, this high absorptive capacity is critical in mediating the absorption of increased intestinal fluid during inflammation or infection also known as diarrhea. Diarrhea occurs via decreased absorption and/or increased secretion of electrolytes and water in the mammalian intestine. Diarrhea is a multifactorial disorder caused by intestinal viruses, parasites, bacteria, food intolerance, medications, and intestinal disorders (50, 84, 113, 119) .
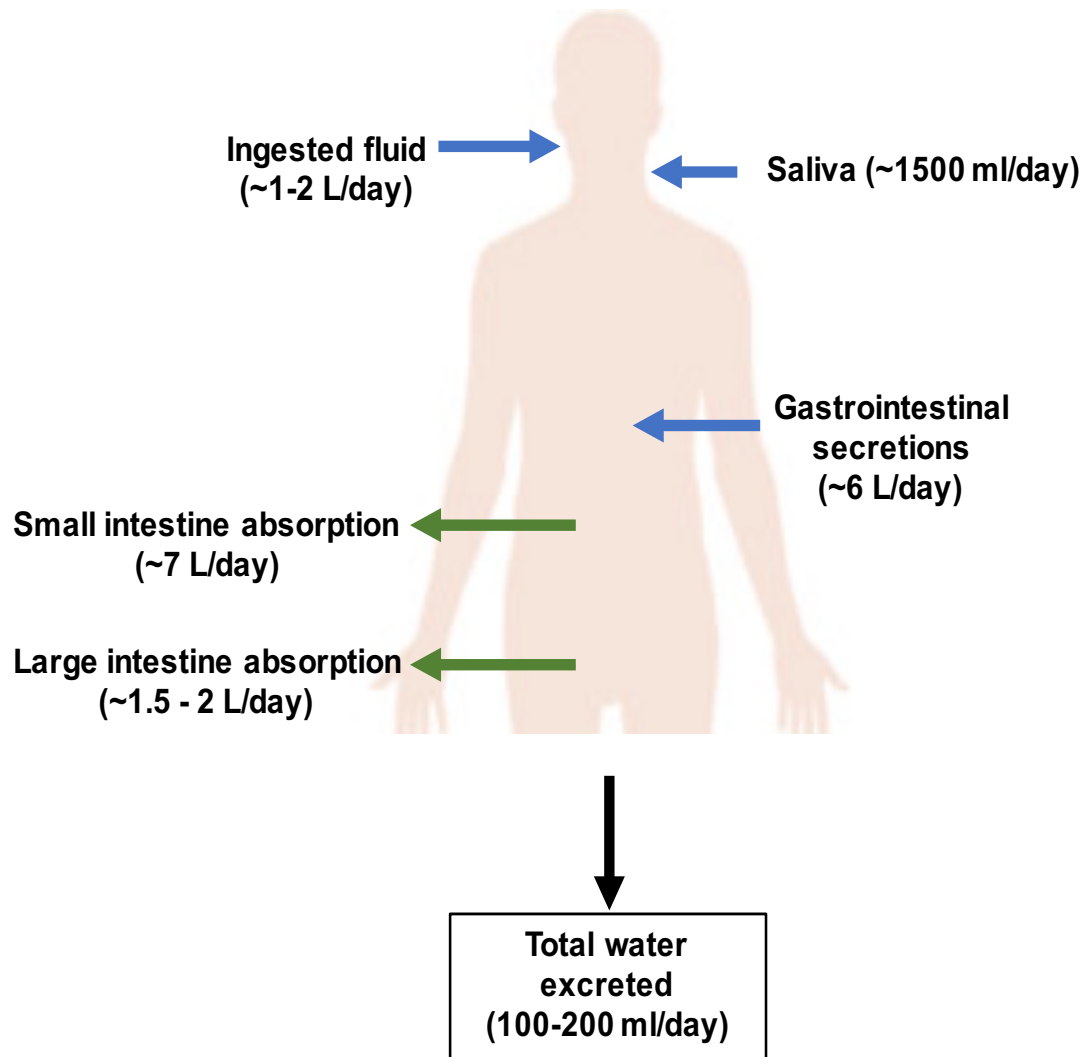
Figure 1: Fluid Homeostasis in the Human Intestine. Adapted from information found in (73).

1.1   The ion transport basis of diarrhea

Diarrhea is the primary cause of mortality and morbidity in children under the age of 5 in developing countries with an estimated 700,000 children dying each year from complications of diarrhea (30). Although there have been reductions in childhood mortality from diarrhea in recent years, diarrhea remains a primary reason for hospitalization especially for children in developing countries. Risk factors for diarrheal disorders include poor hygiene, malnutrition, poverty, and diminished access to suitable healthcare (31) As mentioned previously, the pathophysiology of diarrhea is multifactorial and eventually occurs due to increased secretion and/or decreased absorption in the gastrointestinal tract **(Figure 2).** Water absorption is osmotically coupled to the transport of solutes including Na^+, Cl^-, and nutrients across intestinal epithelial cells. The absorption of these solutes establishes an osmotic gradient across intestinal epithelial cells, thereby allowing for the passive diffusion of water. The intestinal transport of Na^+ and Cl^- occurs through various mechanisms including: (1) secretion of Cl^- via CFTR, CaCC and ClC-2; (2) electrogenic Na^+ absorption through ENaC and other nutrient co-transporters; and (3) electroneutral NaCl absorption (120). These secretory and absorptive mechanisms are described in detail below.

Lumen
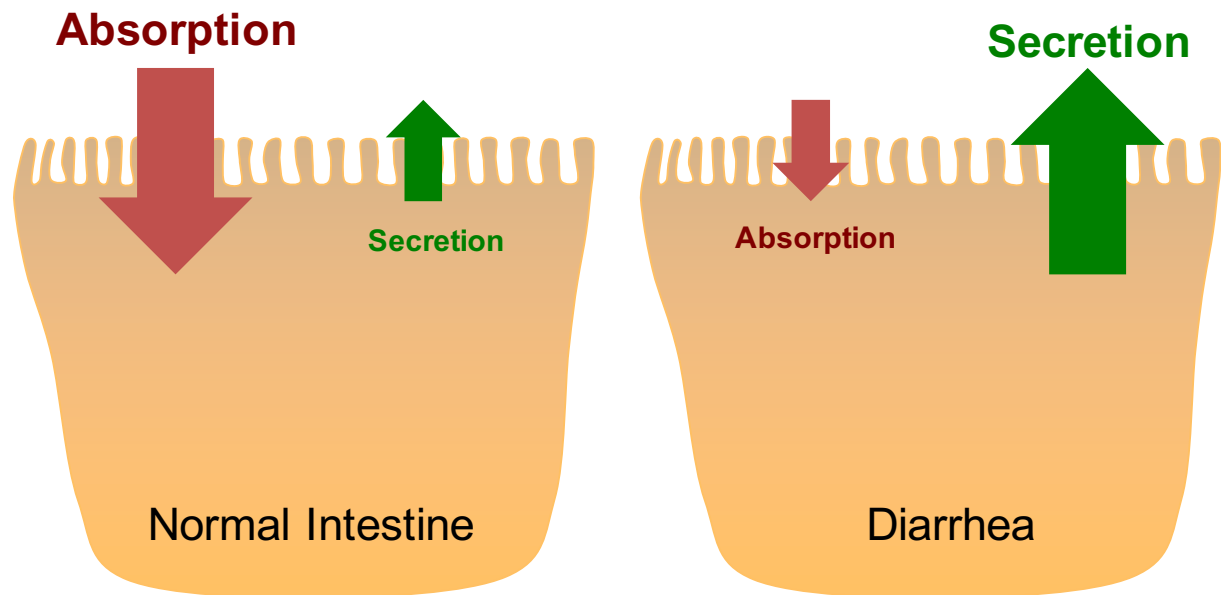
Figure 2: Diarrhea is caused by decreased absorption and/or increased secretion of solutes in the mammalian intestine

1.1.2   Chloride Secretion

There are currently three channels known to secrete Cl⁻ into the intestinal lumen: cystic fibrosis conductance regulator (CFTR); calcium-activated Cl⁻ channels (CaCC); and chloride-channel type-2 (ClC-2) channels (106) **(Figure 3)**. In general, intestinal chloride secretion through these apical channels requires the basolateral uptake of Cl⁻ through the Na⁺/K⁺/Cl⁻ symporter NKCC1. NKCC1 activity is driven by the Na⁺ gradient created by the Na⁺/K⁺ ATPase. Finally, the secretion of K⁺ through basolateral potassium channels creates the electrochemical gradient necessary to force apical secretion of Cl⁻ (154) **(Figure 3)**.The primary transporter responsible for apical chloride secretion is CFTR, a cAMP-sensitive Cl⁻ channel predominantly expressed along the crypt-villus axis in the

mammalian intestine (18, 66, 106). Mutations in CFTR lead to an increase in Cl⁻ secretion and cause cystic fibrosis (CF), an autosomal recessive disorder characterized by heavy production of thick mucus leading to inflammation and infection in the lungs, pancreas, gut, and testes (18). Additionally, some CF patients experience chronic constipation further emphasizing the role for CFTR in intestinal chloride secretion. Intracellular Ca^{2+}, cGMP, and cAMP are all known activators of CFTR activity (47, 106, 138). Another Ca^{2+}-dependent route for chloride secretion is via the calcium-activated Cl⁻ channel (CaCC). While less is known about these channels, electrode-based studies have convincing evidence for a cAMP-independent, calcium-dependent pathway of Cl⁻ secretion through CaCC (8, 106). The final channel responsible for Cl⁻ secretion is the ClC-2 channel, which are located close to tight junctions on the lateral membrane of enterocytes (106) Although Cl⁻ secretion via ClC-2 has been shown in cultured cells, ClC2 KO mice do not exhibit secretory diarrhea, obstructions, or increased mortality (172). Thus, the overall contribution of ClC-2 to intestinal chloride secretion remains poorly understood.

Lumen
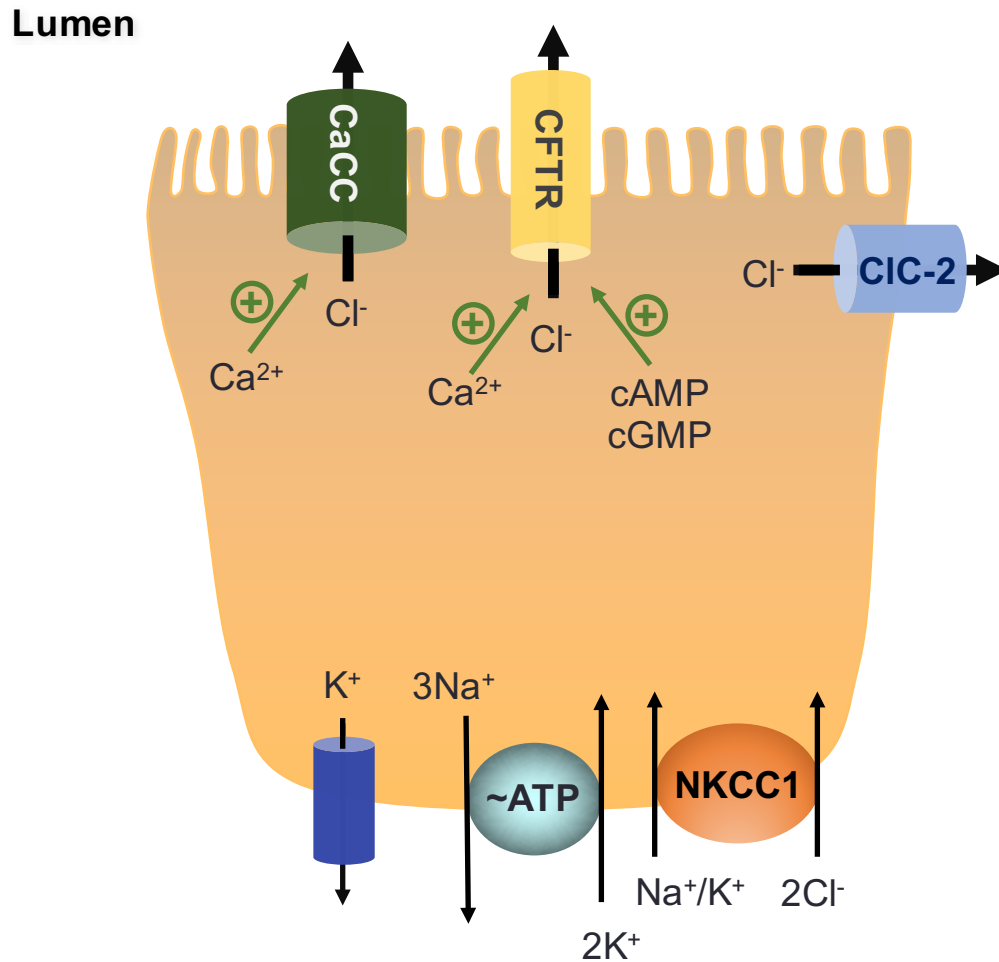
Figure 3: Intestinal luminal chloride secretion is mediated by CFTR, Calcium-dependent Chloride Channels, and ClC-2

1.1.3 Electrogenic Sodium Absorption

One method of intestinal Na^+ absorption is electrogenic Na^+ absorption through the apical sodium channel ENaC. ENaC is located in the apical membrane of polarized epithelial cells in the colon, lung, and kidney (74). ENaCs form heterotrimeric channels that facilitate passive, electrogenic, and selective Na^+ absorption across the apical

membrane (97). ENaCs are predominantly expressed in the rectum and distal colon, where they are critical components of sodium absorption (97). ENaC function and expression has also been linked to inflammatory bowel disease. Specifically, the increased diarrhea seen in patients with ulcerative colitis (UC) has been linked to the downregulation of ENaC (120). On a molecular level, the basolateral Na^+/K^+ ATPase actively pumps out three Na^+ ions for uptake of two K^+ ions resulting in a negative electrochemical gradient. This action allows for the passive diffusion of sodium ions across the apical membrane through ENaC **(Figure 4)**. Sodium absorption through ENaC is stimulated by various glucocorticoids and hormones including aldosterone (130) **(Figure 4)**. Amiloride, on the other hand, inhibits ENaC function and is commonly used as a diuretic (97, 130). Interestingly, studies have shown that ENaC directly interacts with CFTR to modulate CFTR activity (11). This interaction, and its overall contribution to pathophysiological disorders like CF, remains an ongoing area of research.
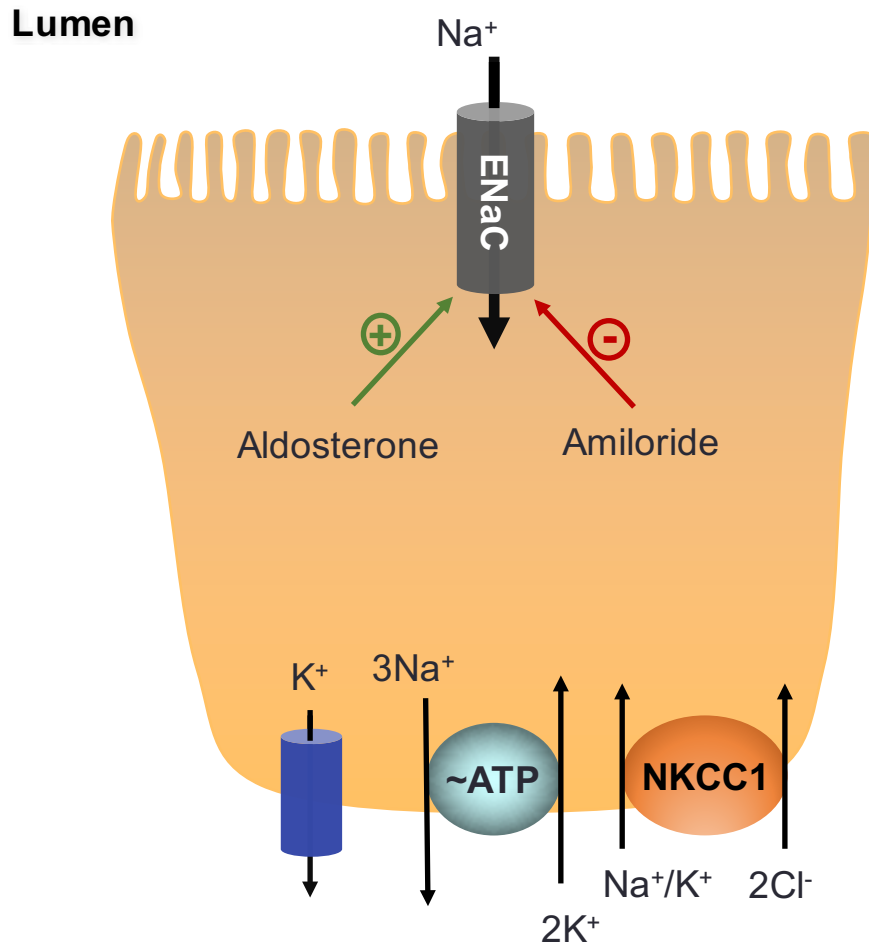
Figure 4: ENaC Na$^+$ channel mediates electrogenic sodium absorption in the mammalian intestine

1.1.4 Electroneutral NaCl Absorption

Na$^+$ and Cl$^-$ absorption occurs primarily via an electroneutral NaCl mechanism, which is found mainly in the ileum and colon of the mammalian intestine (74). The coupled operation of luminal membrane Na$^+$/H$^+$ and Cl$^-$/HCO$_3^-$ exchangers is the predominant route for electroneutral NaCl absorption (37, 40, 120). The ion exchangers responsible

for electroneutral Na^+ and Cl^- absorption, belonging to the SLC9 and SLC26 families, respectively, are described in further detail in later sections. Similar to the chloride secretion and sodium absorption mechanisms described earlier, electroneutral NaCl absorption is powered by the basolateral Na^+/K^+ ATPase pump **(Figure 5)**. The efflux of Na^+ ions through the Na^+/K^+ ATPase pump creates a gradient for apical Na^+ absorption from the intestinal lumen. The SLC9 family transports Na^+ across the apical membrane in exchange for the efflux of H^+. This creates an alkaline environment inside enterocytes, which activates Cl^-/HCO_3^- exchange via the SLC26 family **(Figure 5)**. Inside the cell, carbonic anhydrase (CA) generates the H^+ and HCO_3^- ions needed for Na^+ and Cl^- absorption **(Figure 5)**. This finding is supported by studies showing that NaCl absorption is dependent on CA activity in the mammalian intestine (50). In addition to the transepithelial absorption of NaCl, Na^+/H^+ and Cl^-/HCO_3^- exchangers also play critical roles in intracellular pH. This role is best illustrated by the metabolic acidosis and alkalosis seen in patients with congenital sodium and chloride diarrheas, respectively (67, 161). An introduction to the ion transporters affected by these diseases and their role in intestinal electroneutral NaCl absorption is described below.

Lumen
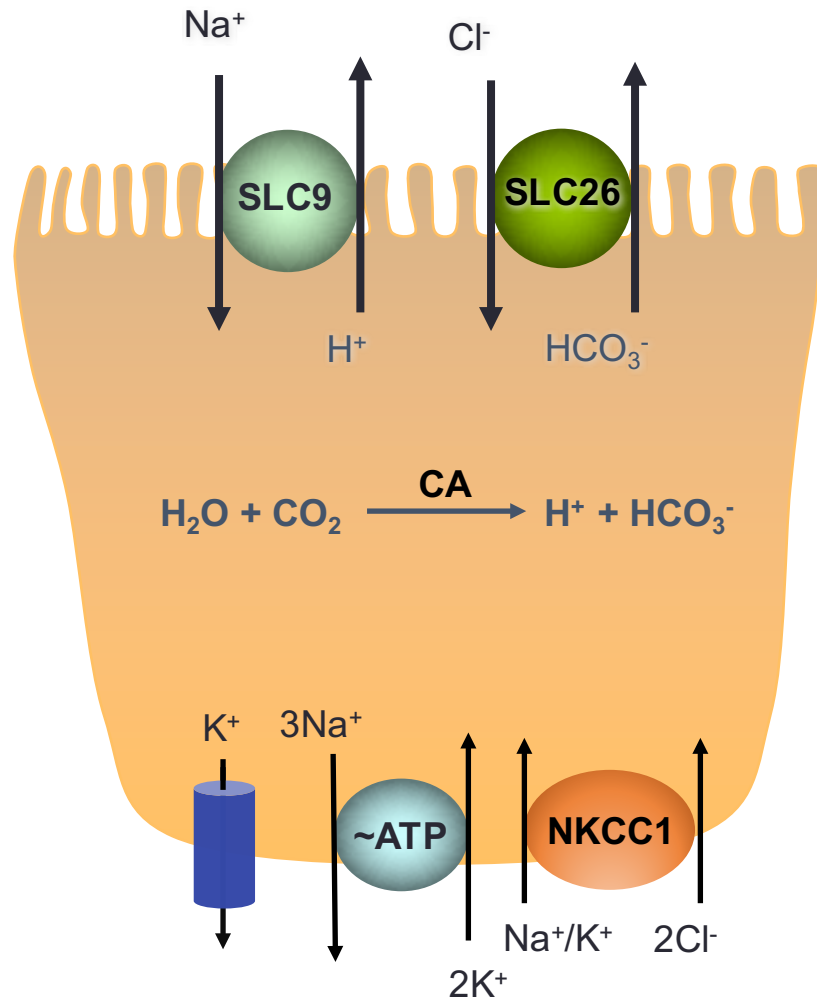
Figure 5: Electroneutral NaCl absorption is mediated by the SLC9 family of Na$^+$/H$^+$ exchangers and the SLC26 family of Cl$^-$/HCO$_3^-$ exchangers

1.2   The SLC9 Family of Na$^+$/H$^+$ Exchangers

The Na$^+$/H$^+$ exchangers, belonging to the SLC9 gene family, play a critical role in

Na$^+$ and water absorption and pH homeostasis (both in the cytosol and organelles) (37).

There are 11 known mammalian isoforms in the NHE family (NHE1-NHE11). Of these,

four NHEs are expressed in intestinal epithelial cells. NHE1 is a basolateral exchanger, while NHE2, NHE3, and NHE8 localize to the apical membrane (37) **(Figure 6).** The four intestine-specific NHEs will be described in the following sections.

1.2.1 SLC9A3 (NHE3)

NHE3 (SLC9A3) is the primary mediator of intestinal and renal Na^+ absorption in the human intestine (37, 38, 50). NHE3 is expressed in a variety of tissues including the gall bladder, colon, small intestine, and kidney. In the mammalian intestine, NHE3 is predominantly expressed in the ileum and proximal/mid-colon with the functional coupling of NHE3 to Cl^-/HCO_3- exchanger DRA (SLC26A3) being the main route for electroneutral NaCl absorption in the ileum and colon (37, 138). The importance of NHE3 in intestinal sodium absorption has been shown in patients with congenital sodium diarrhea (CSD). CSD is caused by a genetic loss of function mutation in NHE3 resulting in impaired Na^+ absorption, diarrhea, and metabolic acidosis (67). Additionally, NHE3 KO mice exhibit mild diarrhea, increased fluid retention in the intestine, reduced blood pressure, and higher mortality rates without proper Na^+ supplementation (37, 163).

NHE3 has also been implicated in various inflammatory and infectious models of diarrhea. Studies have shown that mucosal NHE3 function is decreased in patients with IBD, with both mRNA and protein expression levels decreasing as well (mRNA only in CD patients) (37, 92, 138). Studies have also shown that NHE3 function is significantly decreased in cells infected with EPEC (enteropathogenic *E. coli*) through the bacterial effector EspF (60). Pro-inflammatory cytokines IFN-γ and TNF-α have been shown to downregulate NHE3 expression and/or function both in animal (27, 125) and cell culture

models (4). On the other hand, NHE3 mRNA and protein levels, along with Na^+/H^+ exchange activity, were increased in the presence of probiotic *Lactobacillus acidophilus* or its culture supernatant (141).

1.2.2 SLC9A2 (NHE2)

NHE2 (SLC9A2) is localized to the brush border membrane of the small intestine, colon, and gallbladder (37). It is also expressed in the stomach, endothelial cells of the blood brain barrier, and various parts of the kidney (37). In the small intestine, NHE2 is localized to the brush border of villus and upper crypt cells while its localization in the proximal and distal colon is in the apical membrane of surface and crypt cells (37). While some roles of NHE2 have been identified, the precise physiological significance of NHE2 function in the intestine remains unclear. Few studies suggested that NHE2 might be involved in repair of the intestinal epithelial cell barrier (166). However, NHE2 KO mice do not have diarrhea and NHE2/NHE3 double KO mice do not have more severe diarrhea than NHE3 single KO mice (37, 119).

1.2.3 SLC9A8 (NHE8)

NHE8 is ubiquitously expressed in both human and mouse, but is predominantly expressed early in development. NHE8 is localized both intracellularly and at the apical membrane in the kidney and intestine. Although NHE8 is the primary intestinal brush border NHE in neonates, NHE8 KO mice (2-3 weeks old) do not have a diarrheal phenotype (165) thereby limiting its possible involvement in electroneutral NaCl absorption.

1.2.4 <u>SLC9A1 (NHE1)</u>

NHE1 is expressed in most mammalian cell types including cardio myocytes, fibroblasts, and intestinal epithelial cells (37). In intestinal epithelial cells, NHE1 is expressed in the basolateral membrane thus limiting its contribution to luminal sodium absorption (37, 97). Important functions of NHE1 include its mediation of cell alkalization and restoration of cellular volume through its efflux of H^+ and absorption of Na^+ (97). Interestingly, the role of NHE1 in IBD remains unclear as different studies have reported both increases and decreases in NHE1 expression (44, 144).
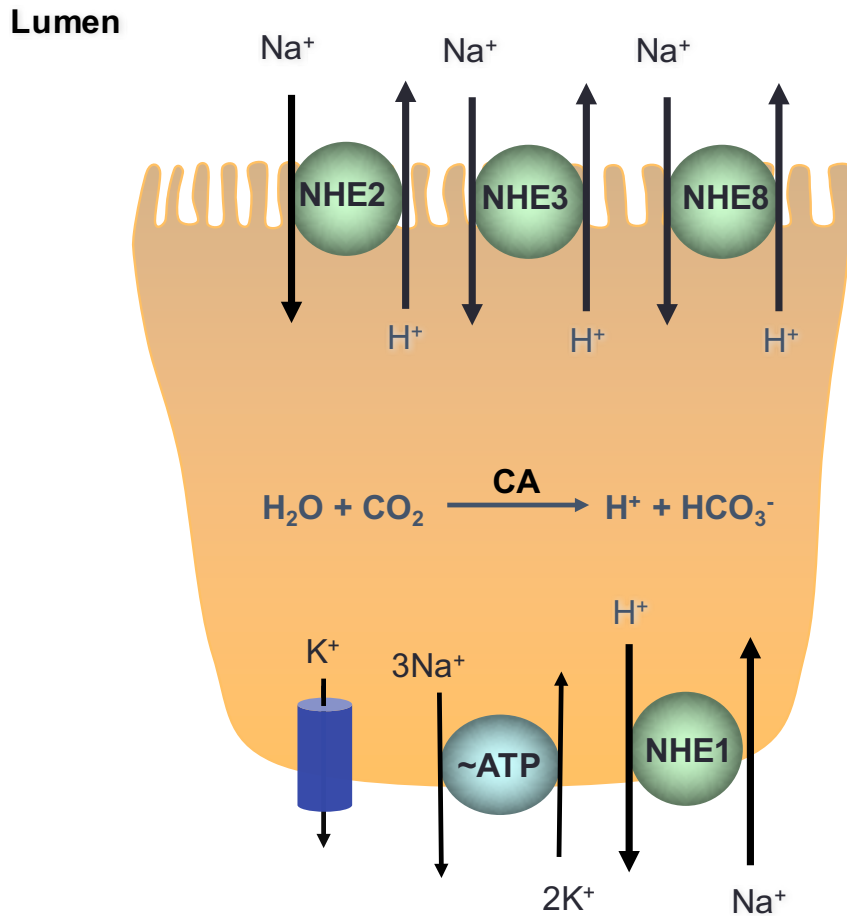
Figure 6: Na$^+$/H$^+$ exchangers mediate electroneutral Na$^+$ absorption in the human intestine

1.3   The SLC26 Family of Cl$^-$/HCO$_3^-$ Exchangers

The SLC26, or sulfate permease family, consists of 11 highly conserved, tissue-specific anion transporters. The SLC26 family are known to transport a range of mono- and divalent anions including, oxalate, SO_4^{2-}, Cl^-, I^-, HCO_3^-, OH^-, and NO_3^- although the specificity for each anion varies considerably amongst the SLC26 transporters (3, 50, 105) Two of these family members, SLC26A3 and SLC26A6, are known to play a critical

role in Cl^- /HCO_3^- exchange in the mammalian intestine and will be described in the following sections **(Figure 7)**.

1.3.1 SLC26A3 (DRA)

SLC26A3, also known as DRA or <u>D</u>own-<u>R</u>egulated in <u>A</u>denoma, was originally considered as a possible tumor suppressor gene as its expression was significantly downregulated in carcinomas and adenocarcinomas. DRA is primarily expressed in the duodenum and colon with limited expression in the ileum and jejunum. In Caco2 cells, an intestinal epithelial cell line, DRA expression is only detected in post-confluent Caco2 cells and its predicted molecular weight ~70 kDa (50, 85). Expression of DRA in the murine intestine is similar to the regional expression pattern seen in humans with the highest expression seen in the cecum, distal colon, and proximal colon (50, 120). Mouse DRA is detected at ~85 kDa; this higher molecular weight is thought to be due to the glycosylation of DRA which also results in a larger molecular weight in rabbits (50).

Although DRA was originally characterized in adenomas (135), it has now been established as the main chloride transporter involved in electroneutral sodium chloride absorption via its functional coupling to NHE3 (47, 74, 138) **(Figure 5)**. The contribution of DRA to electroneutral chloride absorption is evidenced by its dysfunction in a rare genetic disorder called congenital chloride diarrhea (CLD) (161). CLD is characterized by decreased Cl^- absorption, metabolic alkalosis, and profuse chloride-rich diarrhea (>90 mmol/L vs. 10-15mmol/L in normal individuals). Furthermore, this aberrant chloride absorption and subsequent diarrhea seen in CLD patients is fatal without lifelong electrolyte supplementation (161). Evidence for DRA as the primary candidate for

vectorial Cl⁻ absorption is also supported through studies in knockout mice. DRA KO mice exhibit decreased Cl⁻ absorption and a severe diarrheal phenotype similar to that of CLD patients (161)

1.3.2 SLC26A6 (PAT-1)

SLC26A6, also known as putative anion transporter 1 or PAT-1, is Cl^-/HCO_3^- exchanger that is predominantly expressed in the ileum, jejunum, and duodenum with limited expression in the colon. This follows an expression pattern opposite to that of DRA, which has the highest expression in the cecum and colon (50, 120). Like DRA, PAT-1 is expressed in the apical membrane of intestinal enterocytes and has an estimated molecular weight of ~90 kDa (3, 159).

While PAT-1 mediates the exchange of Cl⁻ and bicarbonate along the length of the intestine, studies suggest that it is most important for chloride absorption in the upper GI tract (158). Additionally, some reports have suggested that PAT-1, like DRA also functionally couples to NHE3 to mediate NaCl absorption (171)

As mentioned earlier, loss of DRA in DRA KO mice causes severe diarrhea and decreased chloride absorption (136). On the other hand, PAT-1 KO mice do not have symptoms of diarrhea although their Cl^-/HCO_3^- exchange activity is markedly decreased (159). Interestingly, while PAT-1 KO mice did not have diarrhea, these animals exhibited altered oxalate absorption in the small intestine leading an increase in kidney stone formation (159). Thus, PAT-1 has emerged as a regulator of oxalate secretion in the small intestine, whereas DRA is known predominantly for its role in electroneutral NaCl absorption.
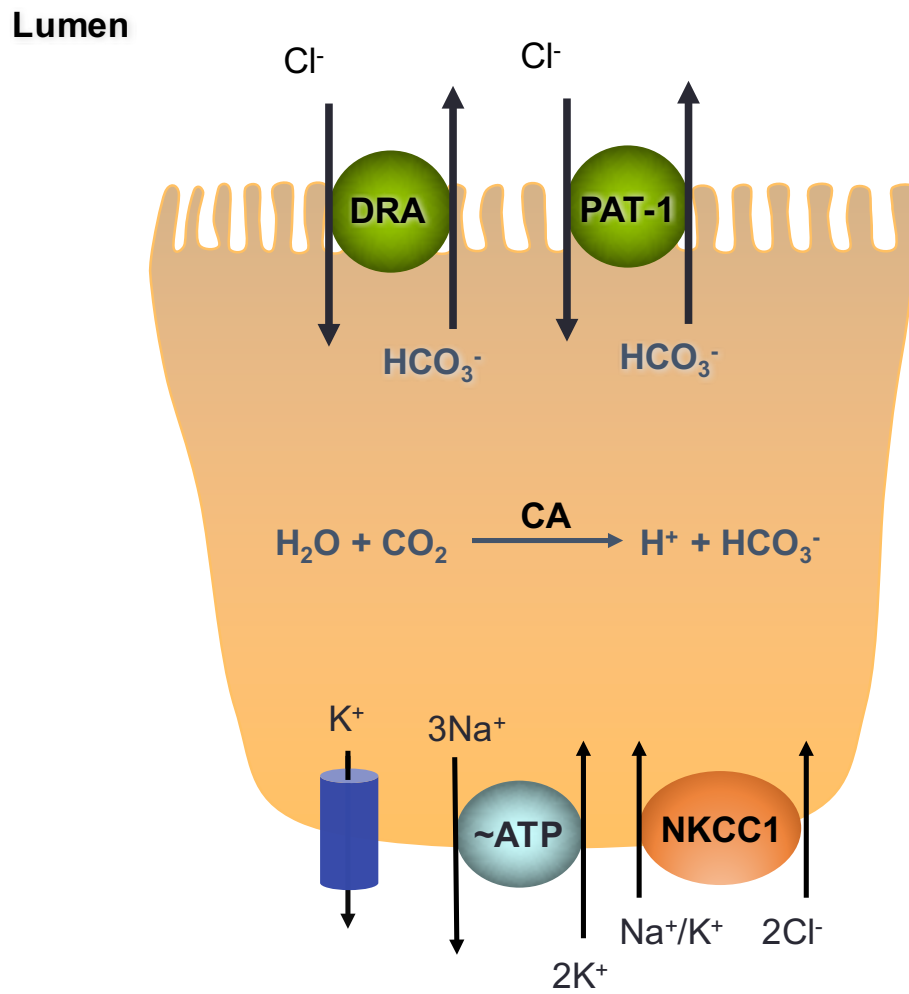
Figure 7: Intestinal Cl⁻/HCO₃⁻ exchange is mediated by SLC26 members DRA (SLC26A3) and PAT-1 (SLC26A6)

1.4   DRA and NHE3 dysregulation in diarrheal disorders

In addition to its role in CLD, DRA function and expression has been shown to be altered in a variety of inflammatory and infectious intestinal disorders including IBD. Inflammatory bowel disease (IBD) is a general term to describe disorders characterized by chronic inflammation and diarrhea in the intestinal tract (104, 120). Common types of IBD include Crohn's disease (CD) and Ulcerative colitis (UC). UC is inflammation predominantly localized to the intestinal lining of the colon whereas inflammation caused by CD can occur anywhere in the digestive tract (104). Studies by Yang et al found that DRA mRNA and protein expression were drastically reduced in patients with UC (168). In murine models of inflammation, DSS-induced colitis caused a significant reduction in DRA mRNA and protein expression without a significant loss of colonic epithelium in these animals. In another study, a decrease in DRA mRNA expression was also found in IL-10 KO mice with the reduction in DRA directly linked to the intestinal inflammation of these animals and not the specific loss of IL-10 (168). In addition, mice overexpressing TNF-α also exhibited a significant loss in DRA mRNA and protein levels (164). Dysregulation of DRA function and expression is also seen in infectious models of diarrhea. Infection with *Citrobacter rodentium*, a murine pathogen closely related to enteropathogenic *E. coli* (EPEC), led to significant loss of DRA mRNA and protein (83). Similarly, Caco2 cells infected with EPEC had decreased function and surface levels of DRA due to microtubule disruption and subsequent alterations in endocytosis/exocytosis (51, 54) . Taken together, these studies highlight the critical role of DRA in chloride and water absorption in the mammalian intestine.

Similarly, NHE3 has also been implicated in various intestinal pathologies including inflammatory bowel disease (IBD), EPEC infection, and congenital sodium diarrhea (61, 67, 144). Thus, electroneutral electrolyte absorption by both NHE3 and DRA represents a therapeutic target for diarrheal diseases. One such diarrheal disease is *Clostridium difficile* infection (CDI), which is the primary cause of hospital- and antibiotic-associated diarrhea in the United States (39). Interestingly, studies using *Clostridium difficile* TcdB have shown internalization of NHE3 from the apical surface in various cell lines after toxin administration (57). Furthermore, decreased NHE3 expression and function were also shown in patients with CDI (42). However, whether *C. difficile* toxins affect DRA *in vitro* has not been explored.

1.5 *Clostridium difficile* infection

Clostridium difficile is a gram-positive, obligate anaerobe belonging to the Firmicutes phylum responsible for *Clostridium difficile* infection (CDI). CDI is an infectious diarrhea characterized by symptoms ranging from self-limiting diarrhea to pseudomembranous colitis, sepsis, and death (1, 137). CDI has become the leading cause of nosocomial diarrhea in the United States resulting in an estimated 14,000 deaths and hospital costs up to $4 billion annually (1, 137). Additionally, the high recurrence rate of CDI (estimated at 20-30%) results in increased costs and comorbidities. Until recently, CDI was primarily found in hospital settings among the elderly and immunocompromised, but the emergence of hypervirulent strains and a drastic increase in community acquired infections illustrate the rapidly changing epidemiology of CDI. The majority of CDI cases occur due to prior antibiotic treatment. The use of broad spectrum antibiotics including

clindamycin, cephalosporins, penicillins, and fluoroquinolones change the composition of the gut microbiota allowing *C. difficile* to flourish.

1.5.1 *C. difficile* pathogenesis

C. difficile is an obligate anaerobe belonging to the Firmicutes phylum, and is acquired through the fecal-oral transmission of spores. *C. difficile* spores are exceptionally hardy and can survive in a variety of environments (39, 137). Given this, *C. difficile* infection is most commonly acquired in hospitals and, until recently, was rarely found outside of hospital settings (33). However, recent studies have shown that *C. difficile* epidemiology is affecting different demographics with 1/3 of reported cases occurring outside of hospitals (33, 137).This is explained, in part, by the widespread use of antibiotics, predominantly penicillins, cephalosporins, and clindamycin. Under normal circumstances, the human gut consists of a wide variety of microbes integral energy metabolism, intestinal repair, and immune system maturation (77). However, widespread use of antibiotics decreases microbial diversity in the gut allowing for colonization by pathogenic bacteria. Additional risk factors for CDI include increasing age (>65 years), use of proton pump inhibitors, and IBD, among others **(Figure 8)** (137). Once ingested, *C. difficile* spores germinate and colonize the intestine. It is important to note that not all ingested *C. difficile* causes disease. One reason for this is that normal commensal microbes compete with *C. difficile* for nutrients thereby inhibiting its growth. The loss of commensal bacteria after antibiotic exposure, however, may allow for *C. difficile* to better colonize the intestine. This is due, in part, to the key role of commensal gut bacteria in bile acid metabolism (35, 156). Increased bile acid availability (due to loss of commensal

microbes), specifically taurocholate, has been shown to promote germination of *C. difficile* spores (137, 156).
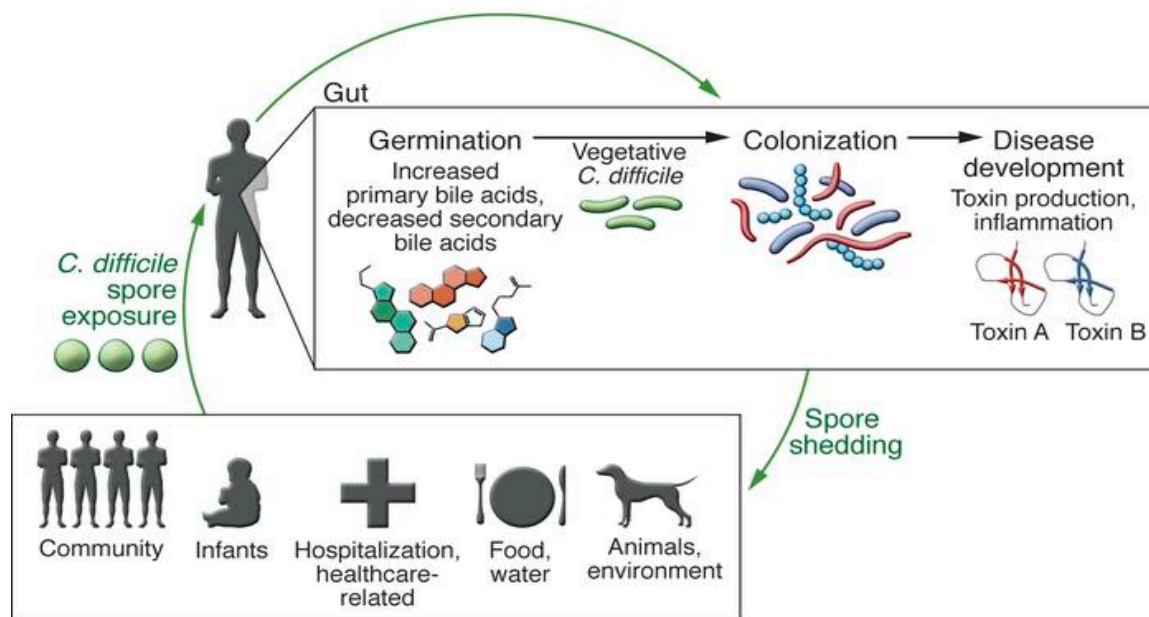
Figure 8: *Clostridium difficile* life cycle and pathogenesis. Used with permission (137)

1.5.2 *C. difficile* toxins: TcdA, TcdB, and CDT

CDI is a toxin-mediated disease relying on the use of three known toxins during pathogenesis. The primary mediators of CDI are large glucosyltransferases – toxins A (TcdA) and B (TcdB). An estimated 5-30% of clinical isolates produce a third toxin CDT, or binary toxin (19, 49, 156). CDT is an ADP ribosyltransferase that alters actin, but its overall contribution to disease remains poorly understood. Some hypervirulent strains,

like the epidemic BI/NAPI/027 North American strain, produce CDT in addition to higher levels of toxins (147). One established role for CDT is the formation of microtubule-based protrusions from the apical surface of intestinal epithelial cells (133, 134). These protrusions have been shown to increase bacterial adhesion and promote more robust colonization in the intestinal lumen.

1.5.3 TcdA and TcdB

TcdA and TcdB (*tcda* and *tcdb*) are encoded by a 19.6 kb pathogenicity locus *PaLoc* along with three other additional genes –*tcdR, tcdE,* and *tcdC* –encoding an RNA polymerase sigma factor, a toxin repressor, and bacteriophage holin for toxin secretion, respectively (21, 147). TcdA and TcdB are large (308 and 207 kDa, respectively) monoglucosylating toxins sharing 66% sequence similarity and 48% sequence identity (2) **(Figure 9)**. Each toxin consists of four domains: (A) The GTD domain responsible for the glucosyltransferase activity of the toxins; (B) the receptor binding domains consisting of Ca^{2+}-binding repeats forming combined repetitive oligopeptide structures (CROPs); (C) the cysteine protease domain responsible for toxin cleavage and (D) a hydrophobic region allowing for acidification of endosomes to promote toxin release (35, 147) **(Figure 9)**.
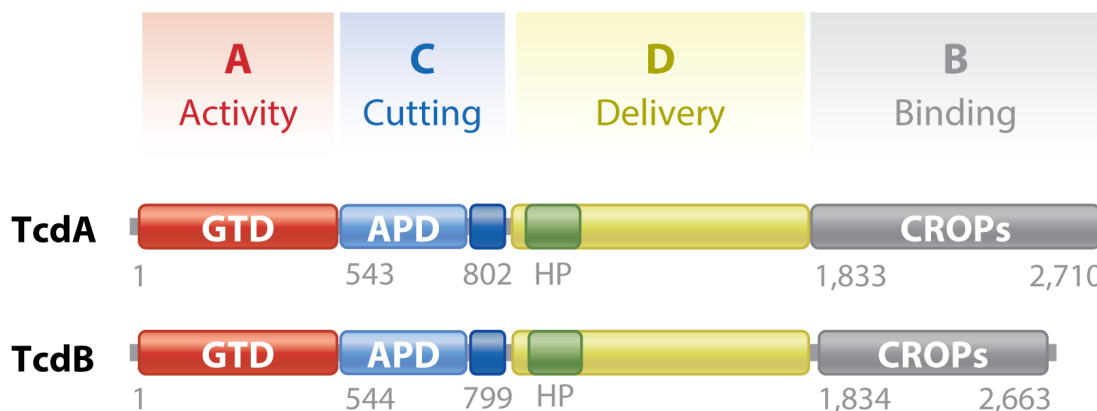
Figure 9: The four domains of *C. difficile* toxins TcdA and TcdB. Used with permission (2)

1.5.4   Cellular receptors of TcdA and TcdB

Although TcdA and TcdB are taken up by the same general process, they are known to have different receptors. Various TcdA receptors are known including isomaltase (rabbit intestinal epithelial cells), Lewis I, X, Y, receptors (human intestinal epithelial cells) (2). Most recently, glycoprotein gp96 has been nominated as another receptor for TcdA (107). Gp96 is expressed on the apical membrane of human colonocytes and in the cytoplasm. However, anti-gp96 antibodies only partially inhibit TcdA-induced cytotoxicity suggesting that gp96 is not the main receptor for TcdA (107). Thus, it is unclear what major receptor is responsible for the pathophysiological effects of TcdA is and what cell types it is expressed in.

Receptors for TcdB have also recently been identified. Utilizing genetic screening techniques like TALEN along with CRISPR/Cas9 gene knockout, CSPG4 has recently

been identified as a receptor for TcdB (170). CSPG4, chondroitin sulfate proteoglycan 4, is a membrane bound proteoglycan that facilitates both TcdB binding and internalization into host cells (170). It has also been theorized that this surface proteoglycan plays a role in cell migration, induction of cell polarity, and proliferation (94). CSPG4 has been found in numerous cell types including mesenchymal stem cells, skeletal myoblasts, oligodendrocyte precursors, and HeLa and HT29 cell lines (170). Another receptor identified for TcdB using the aforementioned techniques is the Wnt receptor Frizzled (FZD) (151). FZD receptors are critical components of the Wnt signaling pathways that regulate embryonic development, stem cell development, and cancer (78). Unlike binding to other known receptors, TcdB does not interact with FZD via its CROPs domain (152). Furthermore, TcdB binding to FZD blocks its binding to Wnt thus inhibiting induction of Wnt-dependent signaling (152).The last putative TcdB receptor is the poliovirus receptor-like 3 (PVRL3), an immunoglobulin-like protein related to the poliovirus receptor PVR (also called nectin-3) (86). Although PVRL3 is expressed in epithelial cells, its overall contribution to TcdB-mediated cytotoxicity remains unclear as PVRL3 was not identified in the CRISPR/Cas9 screen. Additionally, recombinant PVRL3 does not block TcdB induced cytotoxicity whereas recombinant FZD does (86, 152).

1.5.5 TcdA and TcdB mechanism of action

Upon colonization in the colon, *C. difficile* releases toxins that are delivered to the host cell cytosol in seven distinct steps: (1) toxin binding to host cell receptors; (2) receptor-mediated endocytosis of toxins into cell; (3) endsomal acidification mediated by *tcdD* hydrophobic region; (4) pore formation inside the cellular endosome; (5) Endosomal

release of glucosyltransferase domain (GTD) into the host cytosol; (6) inactivation of Rho family GTPases and (7) downstream effects in host cells (21) **(Figure 10)**.

After endosomal release of the GTD domain, both toxins A and B irreversibly inactivate Rho family GTPases, including RhoA, B, C, Rac1-3, Cdc42, and RhoG TcdA and TcdB both mono-*O*-glycosylate Rho at Thr37 and all other Rho GTPases at Thr35, a critical component of the effector switch I region. This switch I effector region is conserved across the Ras superfamily of GTPases and is the region responsible for GTP-binding and subsequent activation of GTPases (26). Additionally, both toxins A and B are known to bind each Rho GTPases with varying specificities (21). It is widely accepted that much of *C. difficile* pathogenesis is attributed to the inhibition of Rho proteins and their downstream effectors. Rho GTPases are involved in several cellular functions including cytoskeletal organization, cytokine production, regulation of cell cycle progression and division, and regulation of phagocytosis (35, 103, 147, 162). These Rho-dependent changes, in addition to known Rho-independent functions (24) comprise the trademark cytotoxic and cytopathic effects of TcdA and TcdB (21, 117, 147). The cytopathic effects of both TcdA and TcdB include various morphologocial changes including cell rounding, cell shrinking, increased epithelial cell permeability, loss of tight junction complexes, and alterations in the actin cytoskeleton (21, 147). These various pathologies all contribute to the diarrheal phenotype commonly associated with CDI (35). After the initial cytopathic events, cell adherence is also reduced thus causing increased apoptosis and cell death (70, 98, 110). TcdA and TcdB also cause cytotoxic effects in infected cells. These effects include the inactivation of RhoA, which leads to the downstream production of pro-apoptosis genes and activation of the inflammasome (48). In addition to apoptosis, *C.*

difficile toxins can also cause cell death via necrotic mechanisms (24), although the role of toxins' glucosyltransferase activity during necrosis remains unclear.
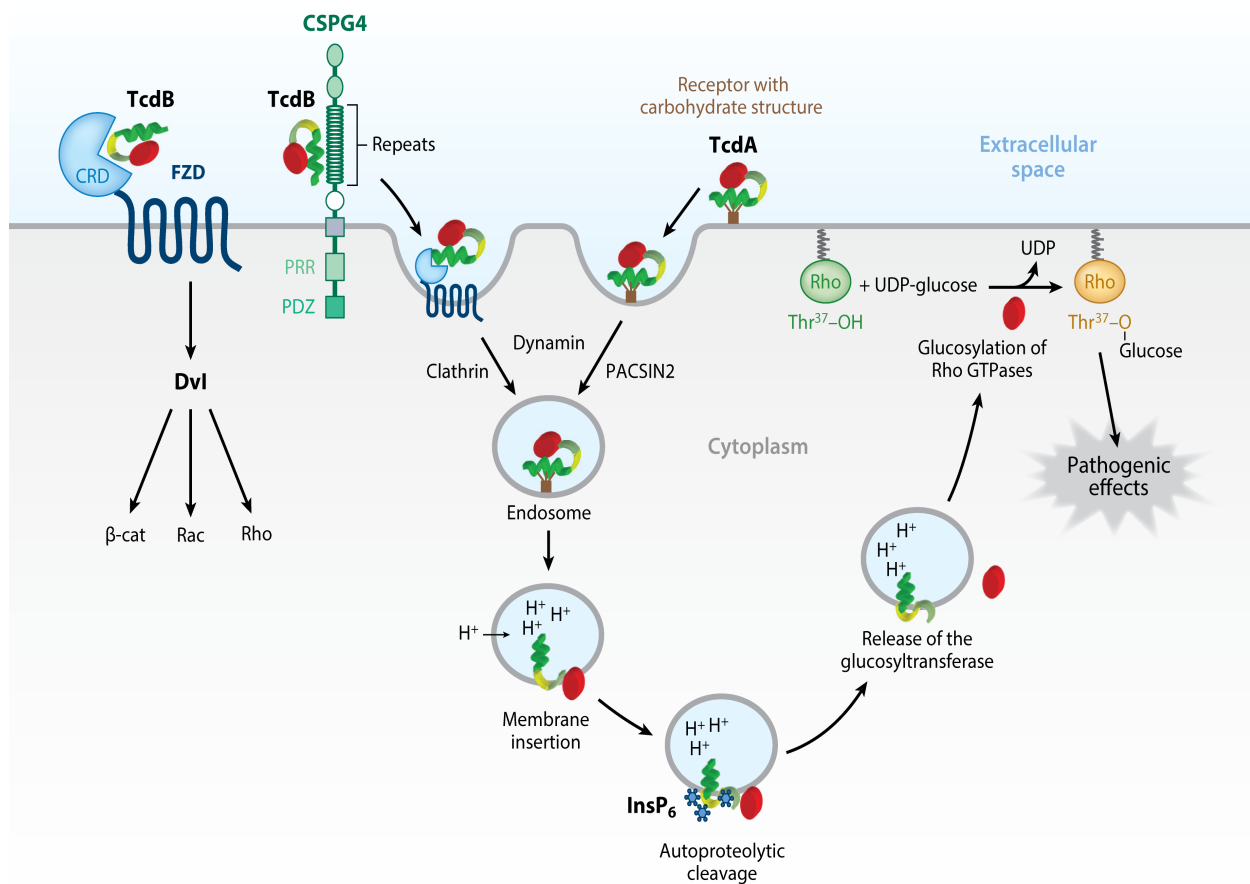
Figure 10: *Clostridium difficile* delivers TcdA and TcdB to host cell cytoplasm via receptor-mediated endocytosis. Used with permission (2)

1.5.6 *C. difficile* Transferase (CDT)

In addition to the primary cytotoxins TcdA and TcdB, an estimated 10% of *C. difficile* clinical isolates produce a third toxin, *C. difficile* transferase (CDT) or binary toxin (1, 49, 140). Unlike toxins A and B, CDT is an actin disrupting toxin belonging to the family of ADP-ribosylating toxins that includes *C. perfringens* iota toxin and *C. botulinum* C2 toxin, among others (49, 114). The genes encoding the two subunits of CDT (CDTa and CDTb) are not located in the PaLoc, but rather in a separate 6.2 kb region named the CDT locus or CdtLoc (1, 49) (**Figure 11A**). CDT consists of two separate toxin components: CDTa and CDTb, the enzymatic and binding subunits, respectively. CDTa is a 48 kDa protein that shares 80-85% sequence similarity with the enzymatic components of other ADP-ribosylating toxins (49). The binding subunit, CDTb, also shares sequence identity with various family members, but this similarity ranges from ~40-80% depending on the toxin (49).
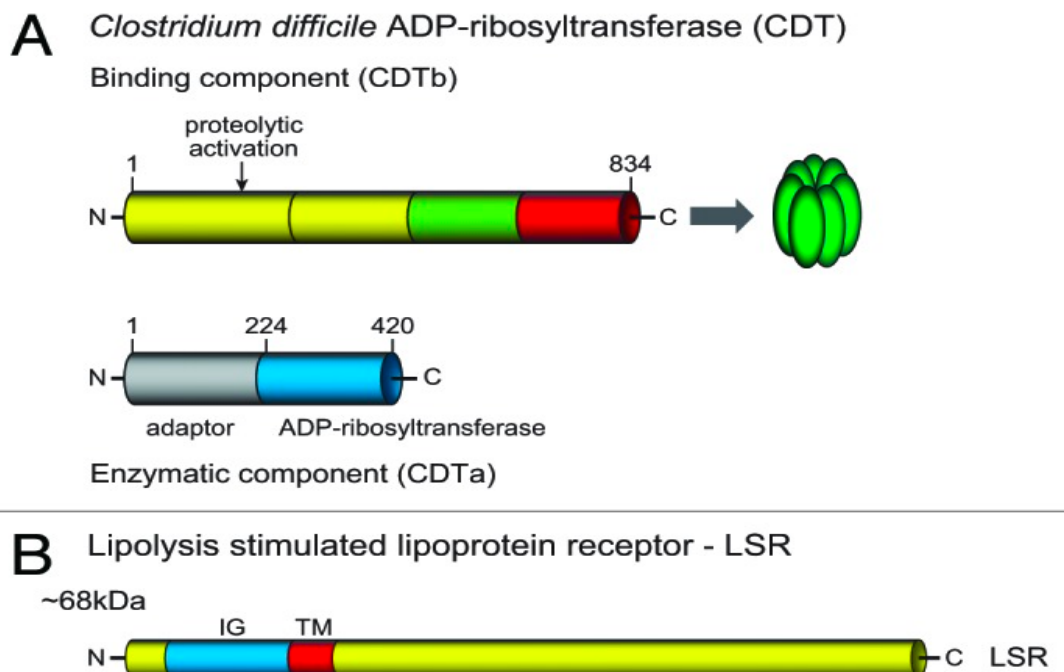
Figure 11: CDT consists of two polypeptides, CDTa (enzymatic component) and CDTb (receptor binding domain) and binds to lipolysis stimulated lipoprotein receptor (LSR). Used with permission (49) under open access license

1.5.7 <u>CDT uptake and mechanism of action</u>

In 2013, studies by Papatheodorou et al identified the CDT receptor using gene trapping in haploid (HAP1 cells) (114). Lipolysis-stimulated lipoprotein receptor (LSR) is a 68 kDa single-pass transmembrane protein that is highly expressed in the liver, small intestine, colon, kidney, lung, adrenal glands, testes, lung, and ovaries **(Figure 11B)** (49, 114). Early on, LSR was shown to be important in clearance of lipoproteins (169). Recent evidence has also emerged showing that LSR is essential for the maintenance of

epithelial tricellular junctions (102). Interestingly, all clostridial iota-like toxins use LSR for receptor-based entry into host cells (114).

Upon release into the intestinal lumen, CDTb heptamers interact with LSR forming a complex that is internalized into host cells (1, 49, 114) **(Figure 12).** After endocytosis, CDTb forms pores in the acidified endosome allowing for the release of the enzymatically active CDTa. Once in the cytosol, CDTa ADP-ribosylates actin at Arg177, thus trapping actin in its monomeric form. This ribosylation prohibits actin polymerization and induces destruction of the actin cytoskeleton. Near the cell surface, the dissolution of cortical actin by CDT leads to the formation of microtubule-based protrusions from intestinal epithelial cells (2, 133). These protrusions are known to increase bacterial adherence 4-5 fold during *C. difficile* colonization, both *in vitro* and *in vivo* (134, 140) **(Figure 12).** Moreover, studies have also shown that patients infected with CDT[+] *C. difficile* strains have a drastic increase in peripheral WBC and 30 day mortality rates (49, 52). Thus, while insights into the precise pathogenic role of CDT remain scarce, *C. difficile* binary toxin may represent an important virulence factor in CDI and remains an active area of toxin-mediated CDI research.
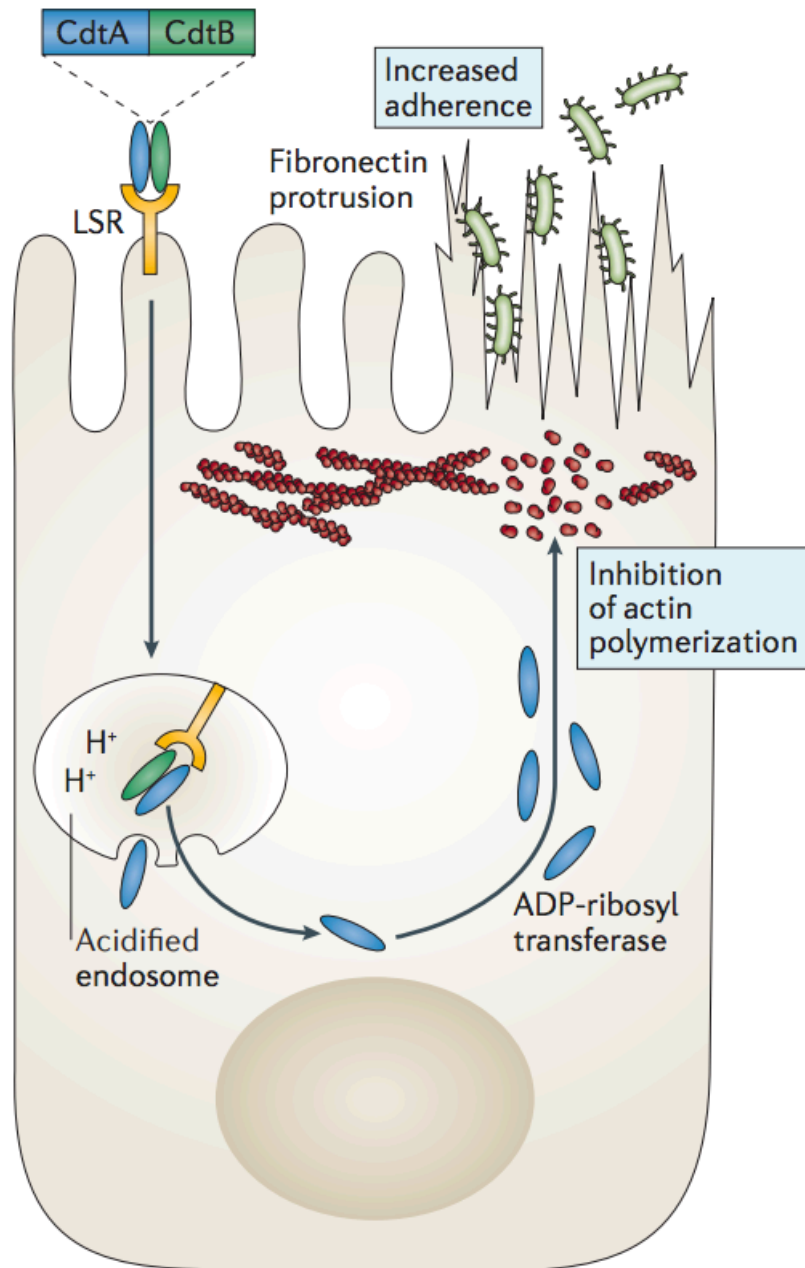
Figure 12: Binary toxin CDT is an ADP-ribosyltransferase consisting of two subunits: CDTa and CDTb. Used with permission (1)

1.5.8 Animal model of CDI

While both TcdA and TcdB are homologous enterotoxins that inactivate Rho GTPases, the overall contribution of each toxin to CDI pathogenesis remains heavily debated. This is perhaps most evident in the various animal models of CDI. Historically, the majority of CDI animal studies have been conducted in hamsters, but disease models have also been established in rabbits, guinea pigs, mice, and rats (22, 95, 156). Hamster CDI is easily induced through antibiotic exposure prior to infection with the primary damage occurring in the cecum with secondary inflammation seen in the ileum (19). Golden Syrian hamsters are easily colonized by *C. difficile*, however, they quickly develop fulminant colitis and many succumb to infection within days (147). This severe infection is not an accurate depiction of the self-limiting disease primarily seen in humans (33, 39, 143). Additionally, the lack of hamster-specific reagents and the involvement of the cecum over *C. difficile's* primary human target, the colon, make the hamster model of CDI less useful. TcdA was originally speculated to be the more important toxin in tissue damage due to the high fluid accumulation seen in various animal models including the hamster (19, 153). TcdB, on the other hand, does not induce damage in rabbit, hamster, or mouse ileal loop models —a core technique of CDI animal models (32, 62). However, studies utilizing *ex vivo* human colonic explants showed that TcdB administration caused significantly more cytokine production and epithelial cell barrier damage. Furthermore, a pivotal study conducted by Lyras et al demonstrated that TcdB alone was responsible for disease progression in hamsters (95). This finding was further evidenced by the identification of TcdA$^-$, TcdB$^+$ strains caused the full spectrum of disease in humans (95).

In the past decade, Chen et al developed a conventional mouse model of CDI using an antibiotic cocktail to establish *C. difficile* colonization in the colon of infected mice (22). This mouse model accurately recapitulates the disease progression seen in human CDI and has been widely adapted, specifically for use with *C. difficile* spores (19, 24, 153). Given that CDI is a toxin-mediated disease, more recent studies have developed an intrarectal toxigenic mouse model of CDI (63). This model, unlike previous models, does not require the extensive biosafety measures of using *C. difficile* spores and is easily induced without prior antibiotic exposure. Interestingly, in this toxigenic model, TcdA-treated mice have significantly more colonic damage and inflammation than those given TcdB alone (63). However, there was evidence that TcdA and TcdB may be acting synergistically as mice given TcdA + TcdB had more severe disease than those given either toxin alone (63).

1.6   Intestinal ion transporters in CDI

The functional coupling of Na^+/H^+ exchanger NHE3 and Cl^-/HCO_3^- exchanger DRA is the predominant route for electroneutral NaCl absorption in the mammalian intestine and has been implicated in a variety of inflammatory and infectious diarrheal diseases (4, 51, 83, 144, 168). Given this, modulation of electrolyte transport has emerged as a potential avenue for therapeutic intervention in cases of diarrhea (82, 85, 141). Interestingly, the role of electroneutral NaCl absorption in *C. difficlie* infection, the most common cause of antibiotic and hospital associated diarrhea, remains poorly understood. Hayashi et al first reported the effects of *C. difficile* toxin B on NHE3 expression in vitro (57). They found that NHE3 was internalized from the apical surface of opossum kidney

cells upon exposure to TcdB (57). Importantly, the overall protein levels of NHE3 remained unchanged indicating that TcdB was causing redistribution, not degradation, of NHE3 (57). More recently, Engevik et al conducted studies using human intestinal organoids (HIOs) and CDI patient stool samples to further investigate the role of NHE3 in CDI (42). These reports found that CDI patients have decreased NHE3 expression in the apical region of intestinal epithelial cells along with a concomitant decrease in NHE3 function evidenced by increased Na^+ and an alkaline pH in stool (42). Taken together, these studies identified NHE3 and electroneutral NaCl absorption as possible targets in CDI pathogenesis.

While there are few studies on NHE3 regulation during CDI, the role of DRA remains entirely unknown. Given this, we hypothesized that C. difficile toxins would decrease DRA expression in *in vitro* and *in vivo* model systems. One possible route of protein downregulation is increased protein degradation through the proteasomal and/or lysosomal pathways discussed below.

1.7 <u>Protein degradation pathways</u>

Protein homeostasis, or proteostasis, is a highly complex process by which cells regulate protein biosynthesis and degradation. Proteostatic regulatory mechanisms are necessary to ensure normal cellular development, aging, adequate response to environmental stressors, and the removal of misfolded proteins (64, 89, 126). Protein degradation by two main pathways, the ubiquitin-proteasome system (UPS) and the autophagy/lysosomal pathway, are the main intracellular systems for proteostasis. In fact, alterations in protein degradation pathways have been implicated in a wide variety of

pathologies including cancers, neurodegenerative disorders, and enteric infections (90, 126).

1.7.1 The ubiquitin-proteasome system (UPS)

The major pathway for protein degradation is through the ubiquitin-proteasome system (UPS), which accounts for 80-90% of all protein degradation (93). Protein degradation by the UPS is known to play a key role in cell cycle progression, DNA repair, immune cell regulation, inflammation, endocytosis, and apoptosis (90, 93, 108). The hallmark of the UPS is its use of ubiquitin as a marker to selectively target proteins for degradation. Ubiquitin (Ub) is a 76-amino acid protein that is covalently attached to lysine residues of proteins to be degraded (108, 126). Proteins are only delivered to the large, multisubunit proteasome for degradation after polyubiquitination (108). The eukaryotic 26S proteasome consists of two large subunits: the catalytic 20S core and two 19S regulatory subunits responsible for stimulating the 20S proteasome to degrade tagged proteins (108, 122). Proteolysis in the UPS consists of three main steps which are outlined in **Figure 13**. First, Ub is linked to a cysteine residue of the activating enzyme, E1, in an ATP-dependent manner. This activated form of ubiquitin is then transferred to E2, a conjugating enzyme, to form a thiol-ester bond. Finally, ubiquitin is transferred from E2 to the target protein by E3 RING ubiquitin ligases. An alternative third step also occurs during which HECT E3 enzymes receive activated ubiquitin from E2 prior to transferring it to the target protein (93) **(Figure 13)**. After this three-step cascade, the process is repeated with E2/E3 or E4 enzymes to achieve polyubiquitination of the target proteins. This polyubiquitination tag is then recognized by the 19S proteasome in an ATP-

dependent manner and is sent to the 20S proteasome subunit for degradation into amino acids and ubiquitin recycling.
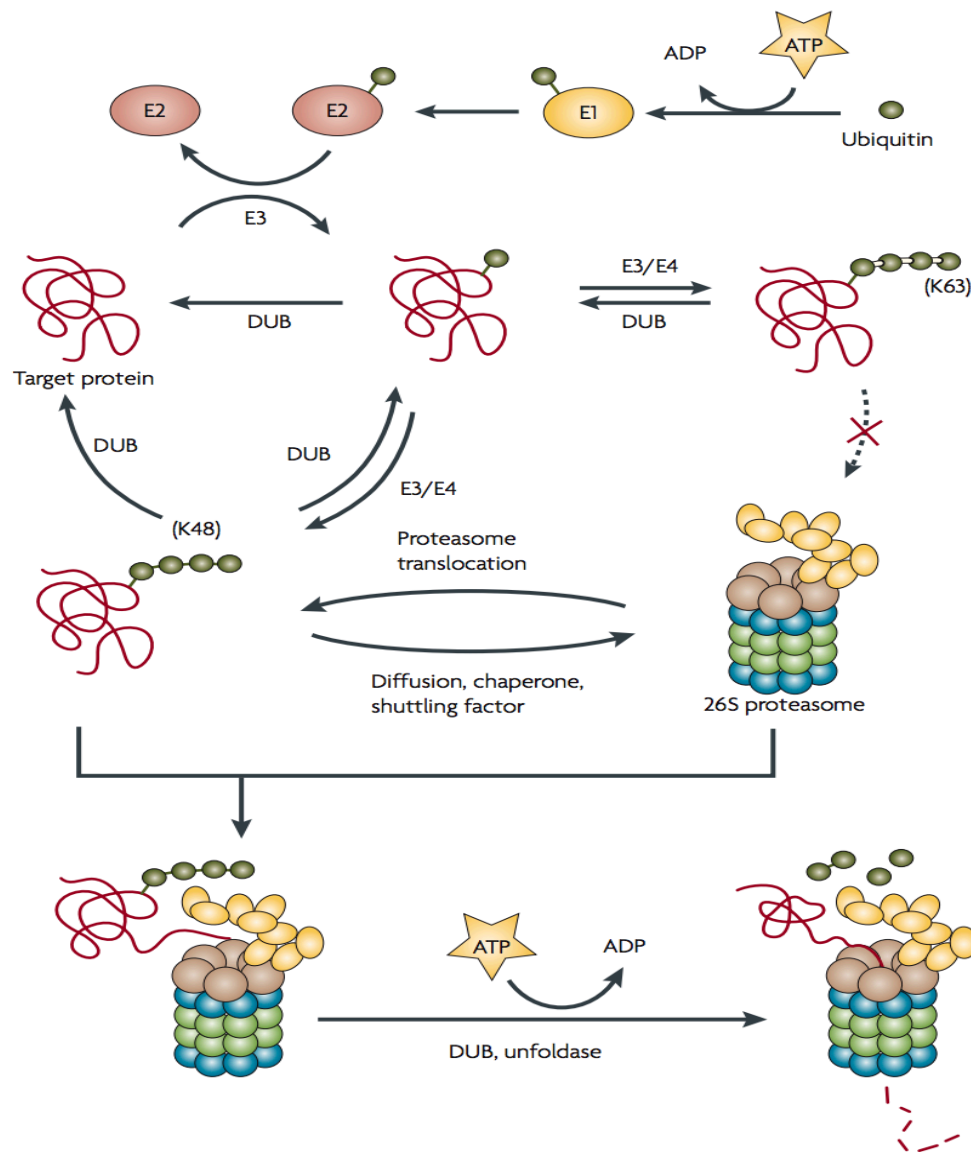
Figure 13: Multi-step ubiquitination targets cytosolic proteins for degradation by the 26S proteasome. Used with permission (148)

1.7.2 <u>Lysosomes and autophagy</u>

While the proteasome is responsible for the cytosolic degradation of small misfolded proteins, some proteins and damaged organelles are too large for degradation by the UPS (96). In these cases, larger substrates are degraded through the lysosomal and autophagy pathway, hereafter referred to as autophagy (108). In general, autophagy (meaning "self-eating") is the degradation of cytoplasmic molecules within lysosomes after delivery of cargo from double-membraned autophagosomes (10, 43). Autophagy has been implicated in a variety of diseases including Parkinson's, various forms of dementia, and Huntington's disease (10). Additionally, some pathogenic bacteria —such as *Salmonella typhi* and *Mycobacterium tuberculosis*—have also been shown to hijack autophagy to promote survival inside host cells (10, 65). Autophagy is comprised of three distinct processes: chaperone mediated autophagy (CMA), microautophagy, and macroautophagy (96). While all three processes degrade proteins in lysosomes, they recognize and degrade different cargo using distinct mechanisms. CMA selectively degrades cytosolic proteins through use of chaperone proteins including heat shock cognate 70 (hsc70) and heat shock protein 90 (hsp90) (9). Additionally, proteins degraded via CMA must be recognized by the lysosomal receptor LAMP-2A (9). The second autophagic process, microautophagy, occurs by direct engulfment of cytosolic proteins into lysosomes however the mechanism remains poorly understood. Macroautophagy is the best characterized of the three and accounts for the majority of proteins degraded in lysosomes (9, 108). **(Figure 14)**.
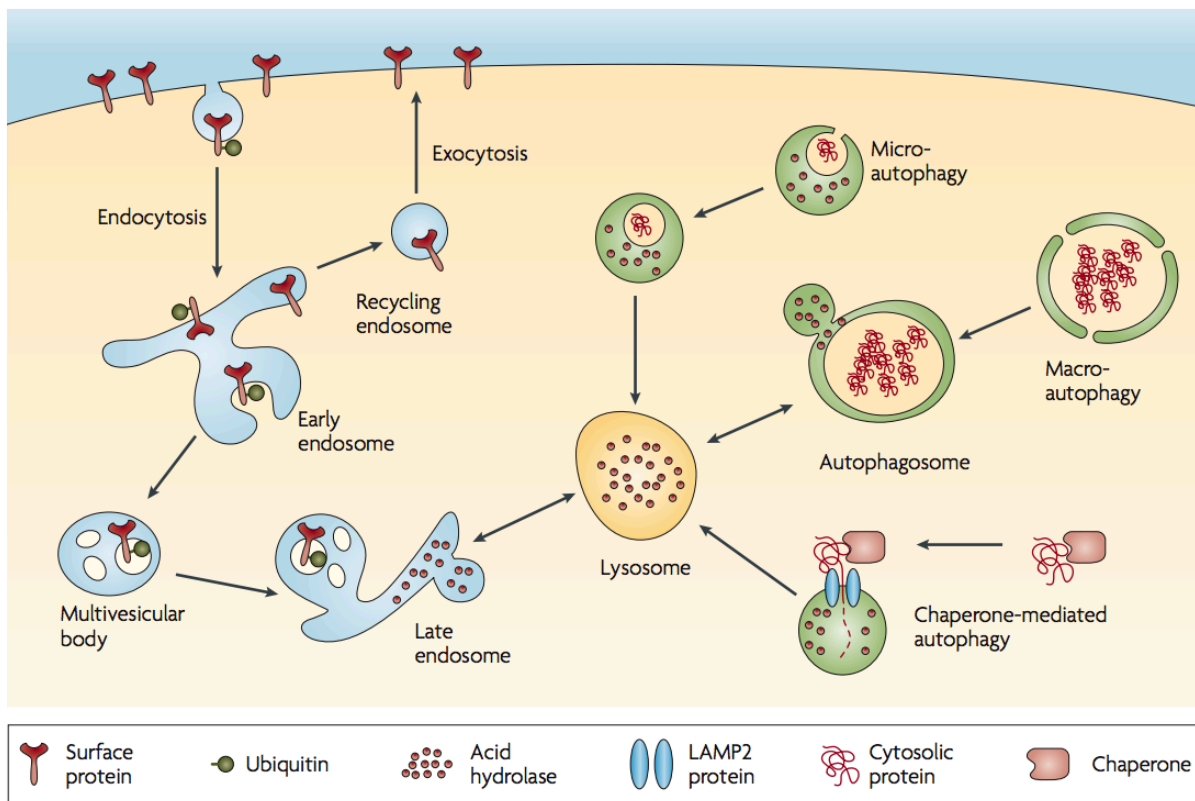
Figure 14: Lysosomal pathways include endocytosis, microautophagy, macroautophagy, and chaperone-mediated autophagy (CMA). Used with permission (148)

1.7.3 Macroautophagy

During macroautophagy, cytosolic cargo is engulfed in a *de novo* formed membrane which seals and matures into a double membrane vesicle known as the autophagosome (43, 79). Under normal circumstances, mTOR and AMPK phosphorylate Unc-like kinases (ULK-1, ULK-2) to inhibit autophagy (10). Upon induction of autophagy during times of stress or nutrient deprivation, ULK-1 is dephosphorylated and activated in

complex with ATG13, FIP200, and ATG101 (65) **(Figure 15).** ULK-1 then phosphorylates and activates Beclin-1, the mammalian homolog of Atg6, in complex with ATG14L and other autophagy proteins. The ULK-1 /Beclin-1 complexes then localize to the forming phagophore prior to autophagosome elongation. Autophagosome elongation is initiated by two different ubiquitin-like conjugation complexes, the first being the ATG5-ATG12 complex (65). The ATG5-ATG12 complex first binds to ATG16(76)L1, creating an E3-like complex that facilitates formation of the second ubiquitin-like complex. The ATG5-ATG12-ATG16L1 complex next facilitates the localization of ubiquitin-like conjugate, microtubule associated light chain 3 (LC3) to the phagosome membrane. Once at the membrane, ATG7, along with the ATG5/12/16L1 complex, conjugates LC3 to phosphatidylethanolamine (PE). This lipidation of LC3 to LC3-PE (also known as the conversion of LC3A to LC3B) initiates closing of autophagosomes, fusion with lysosomes, and subsequent degradation of lysosomal contents (10, 58, 65) **(Figure 15)**. Interestingly, bacterial pathogens are known to be both activators and inhibitors of autophagy depending on the specific pathogen and the stage of infection (65).
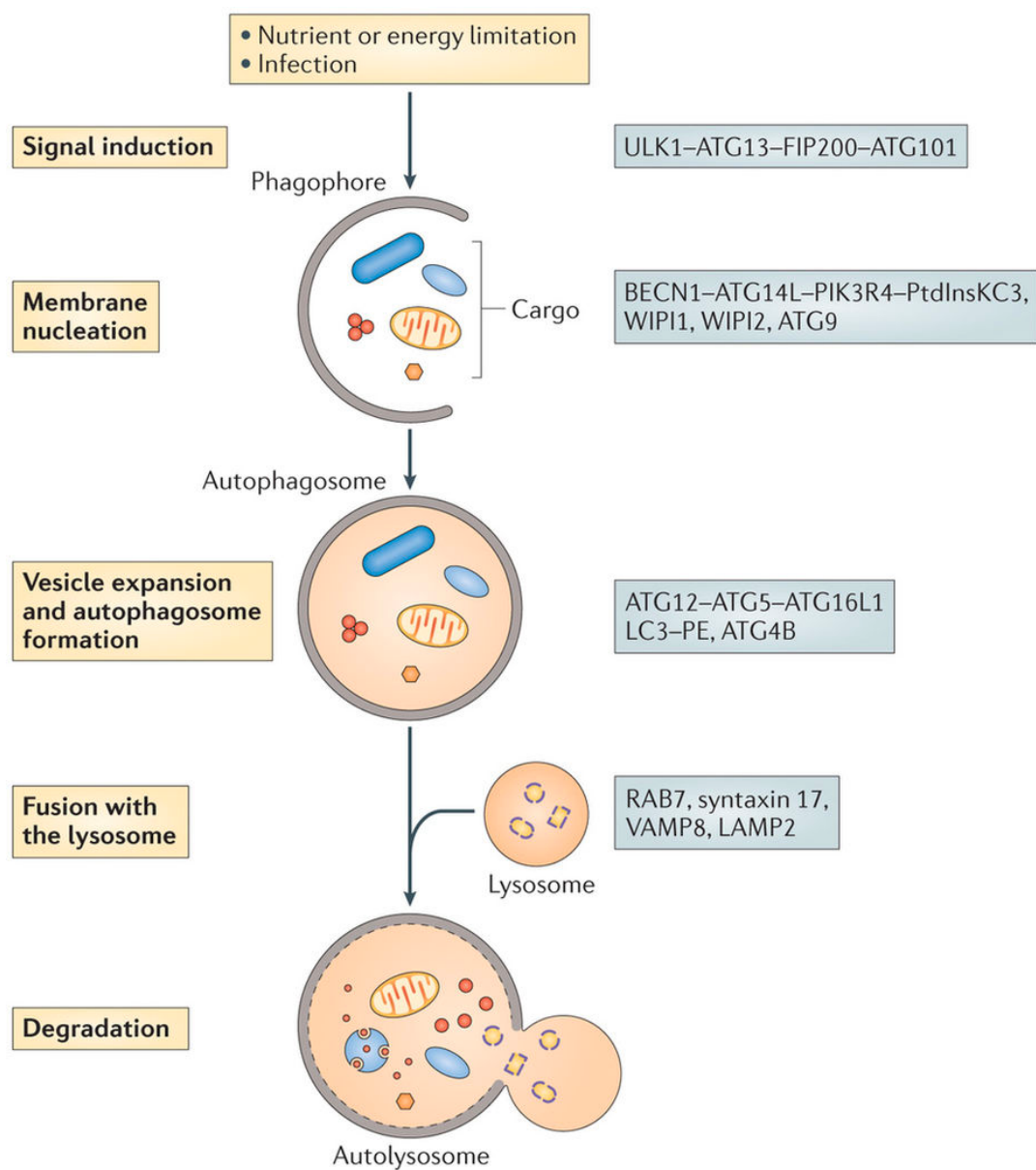
Nature Reviews | Microbiology

Figure 15: Overview of the stages and key regulators of macroautophagy. Used with permission (65)

1.8 Objective and specific aims

While limited studies have been conducted on NHE3, the role of DRA in any model of CDI remains entirely uninvestigated. Therefore, the objective of this thesis was to elucidate the role of DRA in *C. difficile* infection in a range of model systems including various intestinal epithelial cell lines, a toxigenic mouse model, and human CDI patients. To do this, the following specific aims were pursued:

1. Investigate the effects of *C. difficile* toxins on intestinal epithelial Cl^-/HCO_3^- exchanger DRA *in vitro*

2. Determine the mechanism(s) underlying DRA protein downregulation *in vitro*

3. Explore the effects of *C. difficile* toxins on DRA expression *in vivo* and in human CDI

2. Materials and Methods

2.1 Purified *C. difficile* toxins

C. difficile toxins were purchased from List Biological Laboratories (Campbell, CA). Toxin A (#152C) was dissolved in molecular-grade water and stored at 4°C at a concentration of 100 µg/ml. Toxin B (#155L) was stored at 4°C at a concentration of 200 µg/ml. Binary toxin CDTa (#158A) and CDTb (#157A) were dissolved in molecular-grade water and both stored at concentrations of 40 ng/µl at -20°C. TcdA and TcdB glucosyltransferase mutants, TcdA DXD and TcdB DXD, (TcdA D285/287N, TcdB D286/288N) were kindly provided by Dr. Borden Lacy (Vanderbilt University). These toxins were created via double point mutations in the glucosyltransferase regions of TcdA and TcdB (24, 25). These toxins, hereafter called TcdA DXD and TcdB DXD, lack a functional glucosyltransferase domain and cannot glucosylate Rho family GTPases. All other functional domains in the DXD mutants remained intact. WT toxins A and B from the VPI 10463 background used to make the DXD mutants were also provided by the Lacy lab. All four toxins (WT TcdA Lacy, WT TcdB Lacy, TcdA DXD, and TcdB DXD) were aliquoted and stored at -20°C.

2.2 Cell culture

Caco-2 and T-84 cells were purchased from the American Type Culture Collection (ATCC, Manassas, VA) and grown in T-75 plastic flasks at 37°C and 5% CO_2 -95% air environment. T84 and Caco-2 cells were grown in DMEM and EMEM, respectively (ATCC) supplemented with 10% fetal bovine serum (FBS), 100 units/ml penicillin, 100 µg/ml streptomycin, and 2 mg/liter gentamicin. Caco2 cells were plated on 24-well plates (Costar, Corning, NY) at a density of 2 X 10^4 cells/well. Cells were only used between

passage 25 and 40. Fully differentiated Caco-2 monolayers (10-14 days post-plating) were treated with purified *C. difficile* toxin A, toxin B, and/or CDT binary toxin (CDTa and CDTb) for 6-24h at various concentrations in 1% FBS in EMEM. T84 cells were plated on 24-well plates (Costar, Corning, NY) at a density of 2 X 10^4 cells/well. T84 plates were grown for 5-6 days post plating prior to administration of toxins. Media was changed every 2 days for the duration of Caco2 and T84 growth. The night before toxin treatment, Caco2 and T84 plates were serum-starved. All treatments were done in 1% FBS EMEM for Caco2 cells and 1% FBS DMEM for T84 cells.

2.3   RNA extraction and quantitative real-time PCR (qRT-PCR)

To quantitate mRNA of intestinal ion transporters and cytokines, total RNA from Caco-2 cells and mice colonic mucosa was extracted using RNeasy kit (Qiagen, Hilden, Germany) according to the manufacturer's instructions. The quantity and quality of total extracted RNA was verified using a Nanodrop spectrophotometer. Extracted Caco2 RNA was amplified with Brilliant SYBR Green qRT-PCR Master Mix kit (Agilent Technologies, Santa Clara, CA) by using gene-specific primers listed in **Table 1**. Primers for amplification of mouse mRNA are shown in **Table 2**. The relative mRNA levels of cytokines and intestinal ion transporters were expressed as a percentage of control normalized to GAPDH as an internal control gene. Quantification of relative mRNA levels was calculated using the comparative Ct method ($2^{-\Delta\Delta Ct}$) briefly described below.

The comparative Ct method of qRT-PCR analysis uses an endogenous housekeeping gene (GAPDH, Actin, rRNA) to calculate relative changes in gene expression across treatment groups (132). These genes are commonly used as they are unlikely to change

during treatments. The Ct, or threshold cycle, is the cycle at which the fluorescence reaches a specific threshold value and is registered in the PCR system. This value is indicative of the amount of mRNA present for each specific gene. For example, a Ct value of 29 indicates that the target gene needed 29 cycles of amplification to reach the threshold value set by the machine. To compare, a Ct value of 26 indicates a higher level of target gene expression because the threshold value was reached by the 26th cycle versus the 29th. The normalized Ct value for each sample was calculated using the equation:

ΔCt (normalized target gene expression) = Ct (target gene) - Ct (GAPDH)

The relative gene expression $2^{-\Delta\Delta Ct}$ was then calculated after calculating ΔΔCt and expressed as arbitrary units:

ΔΔCt = ΔCt (normalized target gene expression) - ΔCt (untreated control)

TABLE I: HUMAN PRIMER SEQUENCES USED IN QRT-PCR

Gene	Sequence (5' → 3')
Human DRA	F- TTCAGTTGCCAGCGTCTATTC R- GTGTTTTGCCTCCTGTGCTCT
Human GAPDH	F- GAAATCCCATCACCATCTT R- AAATGAGCCCCAGCCTTCT
Human NHE3	F- TGGCAGAGACTGGGATGATAA R- CGCTGACGGATTTGATAGAGA
Human CFTR	F- GCAGGAAGATGTATGVTTTGA R- CTTTACAACAGCTAGGTCCTG
Human PAT1	F- AGATGCCCCACTACTCTGTCCT R- ATCCACACCACACCTCTGCTT
Human MCT1	F- TCTGTGTCTATGCGGGATTCTT R- TTGAGCCGACCTAAAAGTGGT
Human IL-8	F- TGGCAGTTTTCCTGCTTTCT R- CAGTGGGGTCCACTCTCAAT
Human MDR1	F- GGCAAAGAAATAAAGCGACTGAA R- GGCTGTTGTCTCCATAGGCAAT
Human SERT	F- CAGCGTGTGAAGATGGAGAAG R- TGGGATAGAGTGCCGTGTGT
Human NHE2	F- ACCTGTTCGTCAGCACCAC R- GCTCGCTCCTCTTCACCTT

TABLE II: MOUSE PRIMER SEQUENCES USED IN QRT-PCR

Gene	Sequence (5' → 3')
Mouse DRA	F- TGGTGGGAGTTGTCGTTACA R- CCCAGGAGCAACTGAATGAT
Mouse GAPDH	F-TGTGTCCGTCGTGGATCTGA R-CCTGCTTCACCACCTTCTTGAT
Mouse IL-1β	F- GCAACTGTTCCTGAACTCAACT R- ATCTTTTGGGGTCCGTCAACT
Mouse CXCL1	F- AAAGATGCTAAAAGGTGTCCCCA R- AATTGTATAGTGTTGTCAGAAGCCA
Mouse NHE3	F- GGCCTTCATTCGCTCCCCAAG R- ATGCTTGTACTCCTGCCGAGG
Mouse CFTR	F- CTGGACCACACCAATTTTGAGG R- GCGTGGATAAGCTGGGGAT
Mouse PAT1	F- GAAATGGAGCTGCAGAGGA R- GCTGGAGCAGAAGAGAATGG
Mouse NHE2	F- GTGAAGACTGGGATTGAAGATG R- TCGGGAGGTTGAAGTAGAAGC
Mouse MCT1	F- TTFFACCCCAGAGGTTCTCC R- AGGCGGCCTAAAAGTGGTG
Mouse IL-10	F- GCTCTTACTGACTGGCATGAG R- CGCAGCTCTAGGAGCATGTG
Mouse COX2	F- TGACGAACTATTCCAAACCAGC R- GCACGTAGTCTTCGATCACTATC
Mouse IL-6	F- TAGTCCTTCCTACCCCAATTTCC R- TTGGTCCTTAGCCACTCCTTC

2.4   <u>Protein lysates and Western blotting</u>

Tissue lysates were prepared from mucosal scrapings of the colon and total protein was extracted using RIPA lysis buffer (Cell Signaling, Danvers, MA) supplemented with protease inhibitor cocktail (Roche, Indianapolis, IN). Mucosal scrapings were homogenized using a bullet blender and subsequent sonication (two pulses, 30s each). Lysates were then centrifuged at 13000 rpm for 10 min at 4℃ to remove cell debris. Caco-2 cells were treated with purified TcdA, TcdB, or CDT for various times (6h, 24h). Control cells were treated with equal amounts of vehicle (molecular grade water). After treatment, control and toxin-treated cells were washed with 1X PBS to remove residual media and lysed in 1X Cell Lysis Buffer (Cell Signaling, Danvers, MA) and 1X Protease Cocktail Inhibitor (Roche). Cells were further lysed by sonication (two pulses for 30s each) and the lysates were centrifuged at 13000 rpm for 10 min at 4℃ to remove cell debris. The supernatant of each lysate was collected and the total protein concentration was determined by the Bradford method and stored at -80°C until use. Equal amounts (40-60 µg /sample) of whole cell lysates were solubilized in SDS-gel loading buffer and boiled for 8 minutes. Proteins were loaded on ready-made 7.5% SDS-polyacrylamide gels (Bio-Rad, Hercules, CA) and transblotted to nitrocellulose or PVDF membranes. After transfer, membranes were incubated in blocking buffer for 1h (1X PBS and 5% nonfat dry milk or 1X TBS and 3% bovine serum albumin (BSA)) at room temperature with gentle agitation. The membranes were then probed with affinity purified anti-DRA antibody (1:100 dilution), anti-actin antibody (Invitrogen, AC-15) anti-GAPDH antibody (Sigma Aldrich, #G8795, 1:30000), anti-Rac1 antibody (BD Biosciences, San Jose, CA; m102ab, 1:500), anti-Total Rac1 (EMD Millipore, Burlington, MA; #23A8, 1:20000), anti-MCT-1

(Santa Cruz Biotechnology, Dallas, TX; H70, 1:200), anti-Atg16L1 (Cell Signaling, #8089S, 1:10000), anti-LC3B/A (Cell Signaling, #12741, 1:1000), anti-Beclin (Cell Signaling, #3495, 1:1000) anti-NHE3 (1:6000), and anti-PAT-1 (1:8000) in 2.5% nonfat dry milk (1X PBS) or 1% BSA in 0.1% TBS-Tween-20 overnight at 4°C with gentle agitation. The antibodies for NHE3 and PAT-1 antibodies were graciously provided by Dr. Chris Yun (Emory University) and Dr. Peter Aronson (Yale University), respectively. The membranes were washed four times with wash buffer (1X PBS + 0.1% Tween-20) for 5 min each. Membranes were then probed with HRP-conjugated goat anti-rabbit and anti-mouse antibodies (Santa Cruz, 1:2000) in 2.5% nonfat dry milk (1X PBS) or 1% BSA (0.1% TBS-Tween 20) for 1h at room temperature with gentle agitation. Membranes were then washed (4 x 5 min each) and visualized using Enhanced chemiluminescence detection (Bio-Rad).

2.5   Authentication of reagents

The DRA antibody was raised against the C-terminal amino acid sequence INTNGGLRNRVYEPVETKF of DRA (accession number: BC025671) as previously described (84). The DRA antibody was validated using DRA knockout mice (157) and HEK 293 cells (ATCC 1573), which do not express endogenous DRA (87). The NHE3 antibody was validated using Western blots of mouse ileal (high levels of NHE3) and distal (low levels of NHE3) colonic mucosa. The PAT-1 antibody was validated using immunofluorescent staining of mouse ileum (high PAT-1) and distal colon (low PAT-1). Glucosyltransferase mutants, TcdA DXD and TcdB DXD, were validated by Western blotting to compare Rac1-glucosylated levels in control, wild type toxin and DXD toxin

treated cells. This experiment utilizes a Rac1 antibody (m102ab, BD Biosciences) that only binds to Rac1 that has not been glucosylated at Thr35. Rac1-glucosylated levels were normalized to total Rac1 levels (glucosylated and non-glucosylated) using a separate Rac1 antibody (EMD Millipore #23A8). Use of this antibody allowed for visualization of the direct effects of wild type and DXD mutant toxins on Rac1. These experiments showed that Rac1-glucosylation in cells treated with TcdA and TcdB DXD toxins was not statistically different than untreated cells. This verified that the DXD mutants were true glucosyltransferase mutants not capable of inactivating Rac1 via glucosylation.

2.6 *In vivo* studies

All mice used in our studies were female C57BL/6 between 10-14 weeks of age (Jackson Laboratory, Bar Harbor, ME). All animal studies were conducted at the Jesse Brown Veterans Affairs Medical Center (JBVAMC) under the approval of the University of Illinois at Chicago Animal Care Committee (ACC) and the JBVAMC IACUC animal care committee. The instillation of toxins A and B was performed as described previously (62, 63) with minor modifications. As shown below **Figure 16**, purified TcdA and TcdB were intrarectally administered at 10 µg/mouse in 100 µl PBS. For the co-administration of TcdA and TcdB together, mice were given 5 µg of each toxin, for a total toxin dose of 10 µg. After dilution of toxins in PBS, intrarectal administration was conducted as described previously (63). Briefly, a tube was lubricated with water soluble personal lubricant and intrarectally inserted 3.5 cm. 100 µl of solution was slowly administered while pressure was applied to the anal area to prevent leakage. The tube was then slowly removed and pressure was applied to the anal area for an additional 30 seconds. Mice were euthanized

at 4h post-instillation and colonic tissues were harvested, snap frozen in liquid nitrogen, and stored at -80 °C. The assays listed in **Figure 16** will be described in further detail in later sections.
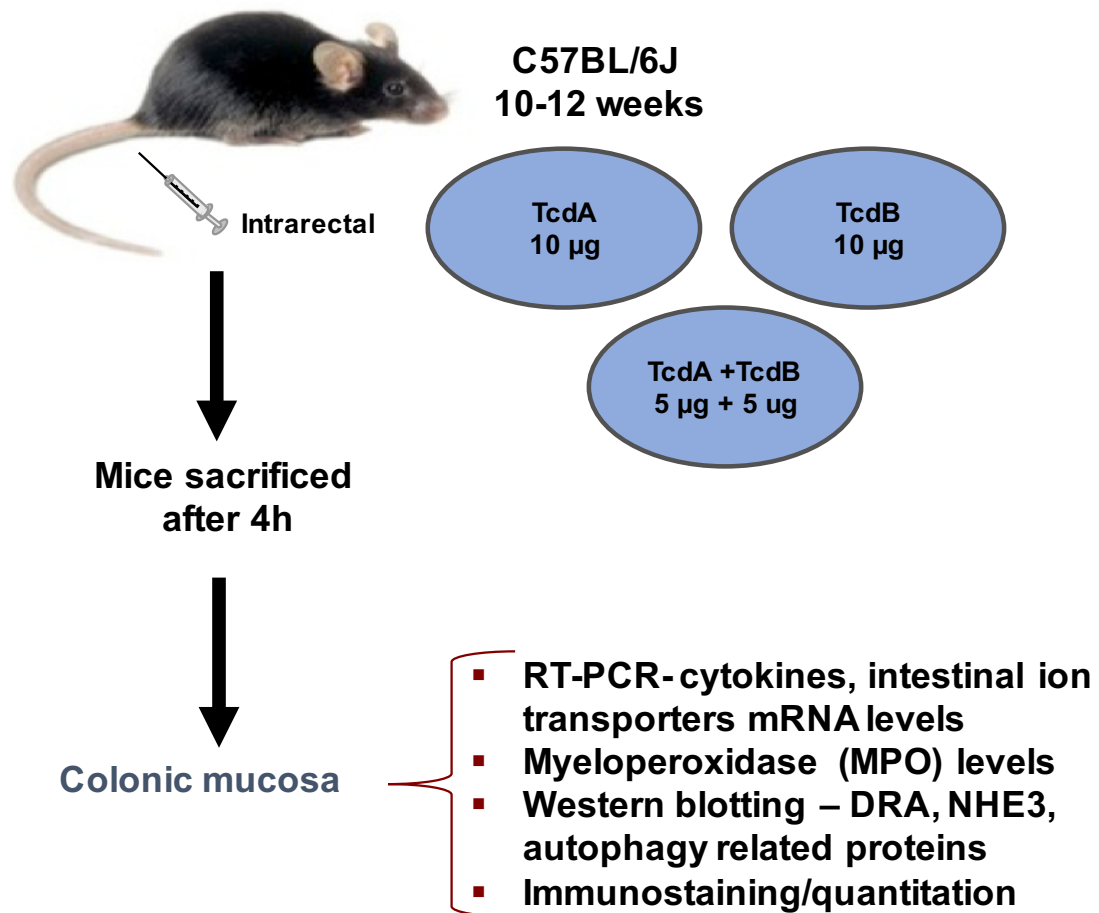
Figure 16: Schematic overview of intrarectal toxigenic mouse model of CDI.

2.7   CDI Patient biopsies

Human patient biopsy sections were kindly provided as slides by Dr. Melinda Engevik of the Versalovic Lab at Baylor University. The patient biopsies were originally given to Dr. Engevik by Drs. Mary Beth and Bruce Yacyshyn (University of Cincinnati). All patients and healthy volunteers provided informed consent consistent with IRB approval at the University of Cincinnati. Volunteers were considered healthy when they presented without previous or current GI symptoms, history of chronic disease or cancer. Colon biopsies were collected, fixed in neutral buffered formalin and paraffin-embedded. Paraffin sections were obtained from de-identified patients with current CDI diagnosis (*C. difficile*-positive ELISA or LAMP toxin test) and no other known morbidity/disorder as previously described (42). CDI positive patients did not have history of Inflammatory Bowel Disease (IBD), colostomy, cancer, small bowel obstruction, or diverticulosis. De-identified patient samples were sectioned, placed on glass slides, and sent to the Dudeja Lab at the University of Illinois at Chicago under Dr. Dudeja's exempt IRB protocol.

2.8   Immunofluorescent staining

Mouse distal colon samples were embedded in Optimal Cutting Temperature compound (OCT) and 5 µm thick sections were applied to glass slides. Sections were fixed with 4% paraformaldehyde in PBS (pH 8.5) for 15 mins at room temperature and permeabilized using Nonidet P-40 in PBS for 5 min. Sections were then placed in blocking solution (2.5-5% normal goat serum) for 2h at room temperature. Sections were then incubated with anti-DRA and anti-villin (Abcam, Cambridge, MA) antibodies in 1% NGS (normal goat serum) for 1h at room temperature. After washing with 1% NGS, sections

were incubated with secondary antibodies Alexa fluor 488 goat anti-rabbit IgG (Invitrogen, Carlsbad, CA) and Alexa Fluor 568 goat anti-mouse IgG (Invitrogen) for 1h then mounted with Slowfade Gold antifade with DAPI (Invitrogen) under coverslips. All sections were imaged on a Carl Zeiss LSM 510 laser-scanning confocal microscope using a 20x objective.

2.9   Histological assessment of inflammation

To assess the severity of TcdA/B induced colitis, formalin fixed paraffin embedded distal colonic tissues were sectioned at room temperature and applied to glass slides in 5 µm thick sections using a microtome. The sections were stained using H&E staining as described previously (63, 114) using a commercially available H&E staining kit (ScyTek Laboratories, Logan, UT) and described below. The stained slides were then mounted with Permount (Fisher Scientific, Waltham, MA) and scored in a blinded manner by a board-certified pathologist. The inflammatory score was assigned based on the following criteria: epithelial cell damage, submucosal edema, neutrophilic infiltration, lymphoid aggregates, submucosal inflammation, necrotic cellular material in lumen, crypt destruction, epithelial apoptosis, and luminal debris/artifact. The scoring system used in each of these subsections was 0 (normal), 1 (mild disease), 2 (moderate disease), 3 (severe disease). Scores were reported on this 0-3 number scale for each category resulting in a total possible score of 30.

2.10   Hematoxylin and Eosin (H&E) staining

Paraffin embedded mouse colonic sections were placed on a warming plate set (60°C) for 10-15 minutes to deparaffinize the sections. Slides were placed in a glass slide holder and submerged in xylene (Fisher Scientific, #X5SK4) two times for 20 minutes each. The slides were then submerged in 100% ethanol, 95% ethanol, and 70% ethanol for 5 minutes each. Slides were then submerged in deionized H_2O (dH_2O) twice for 5 min each before being placed in hematoxylin reagent (ScyTek Laboratories) for 1 min. After hematoxylin staining, slides were submerged twice in dH_2O for 5 mins each. Next, slides were quickly dipped 10-15 times (no more than 30 seconds total) in bluing reagent (ScyTek Laboratories) and subsequently submerged two more times in dH_2O for 5 min each time. After washes, slides were submerged in eosin reagent (ScyTek Laboratories) for 1-2 minutes and then washed twice in dH_2O for 5 mins each. Finally, the slides were submerged in increasing concentrations of ethanol (70%→95%→100%) for 5 mins each. Finally, slides were placed in xylenes for 5 minutes, dried very briefly, and mounted with one drop of Permount and a glass coverslip. Slides were left to dry overnight in the fume hood.

2.11   Myeloperoxidase (MPO) release assay

To assess colonic inflammation in our toxin-treated mice, we utilized myeloperoxidase (MPO) as a marker of colonic neutrophil infiltration and inflammation. The protocol for assessing myeloperoxidase was adapted as described previously (81) and described in detail below.

2.11.1 Preparation of stock reagents

Stock reagents for the myeloperoxidase release assay were prepared as follows: solution A (6.8 g KH_2PO_4 dissolved in 1 L of dH_2O), solution B (8.7 g of K_2HPO_4 dissolved in 1 L of dH_2O). A 50 mM solution of potassium phosphate buffer was made by adding solution B to solution A until a pH of 6.0 was reached. The remaining solutions (A and B) were stored at 4 °C until future use. Hexadecyltrimethylammonium bromide (HTAB) buffer was prepared by adding 5g of HTAB to 1L of 50 mM potassium phosphate buffer and gently heated to dissolve. KH_2PO_4, K_2HPO_4, and HTAB were all purchased from Sigma Aldrich with catalog numbers of 60353, 1151139, and H9151, respectively.

2.11.2 Sample preparation for MPO assay

Mouse distal colon samples were removed from -80°C and placed on ice. The weight of each sample was recorded to ensure that each sample was approximately the same size. Homogenizer beads were added to each sample and HTAB buffer was added according to the tissue weight (weight<25 mg, add HTAB at ratio of 12.5 mg/ml; weight between 25-50 mg, use ratio of 25mg/ml; weight> 50 mg, add buffer at ratio of 50 mg/ml). Tissues were then homogenized for 4 min at 30 Hz. The homegenizer beads were removed and the samples were centrifuged for 6 min (13500 x g, 4°C). Supernatants were collected and the remaining pellet was discarded.

2.11.3 MPO activity assay

Once the reagents were prepared, the o-dianisidine dihydrochloride (Sigma, D2679) solution was made by combining 16.7 mg of o-dianisidine dihydrochloride, 90 mL

of dH$_2$0, and 10 ml of potassium phosphate buffer. Next, we pipetted 7 µl of tissue homogenate (prepared in prior section) in triplicate into a clear polysterene 96 well plate. 50 µl of diluted H$_2$O$_2$ (4 µl 30% H$_2$O$_2$ + 90 µl dH$_2$0) was then added to the o-dianisidine mixture. Next, we added 200 µl of the o-dianisidine mixture (with H$_2$0$_2$) to each well of the 96 well plate. Absorbance was measured at 450 nm using a spectrophotometer taking three readings at 30 second intervals.

2.11.4 Calculation of MPO activity

MPO activity is measured in units (U) of MPO/mg of tissue. One unit of MPO is defined as the amount necessary to degrade 1 µmol of H$_2$0$_2$ per minute at room temperature. One unit of MPO yields a change in absorbance (ΔA) of 1.13 x 10^{-2} nm/min. Changes in absorbance at each time point, then, is calculated using the following equation:

$$[\Delta A(t2 – t1)] / (1.13 \times 10^{-2} \ nm/min) / (tissue \ weight \ in \ mg)$$

Total MPO activity (U/mg tissue) is the average of the above calculation at each time interval.

2.12   Lactate dehydrogenase (LDH) release assay

Lactate dehydrogenase (LDH) release assays were conducted for measurements of toxin-induced cell toxicity using a commercially available Cytotoxicity Detection Kit (Roche, Indianopolis, IN; #11 644 793 001) as described previously (59). Unopened contents of the kit were stored at -20°C until use and stored at 4°C thereafter. The protocol below was adapted from the Roche protocol with no modifications. Cell media

supernatants were collected after treatments and spun down at 300 x g for 10 mins to remove any cell debris. Supernatants were transferred to autoclaved 1.5 ml tubes and used immediately or stored at 4°C for no more than 7 days to diminish loss of LDH activity. Prior to starting, 250 μl of reconstituted lyophilisate (catalyst bottle #1) was added to 11.25 ml of thawed dye solution (bottle #2). This reaction mixture is light-sensitive therefore this step, and all subsequent steps, were conducted in darkened containers in a darkened room. Using a clear polysterene 96 well flat bottomed microplate (Corning, 07-200-706), 100 μl of treatment media (1% FBS supplemented EMEM) was pipetted into 3 consecutive wells. These wells served as the experimental background control (BC). These values were averaged and subtracted from all sample values, LC and HC averages prior to calculation. The next three wells contained 10 μl of control-treated cell supernatant + 90 μl of treatment media. These wells served as the low control (LC) for the experiment and were averaged prior to calculation. The next three wells contained 10 μl of treatment media from Caco2 cells treated with 2% Triton X-100 (Sigma, #X-100-100ml). These wells were averaged and comprised the high control (HC), a value that served as a positive control for cell lysis and cell cytotoxicity. This 1:10 dilution was optimized based on the absorbance limits of the spectrophotometer used. Next, the sample supernatants were pipetted in triplicate in the same 1:10 ratio used in the LC and HC wells (10 μl sample + 90 μl media). 100 μl of the reaction mixture (bottle #1 and #2) was then pipetted into each well, the plate covered in foil, and left at room temperature for 30 mins. After 30 mins, the absorbance was read at 492 nm and the values were added to the equation below.

$$Cytotoxicity\ (\%) = (exp\ value - LC)\ /\ (HC - LC)\ x\ 100$$

2.13   Statistical Analyses

All data were analyzed by Prism (Prism GraphPad Software). Results are expressed as means ± SE and represent the data from three to six independent experiments. Student's t-test or one-way ANOVA with Tukey's multiple comparison test was used for statistical analysis. $p < 0.05$ was considered statistically significant.

3. Experimental Results

3.1   Effects of purified *C. difficile* toxins TcdA and TcdB on DRA *in vitro*

3.1.1 Verification of *C. difficile* toxins TcdA and TcdB

To investigate the effects of *C. difficile* toxins on DRA, we utilized commercially available purified *C. difficile* toxins A and B (TcdA and TcdB). These toxins were purified from *C. difficile* strain VPI 10463, a highly toxigenic and commonly used strain in CDI research (19, 63, 146, 170). Our first experiments sought to validate the efficacy of these purified toxins (List Labs). Given that Rac1 is a well-known target of both *C. difficile* toxins (24, 147), we used non-glycosylated Rac1 levels as markers for toxin efficacy. Contrary to the antibody used to measure total Rac1 levels, the non-glycosylated Rac1 antibody is specific for Rac1 lacking a glucose moiety at Thr35 (103). The glycosylation of Rac1 at Thr35 is *C. difficile*-specific modification, therefore use of this non-glycosylated Rac1 antibody allowed for assessment of the specific loss of Rac1 functionality due to TcdA and TcdB. Both the non-glycosylated and total Rac1 bands are detected at 21 kDa thus membranes were first probed for Rac1-glycosylated and then probed for totalRac1 using the stripping procedure described in the Methods. To assess glycosylated Rac1 levels, low doses of TcdA (0.5-10 ng/ml) (71) or TcdB (0.1-5ng/ml) (45) were administered to the apical side of confluent Caco2 cells. After 24h, control and toxin-treated protein lysates were probed for non-glycosylated Rac1 levels using SDS-PAGE and immunoblotting. We found that both purified TcdA and TcdB significantly decreased active (non-glycosylated) Rac1 in Caco2 cells at 24h without changing total Rac1 levels **(Figure 17)**. These initial experiments verified that *C. difficile* toxins inactivated their molecular target, Rac1, in intestinal epithelial cells at the doses and time points used.
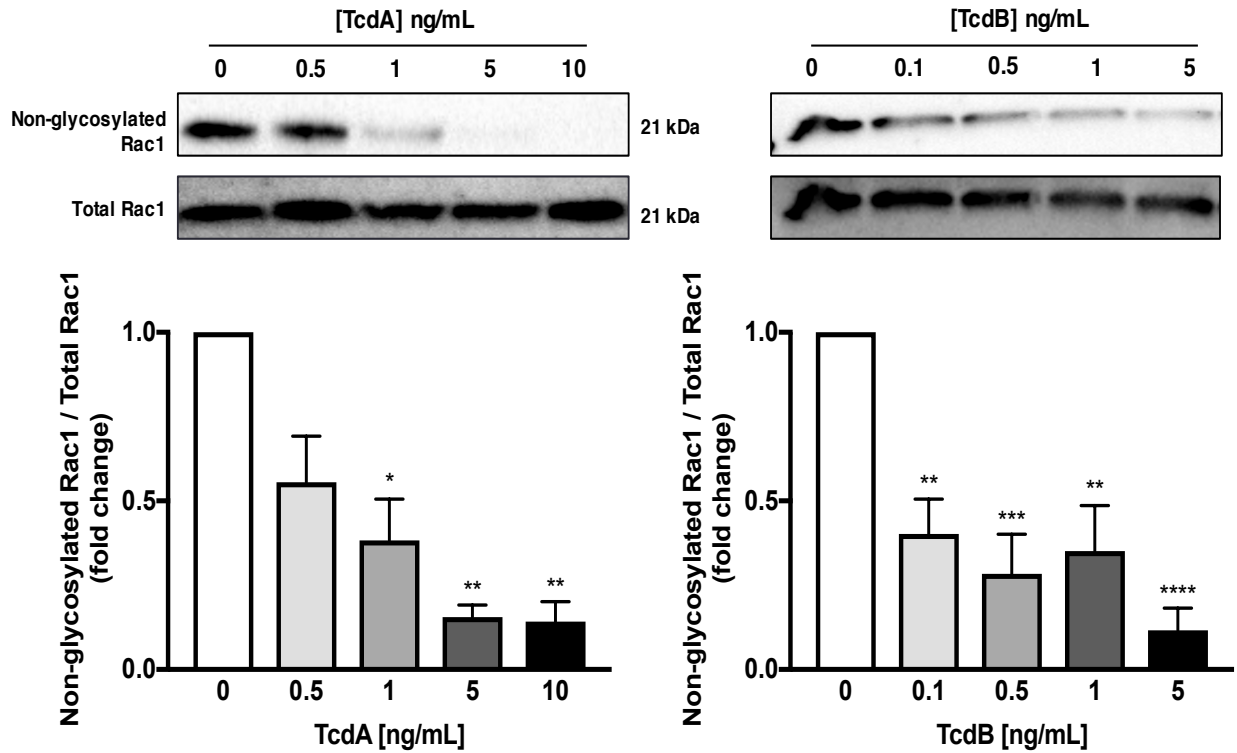
Figure 17: TcdA and TcdB glycosylated and inactivated Rac1 in Caco2 cells
Immunoblots of non-glycosylated Rac1 and total Rac1 levels after 24h treatment with low doses of TcdA (left) and TcdB (right). n=3, asterisks indicate differences between toxin-treated cells and control (*$p < 0.05$, **$p < 0.01$, ***$p < 0.001$, ****$p < 0.0001$).

3.1.2 *C.difficile* toxins A and B decrease DRA protein levels *in vitro*

Previous studies have reported that NHE3 expression is decreased after TcdB administration (57) and in patients with CDI (42). Given that the predominant route for electroneutral NaCl absorption involves the functional coupling of NHE3 to DRA, we next investigated the effect of purified *C. difficile* toxins on DRA protein expression in intestinal epithelial cells. Caco2 cells treated with low doses of TcdA had a significant reduction in DRA protein levels in a dose-dependent manner at both 6h and 24h **(Figure 18)**. Similarly, low doses of TcdB decreased DRA protein levels in a dose dependent manner at both 6h

and 24h **(Figure 19)**. Furthermore, these findings were not found to be cell line specific as these doses of TcdA and TcdB also decreased DRA protein expression in T84 cells, another intestinal epithelial cell line, as well **(Figure 20)**.
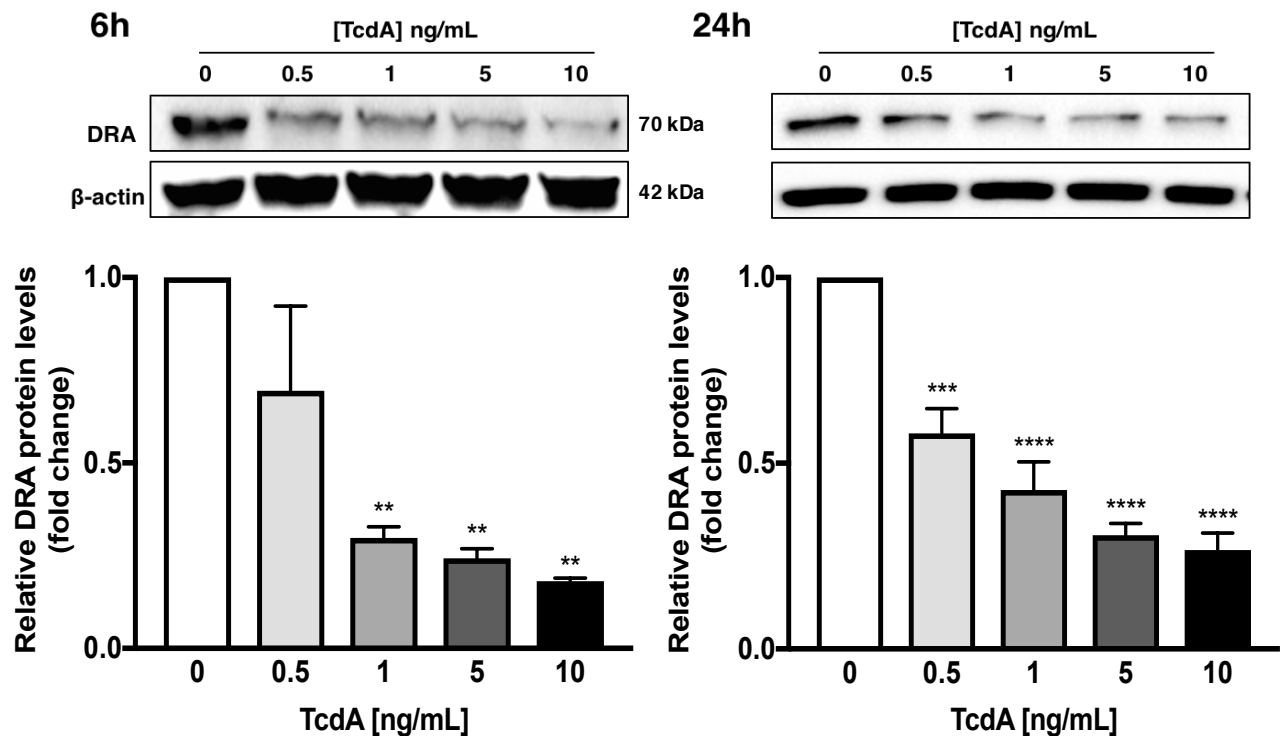
Figure 18: Purified TcdA decreased total DRA protein levels in Caco2 cells
Immunoblots of DRA levels at 6h (left) and 24h (right) post-treatment with 0.5-10 ng/ml of TcdA. DRA levels were quantified and normalized to ß-actin. n=3, asterisks indicate differences between toxin-treated cells and control ($**p < 0.01$, $***p < 0.001$, $****p < 0.0001$).
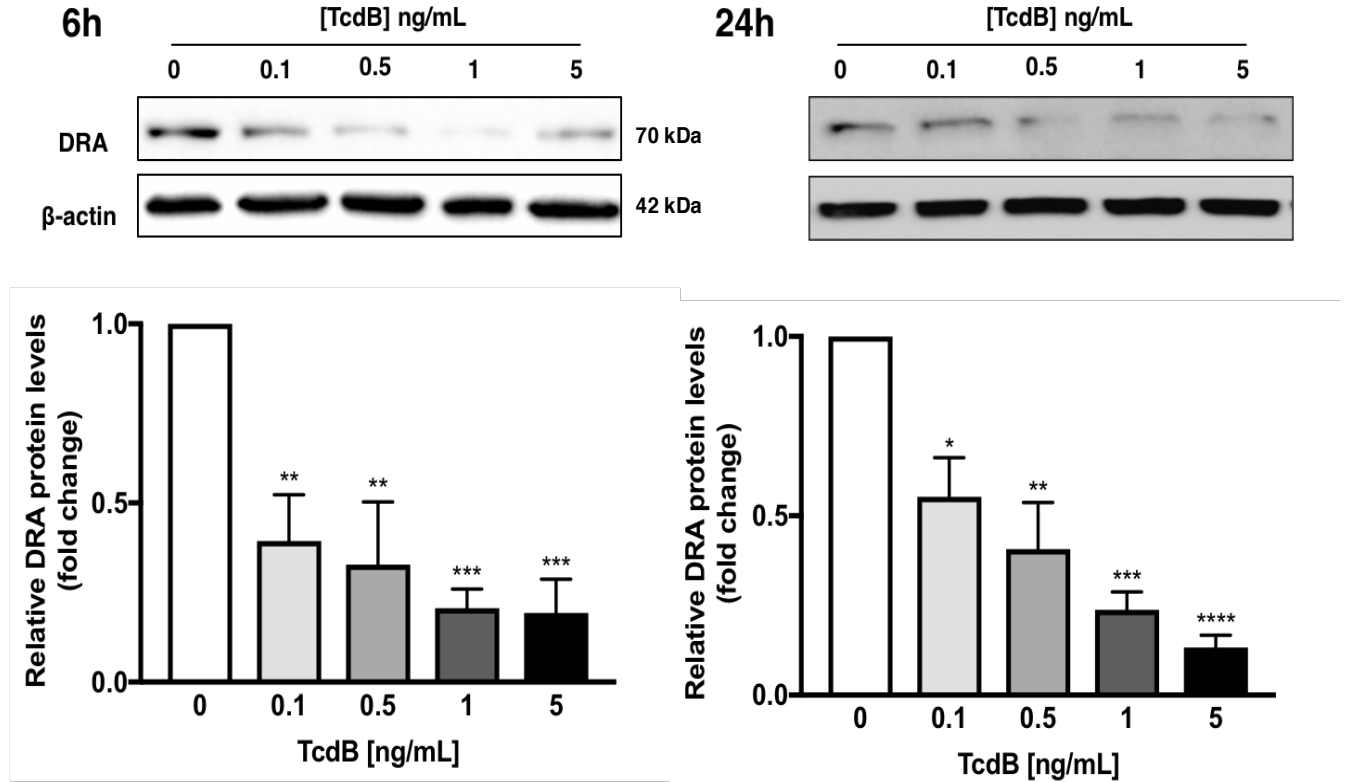
Figure 19: Purified TcdB decreased total DRA protein levels in Caco2 cells
Immunoblots of DRA levels at 6h (left) and 24h (right) post-treatment with 0.1-5 ng/ml of TcdB. DRA levels were quantified and normalized to ß-actin. n=3, asterisks indicate differences between toxin-treated cells and control (*p < 0.05, **p < 0.01, ***p < 0.001, ****p < 0.0001).
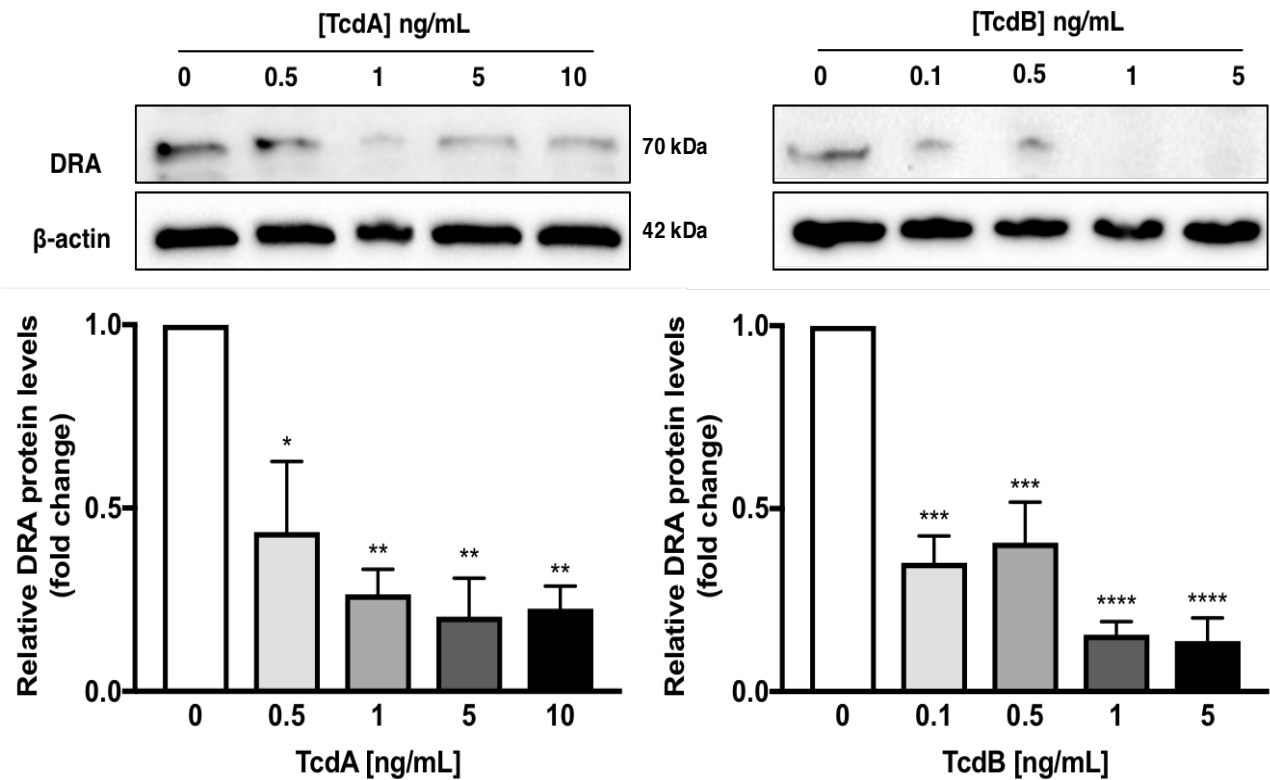
Figure 20: The toxin-mediated decrease in DRA protein is not cell line specific. Immunoblots of DRA levels at 24h post-treatment with TcdA *(left)* or TcdB *(right)* in confluent T84 cells (5-6 days post-plating). DRA levels were quantified and normalized to ß-actin. n=3, asterisks indicate differences between toxin-treated cells and control (*p < 0.05, **p < 0.01, ***p < 0.001, ****p < 0.0001).

3.1.3 Toxin-mediated decrease in DRA protein is not due to increased cell death

To identify whether this marked decrease in DRA protein levels was due to increased cell death, we performed cell viability assays using LDH (lactate dehydrogenase) release as a marker. LDH is found in almost all living cells and is significantly increased after tissue damage (14, 131). Low doses of TcdA did not induce significant LDH release from Caco2 cells at 6h or 24h **(Figure 21)** Similarly, Caco2 cells

treated with low doses of TcdB also did not release significantly more LDH at 6h or 24h

(Figure 21). These results demonstrated that the doses of TcdA and TcdB reduced DRA

protein levels without causing significant cell death.
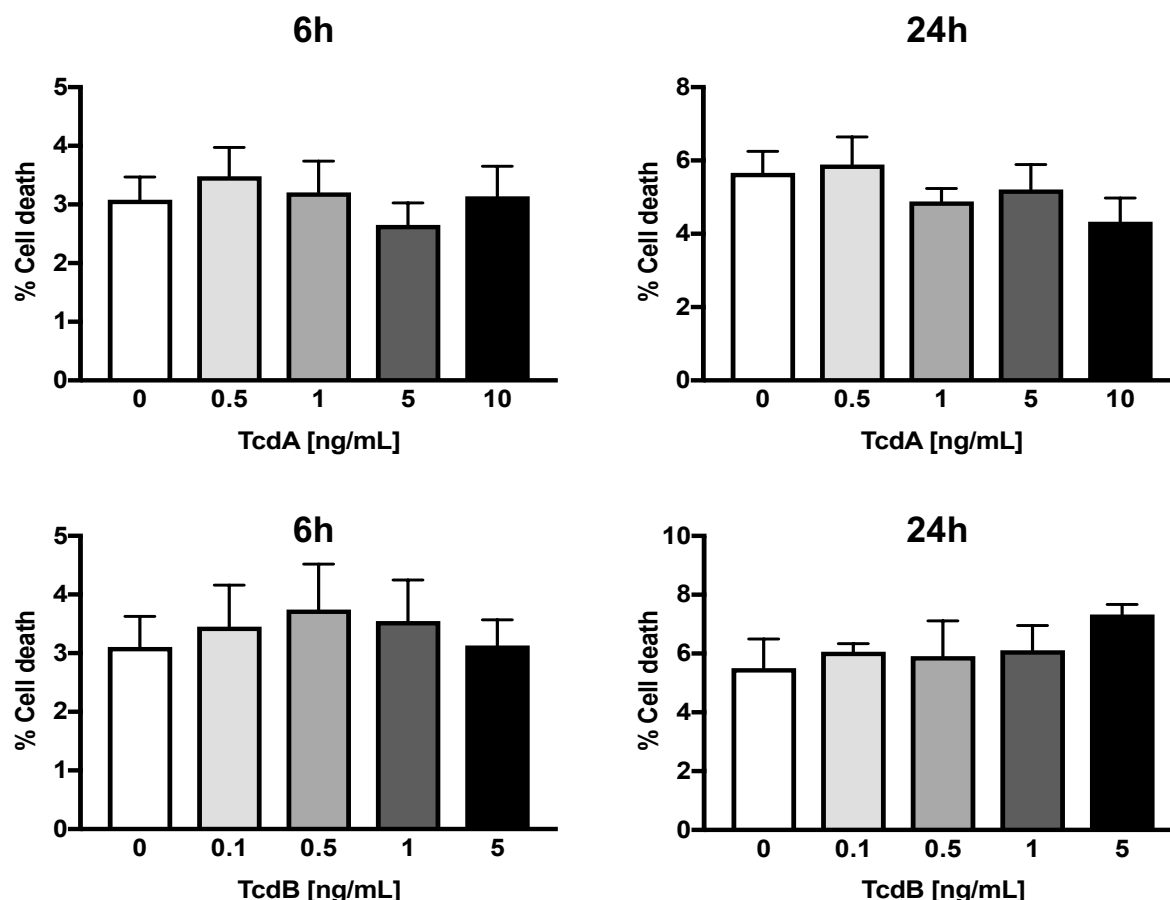
Figure 21: Decrease in DRA protein is not due to increased cell death. Confluent Caco-2 cells were treated with *(top)* purified TcdA (0.5-10 ng/ml) or (*bottom)* TcdB (0.1-5 ng/ml) for 6h and 24h. The treatment media were collected and analyzed for lactate dehydrogenase (LDH) release as described in the Methods. Samples were analyzed using an ELISA plate reader to measure absorbance at 492 nm. LDH levels were quantified and normalized to two controls: cell-free media (EMEM) and cells treated with 1% Triton-X 100 as a positive control (n=5). 0 indicates control (untreated) Caco-2 cells.

3.1.4 Toxin-mediated downregulation is specific to DRA *in vitro*

DRA is functionally coupled to NHE3 in the intestine to mediate NaCl and water absorption (50). Importantly, *C. difficile* toxins have been shown to affect the function and localization of NHE3 both *in vitro* and in patients with CDI (42, 45, 57). Given this, we next examined whether NHE3 was also decreased in response to our purified toxins. In contrast to DRA, we found that protein levels of NHE3 remained unchanged in the presence of varying doses of TcdA and TcdB at 24h **(Figure 22)**.
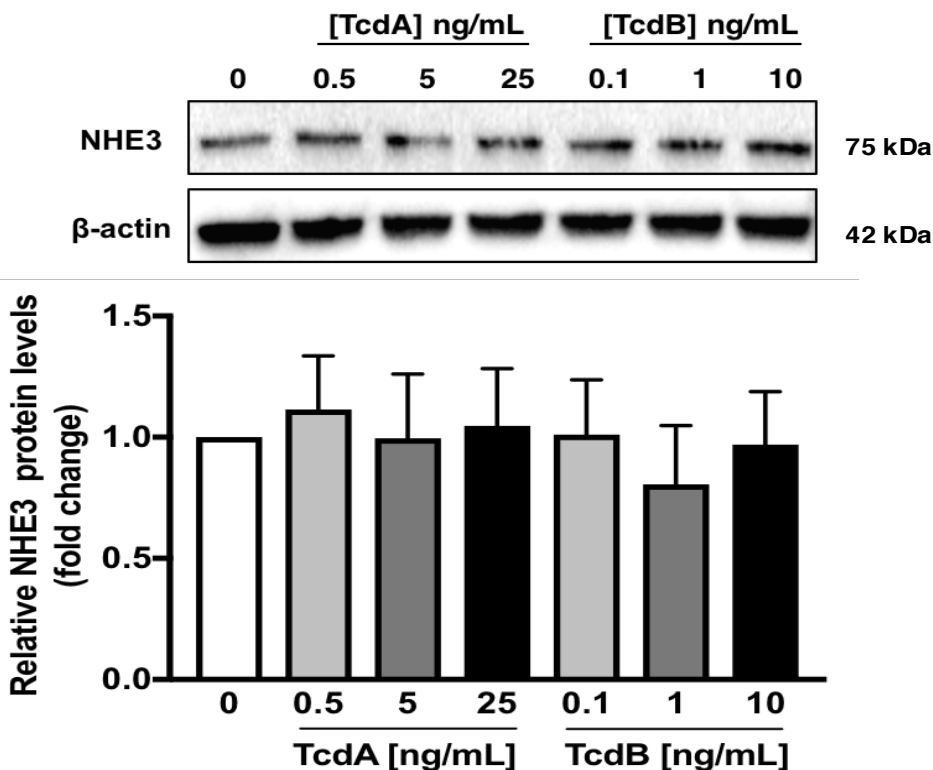
Figure 22: TcdA and TcdB did not alter NHE3 protein expression in Caco2 cells. Confluent Caco-2 cells (14 days post-plating) were treated with purified TcdA or TcdB for 24h. NHE3 levels were quantified and normalized to the housekeeping gene ß-actin (n=3).

Although DRA is the predominant Cl^-/HCO_3^- exchanger responsible for electroneutral NaCl absorption, another member of the SLC26 family, SLC26A6, is also an intestinal luminal Cl^-/HCO_3^- exchanger (40, 50, 69). SLC26A6 (PAT-1) is known to be important in chloride absorption, bicarbonate secretion, and oxalate transport (69, 159). Additionally, some studies have shown that PAT-1 is coupled to NHE3 in the small intestine to mediate electroneutral NaCl absorption (50). Given this, we next investigated whether PAT-1 protein levels were affected by *C. difficile* toxins. We observed that PAT-1 was unaffected by TcdA and TcdB administration at 24h **(Figure 23)**. This finding illustrated that the toxin-mediated decrease in DRA was specific to DRA and not due to an overall decrease in colonic Cl^-/HCO_3^- exchangers.
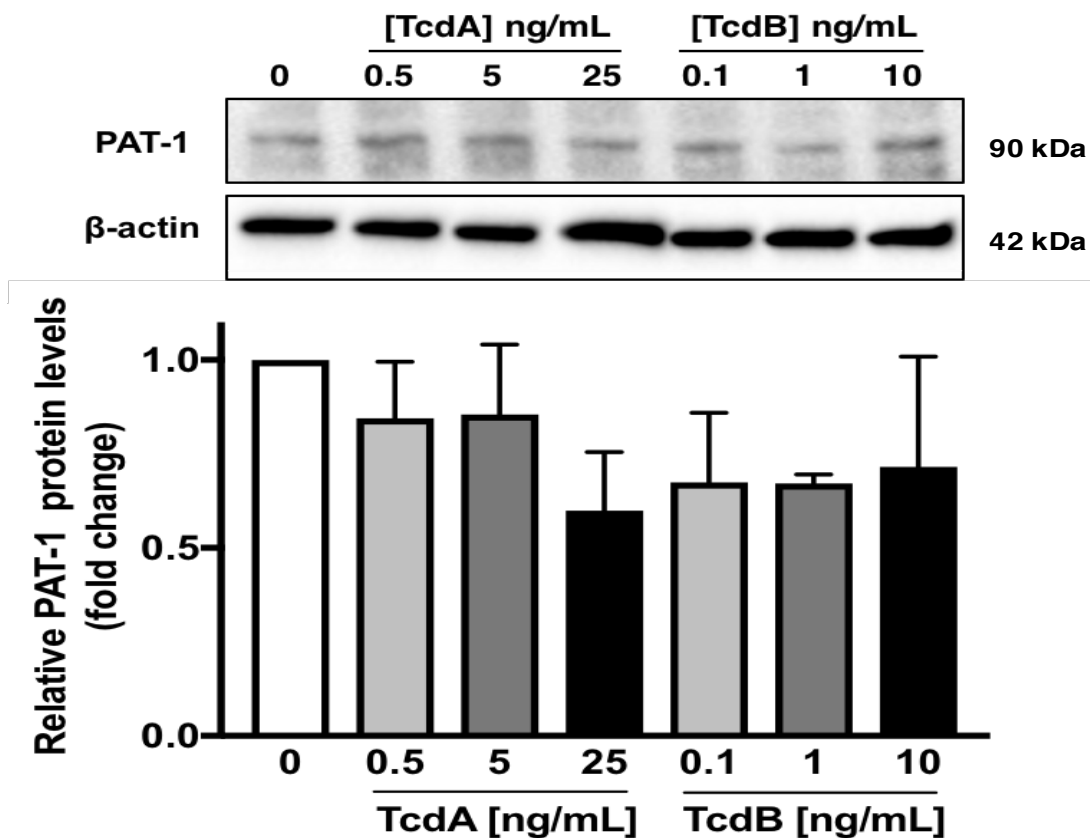
Figure 23: TcdA and TcdB did not alter PAT-1 protein expression in Caco2 cells.
Confluent Caco-2 cells (14 days post-plating) were treated with purified TcdA or TcdB for 24h. Immunoblots of PAT-1 levels were quantified and normalized to the housekeeping gene ß-actin (n=3).

3.1.5 SCFA transporter MCT-1 protein levels are decreased by TcdA

Electroneutral NaCl absorption, while mediated by DRA and NHE3, is also affected by various intestinal metabolites including short chain fatty acids (SCFAs) (82). Butyrate, a key intestinal SCFA, is known to provide nutrients for colonocyte differentiation and proliferation (82). Furthermore, reports have shown that SCFAs play a role in autophagy, immune responses, and barrier function (36, 82, 115). Intestinal epithelial SCFA transporter monocarboxylate transporter 1 (MCT-1) has been shown to play an important role in the H^+-coupled absorption of colonic butyrate (16, 82, 150). Modulation of MCT1 has also been implicated in intestinal inflammation, colon cancer, and enteric infections such as enteropathogenic *E. coli* (EPEC) infection (16, 53, 124, 155). The role, if any, of MCT-1 in CDI, however, had not been investigated. Given this, we next investigated whether MCT1 expression was affected in the presence of *C. difficile* toxins. Interestingly, we found MCT-1 protein levels were decreased only at the highest dose of TcdA (25 ng/ml) but unchanged in the presence of TcdB **(Figure 24)**. Importantly, the drastic decrease in DRA protein levels by TcdA was seen as early as 6h at doses greater than 0.5 ng/ml. Therefore, while TcdA may moderately affect colonic butyrate transport via MCT-1 protein levels, the rapid decrease in protein expression by both toxins was specific to DRA.
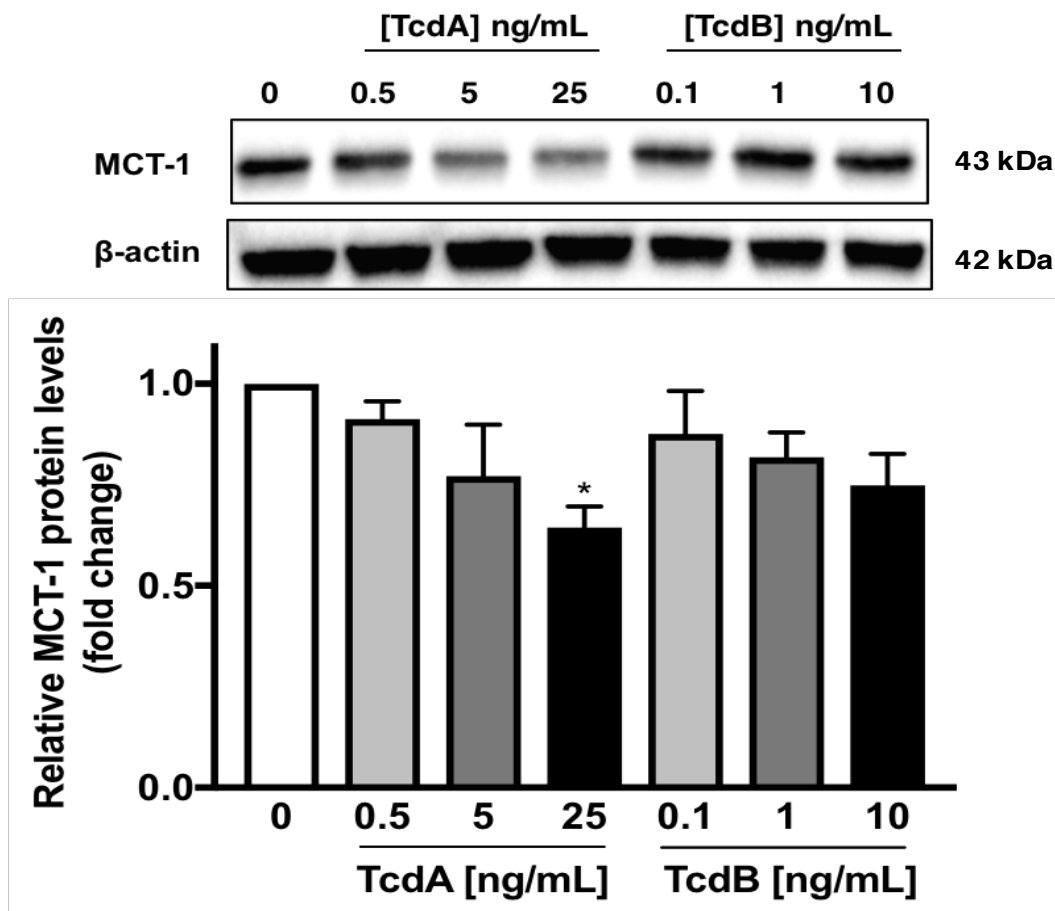
Figure 24: Only the highest dose of TcdA, but not TcdB, decreased MCT-1 protein expression in Caco-2 cells. Confluent Caco-2 cells (14 days post-plating) were treated with purified TcdA or TcdB for 24h. MCT-1 levels were quantified and normalized to the housekeeping gene ß-actin. n=5, asterisks indicate differences between toxin-treated cells and control (*p < 0.05)

3.1.6 Downregulation of DRA protein by *C. difficile* toxins occurs at the post-transcriptional level

Given that bacterial pathogens have been shown to down-regulate DRA at the transcriptional level (83, 129), we next examined how purified toxins would affect DRA mRNA levels. Contrary to DRA protein expression, we found no difference in DRA mRNA

levels in Caco-2 cells with either TcdA or TcdB **(Figure 25)**. This finding illustrated that the toxin-mediated effects on DRA protein levels were likely occurring at the post-transcriptional level.
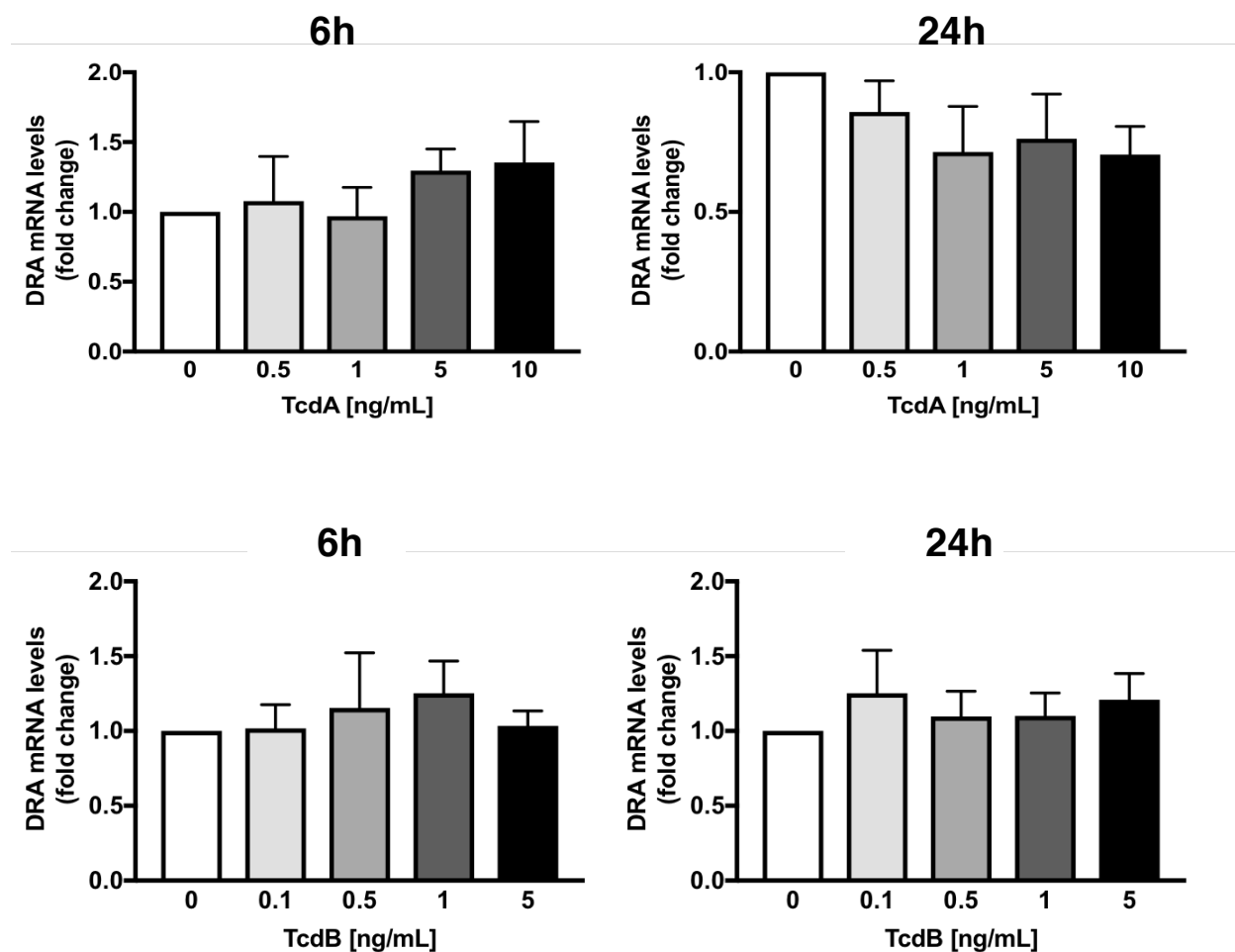
Figure 25: TcdA and TcdB had no effect on DRA mRNA in Caco2 cells. Confluent Caco-2 cells (14 days post-plating) were treated with (*top panel)* purified TcdA (0.5-10 ng/ml) or (*bottom panel)* TcdB (0.1-5 ng/ml) for 6h and 24h. The mRNA levels of DRA were analyzed by RT-PCR and normalized to GAPDH using the gene-specific primers in Table 1. Values are expressed as relative expression compared to untreated cells.

After identifying that DRA mRNA levels were unchanged, we next examined mRNA levels of other key intestinal ion transporters including CFTR, MDR1, NHE2, PAT1, and SERT. As mentioned earlier, CFTR is an intestinal epithelial chloride channel implicated in cystic fibrosis (18). Multi-drug resistance gene 1 (MDR1), or P-glycoprotein, is an apical intestinal transporter known to be important in the efflux of bacterial toxins and xenobiotics into the intestinal lumen (129). NHE2, a member of the NHE3-containing SLC9 family, is another Na^+/H^+ exchanger that mediates intestinal sodium absorption (7), and, like MCT-1, NHE2 function has been implicated in EPEC infection (60). Lastly, dysregulation of SERT, an intestinal serotonin transporter, is known to occur in inflammatory and infectious diarrhea (28, 142). Given the known roles of these ion transporters in diarrheal diseases, we conducted qRT-PCR experiments to evaluate mRNA levels after toxin administration. As shown in **Figures 26** and **27**, we saw no changes in mRNA levels of these transporters at 6h with TcdA or TcdB.
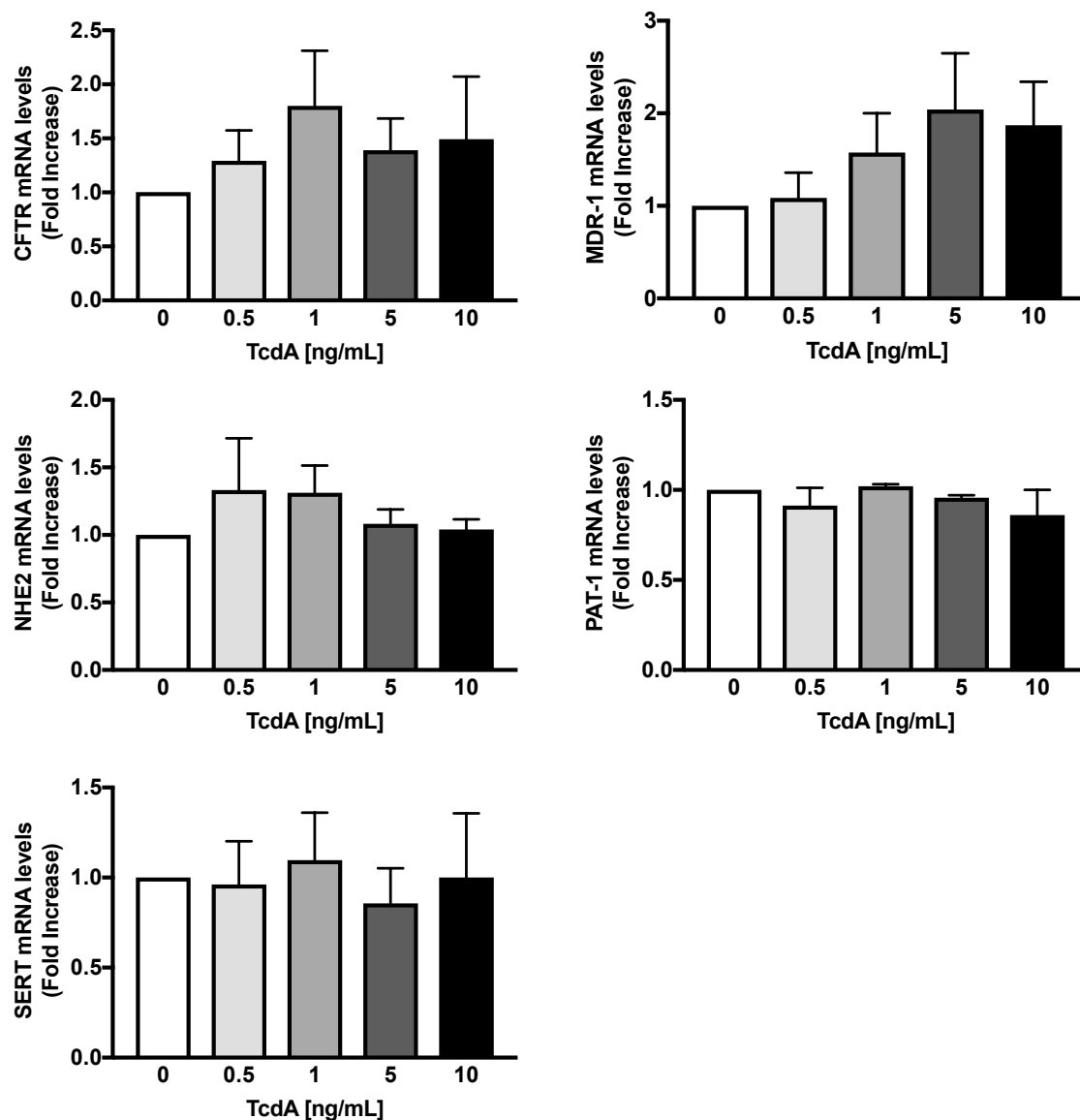
Figure 26: TcdA has no effect on mRNA levels of CFTR, MDR1, NHE2, PAT1, and SERT at 6h. Confluent Caco-2 cells (14 days post-plating) were treated with purified TcdA (0.5-10 ng/ml) for 6h.The mRNA levels of CFTR, MDR1, NHE2, PAT-1, and SERT were analyzed by RT-PCR and normalized to GAPDH using the gene-specific primers shown in Table 1. Values are expressed as relative expression compared to untreated cells.
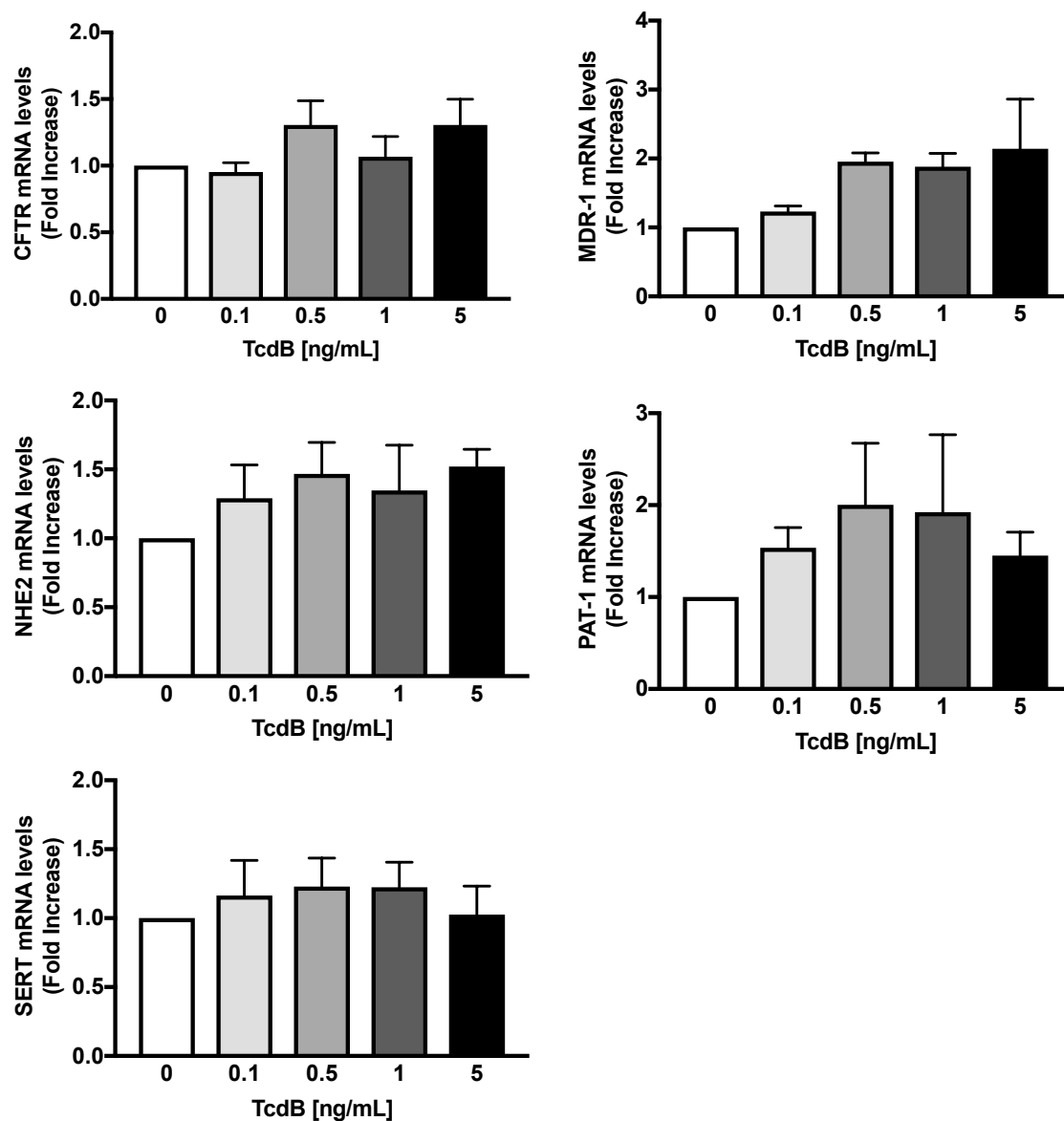
Figure 27: TcdB has no effect on mRNA levels of CFTR, MDR1, NHE2, PAT1, and SERT at 6h. Confluent Caco-2 cells (14 days post-plating) were treated with purified TcdA (0.1-5 ng/ml) for 6h. The mRNA levels of CFTR, MDR1, NHE2, PAT-1, and SERT were analyzed by RT-PCR and normalized to GAPDH using the gene-specific primers shown in Table 1. Values are expressed as relative expression compared to untreated cells.

Although there were no apparent changes in these mRNA levels at 6h, we did observe a significant increase in MDR1 mRNA after 24h treatment with 10 ng/ml of TcdA **(Figure 28)**. TcdB, on the other hand, did not induce changes in transporter mRNA levels even at 24h **(Figure 29)**.
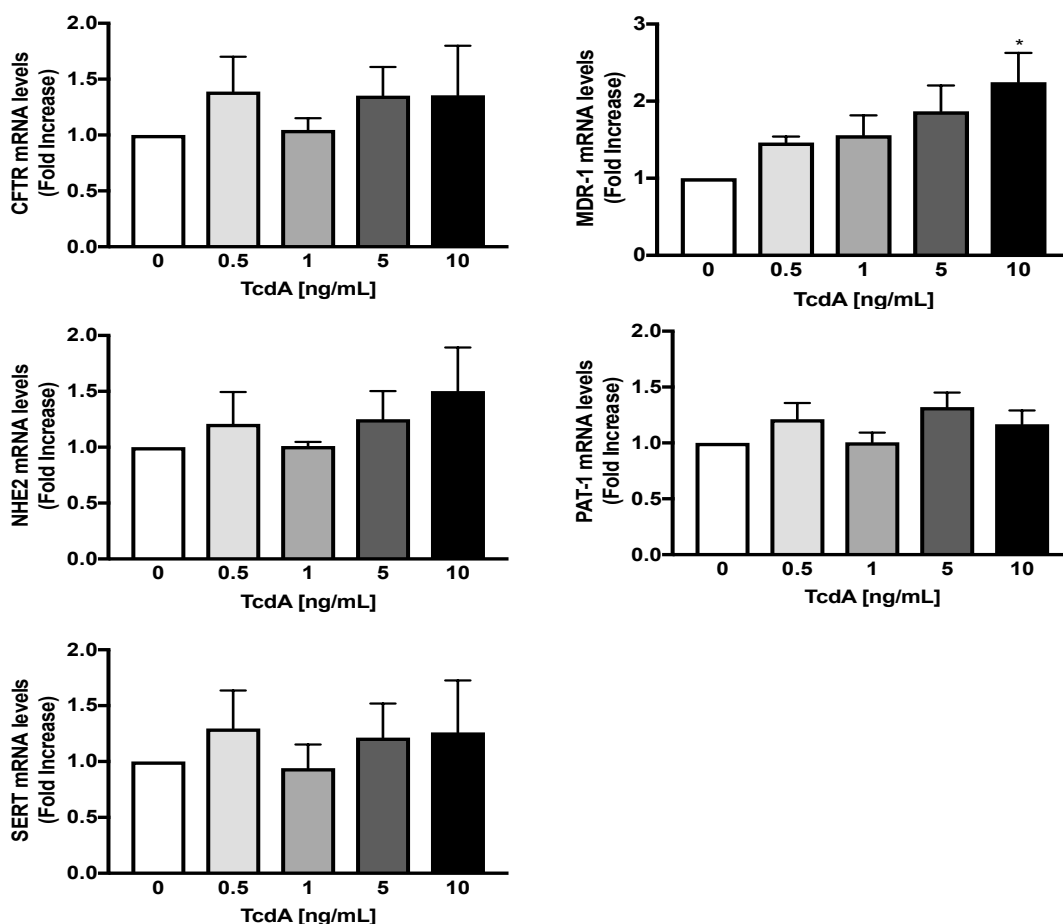
Figure 28: Only MDR1 mRNA levels are increased in the presence of TcdA at 24h. Confluent Caco-2 cells (14 days post-plating) were treated with purified TcdA (0.5-10 ng/ml) for 24h. The mRNA levels of CFTR, MDR1, NHE2, PAT-1, and SERT were analyzed by RT-PCR and normalized to GAPDH using the gene-specific primers in Table 1. Values are expressed as relative expression compared to untreated cells. n=5, (*$p < 0.05$)
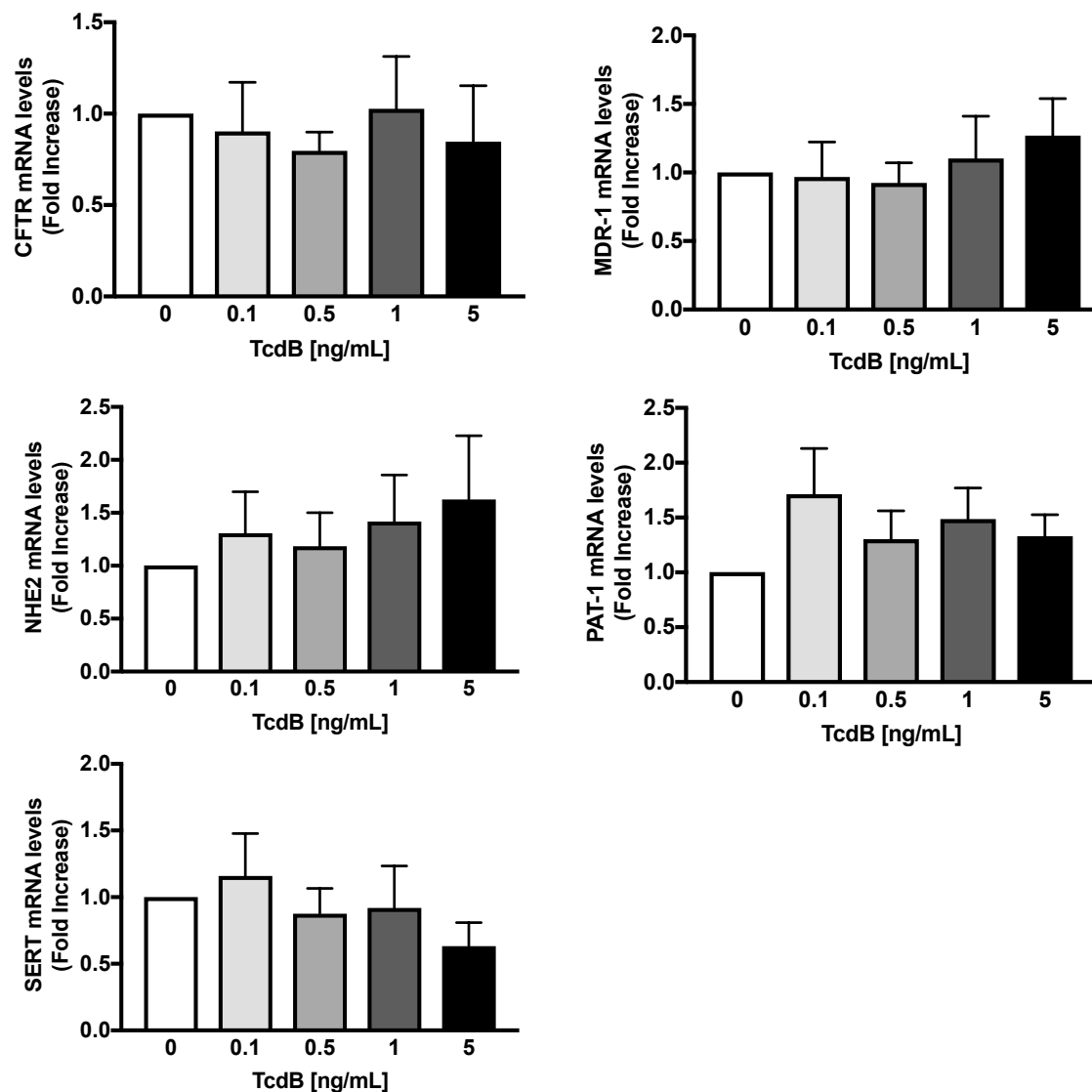
Figure 29: TcdB has no effect on mRNA levels of CFTR, MDR1, NHE2, PAT1, and SERT at 24h. Confluent Caco-2 cells (14 days post-plating) were treated with purified TcdB (0.1-5 ng/ml) for 6h. The mRNA levels of CFTR, MDR1, NHE2, PAT-1, and SERT were analyzed by RT-PCR and normalized to GAPDH using the gene-specific primers in Table 1. Values are expressed as relative expression compared to untreated cells.

3.1.7 Purified TcdB induced IL-8 release *in vitro*

In addition to the intestinal ion transporters, we also examined mRNA levels of interleukin 8 (IL-8) after TcdA and TcdB treatment. IL-8 is an inflammatory chemokine produced by various cell types including macrophages, epithelial cells and endothelial cells (5, 29). Importantly, IL-8 upregulation is frequently reported in cell culture *C. difficile* studies (14, 56). We found that TcdB, but not TcdA, significantly increased IL-8 mRNA levels in Caco2 cells at 24h **(Figure 30).** While prior studies have shown IL-8 production in intestinal epithelial cells after treatment with TcdA, only HT-29 and T84, not Caco2, cells exhibited a significant increase in IL-8 after 24h (99). These findings indicated that while both TcdA and TcdB inactivate Rho GTPases and, in our current findings, decrease expression of DRA protein levels, each toxin is capable of inducing different signaling pathways and immune responses as shown previously (71, 95, 147). Taken together, these results illustrated that the TcdA and TcdB-mediated downregulation of DRA protein likely occurred via a post-transcriptional mechanism. Furthermore, toxins A and B did not alter mRNA levels of other key intestinal ion transporters further indicating that the toxin-mediated effects are specific to DRA *in vitro.*
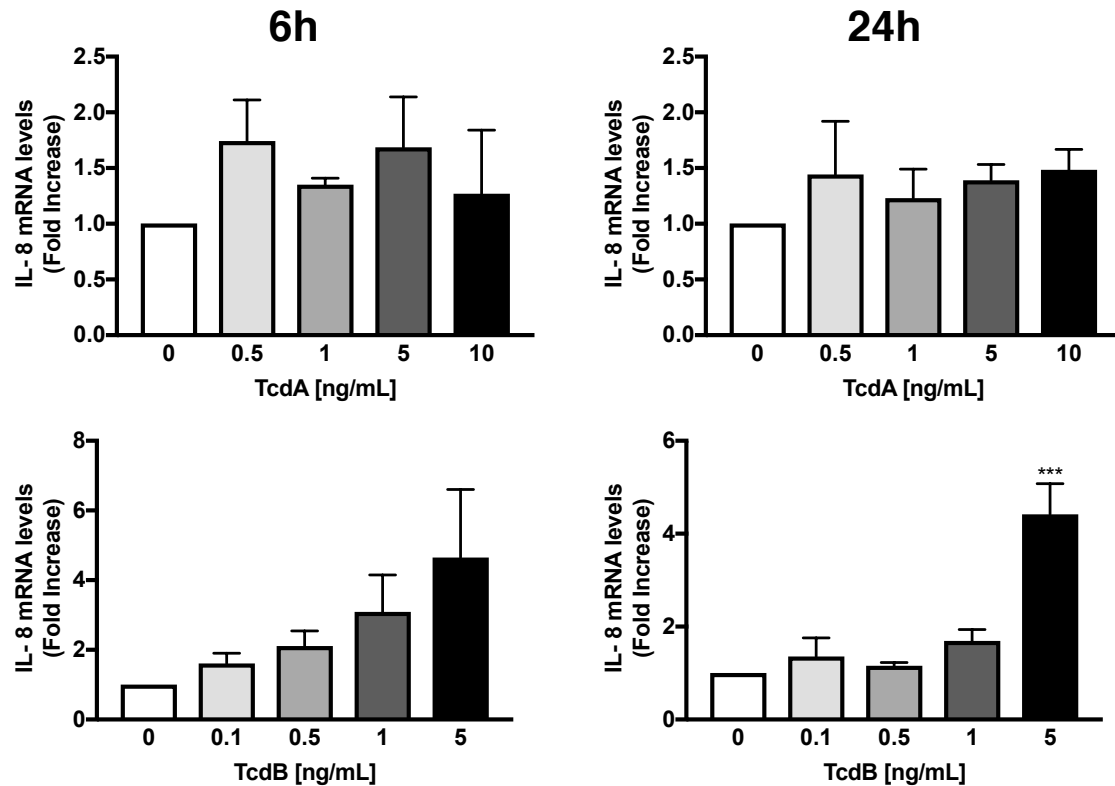
Figure 30: TcdB, but not TcdA, increases IL-8 production in Caco2 cells at 24h. Confluent Caco-2 cells (14 days post-plating) were treated with purified TcdA (0.5-10 ng/ml) or TcdB (0.1-5 ng/ml) for 6h and 24h. The mRNA levels of IL-8 were analyzed by RT-PCR and normalized to GAPDH using the gene-specific primers shown in Table1. Values are expressed as relative expression compared to untreated cells. n=5, (***$p < 0.001$)

3.2   Mechanism(s) underlying DRA downregulation by *C. difficile* toxins

3.2.1 Downregulation of DRA protein is independent of toxins' glucosyltransferase activity

C. difficile toxins A and B are large gluscosyltransferase toxins that specifically modify host cell Rho GTPases such as RhoA, Rac1, Rac2, and Cdc 42 among others (2, 140, 143). The enzymatic glucosyltransferase domain (GTD) irreversibly transfers a UDP-glucose moiety to the switch I (GTP binding) region of Rho GTPases (35). This action locks Rho GTPases in their GDP-bound state thereby halting downstream cascades and recycling of GTPases to the plasma membrane (2, 26). Historically, this inactivation was thought to cause the majority of cytopathic and cytotoxic effects of the toxins , as described earlier (21, 147). Recent studies, however, have identified some GTD-independent effects of TcdA and TcdB (24, 59). Thus, the start of our mechanistic studies focused on whether the toxin-mediated decrease in DRA protein, but not mRNA levels, was specifically caused by the glucosyltransferase domain of each toxin. Through our collaboration with Dr. Borden Lacy at Vanderbilt, we obtained GTD-deficient toxins A and B along with wild type TcdA and TcdB from the same background strain. Utilizing the published crystal structure of both toxins (68), the Lacy lab introduced double point mutations into the glucosyltransferase domain of each toxin (TcdA D285/287N, TcdB D286/288N) (24). These toxins were rigorously analyzed by the Lacy group for their UDP-glucose binding ability to assess the functionality of the mutated GTD domain (23, 24). Although the efficacies of the toxins were verified by the Lacy group, we also examined the efficacy of the DXD mutant toxins prior to use. To ensure that the glucosyltransferase region of each toxin was inactive, we first treated Caco2 cells with 25 ng/mL of TcdA or 10 ng/mL TcdB for 24h. In these studies, we also used the wild type toxins (VPI 10463

background) purchased from List Labs (used in all *in vitro* studies) and those purified by

the Lacy lab. Both wild type toxins from List Labs and the Lacy lab wild type toxins

significantly decreased active, non-glycosylated Rac1 at 24h **(Figure 31)**. In contrast,

both the TcdA DXD and TcdB DXD mutants did not significantly decrease active Rac1

levels **(Figure 31)**. These preliminary experiments confirmed that the DXD mutants were

lacking glucosyltransferase activity and were unable to modify Rho GTPases in Caco2

cells.

After confirming that our DXD mutant toxins were incapable of glycosylating Rho

GTPases, we next investigated whether the toxin-mediated decrease in DRA protein

levels was dependent on Rac1 inactivation. Using the same doses shown in **Figure 31**,

we found that DRA protein levels were significantly decreased after 24h toxin incubation

regardless of the glucosyltransferase activity of either toxin A or B **(Figure 32).** These

results suggested that the downregulation of DRA protein by both TcdA and TcdB was

due to an alternative activity of the toxin and not the inactivation of Rho GTPases by the

GTD domain.
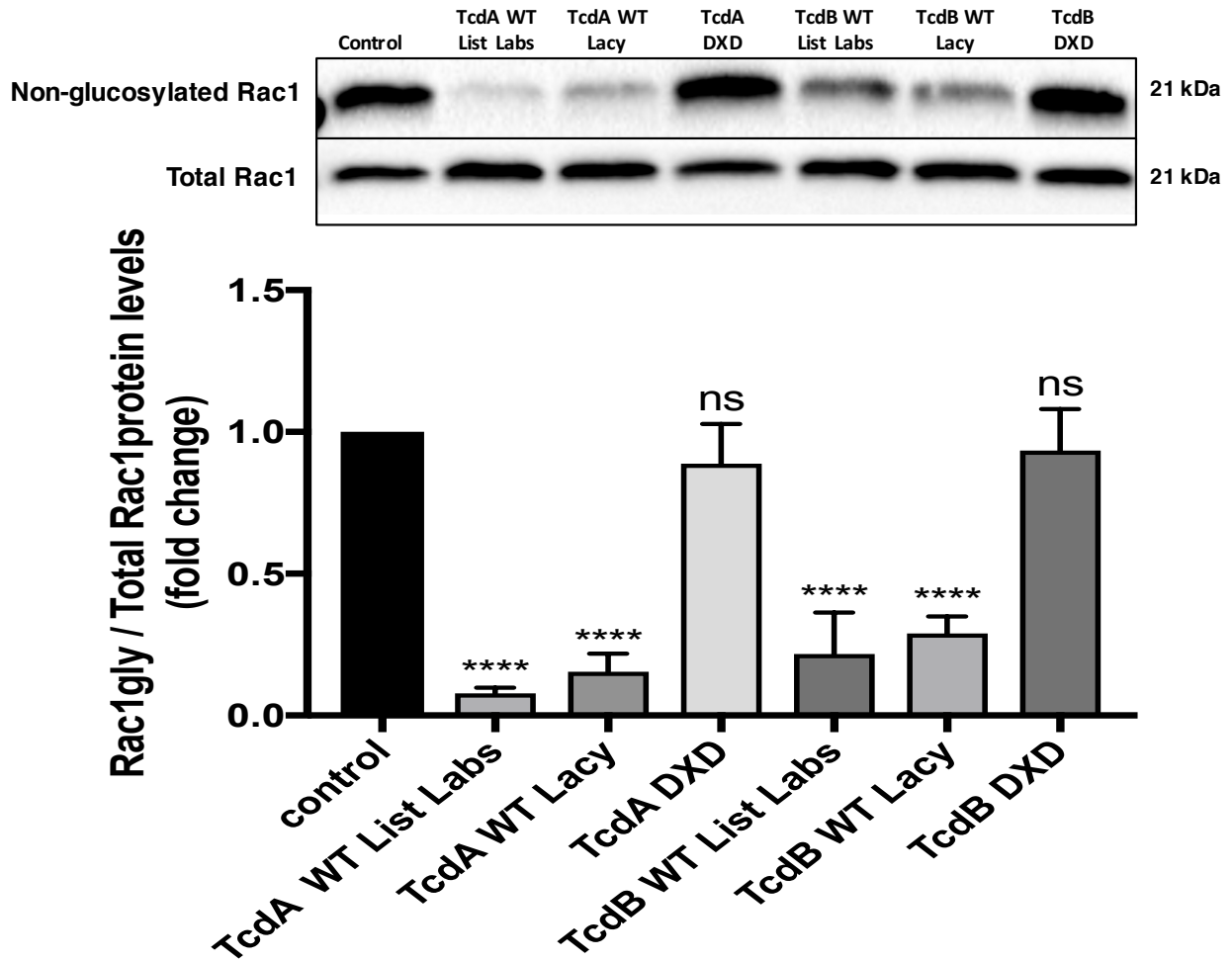
Figure 31: Glucosyltransferase mutants TcdA DXD and TcdB DXD did not inactivate Rac1 in Caco2 cells. Immunoblots of non-glycosylated Rac1 and total Rac1 levels after 24h treatment with 25 ng/ml TcdA (List Labs, Lacy Lab WT, and TcdA DXD) or 10 ng/mL TcdB (List Labs, Lacy Lab WT, and TcdB DXD). n=4, asterisks indicate differences between toxin-treated cells and control (****$p < 0.0001$), ns: not significant
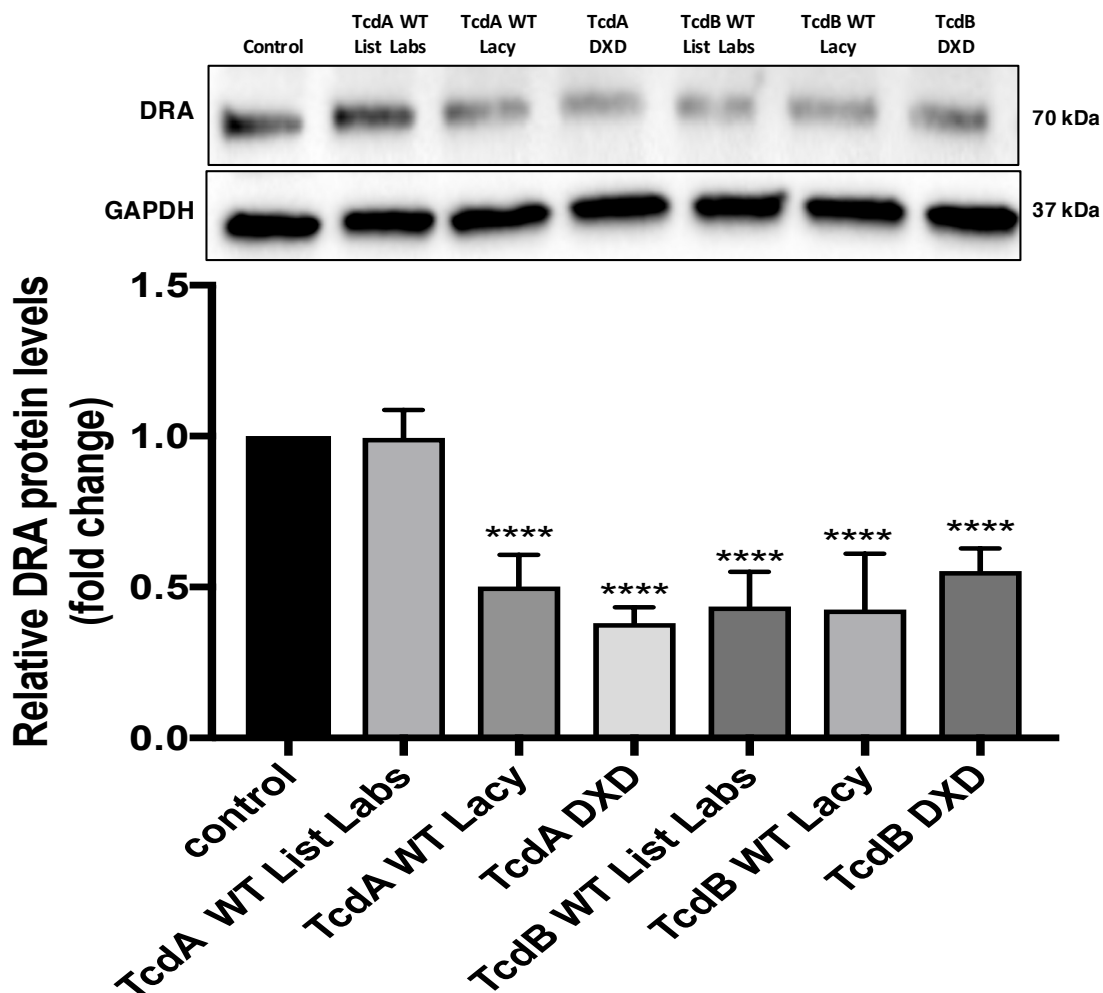
Figure 32: Toxin-mediated decrease in DRA protein levels was independent of glucosyltransferase activity. Immunoblots of DRA protein levels after 24h treatment with 25 ng/ml TcdA (List Labs, Lacy Lab WT, and TcdA DXD) or 10 ng/mL TcdB (List Labs, Lacy Lab WT, and TcdB DXD). n=4, asterisks indicate differences between toxin-treated cells and control (****$p < 0.0001$).

3.2.2 TcdA-mediated decrease in MCT-1 protein required functional GTD domain

Given the GTD-independent effects of toxins A and B on DRA expression levels,

we next investigated whether the TcdA-mediated decrease in MCT-1 protein **(Figure 21)**

was also independent of the GTD domain. Interestingly, we still identified a significant

decrease in MCT-1 protein in the presence of wild type TcdA, but not TcdA DXD **(Figure 33).** These results indicated that MCT-1 protein levels, unlike DRA, are decreased due to the glucosyltransferase activity of TcdA. Purified TcdB, on the other hand, did not alter MCT-1 protein levels regardless of glucosyltransferase activity **(Figures 24, 33).**
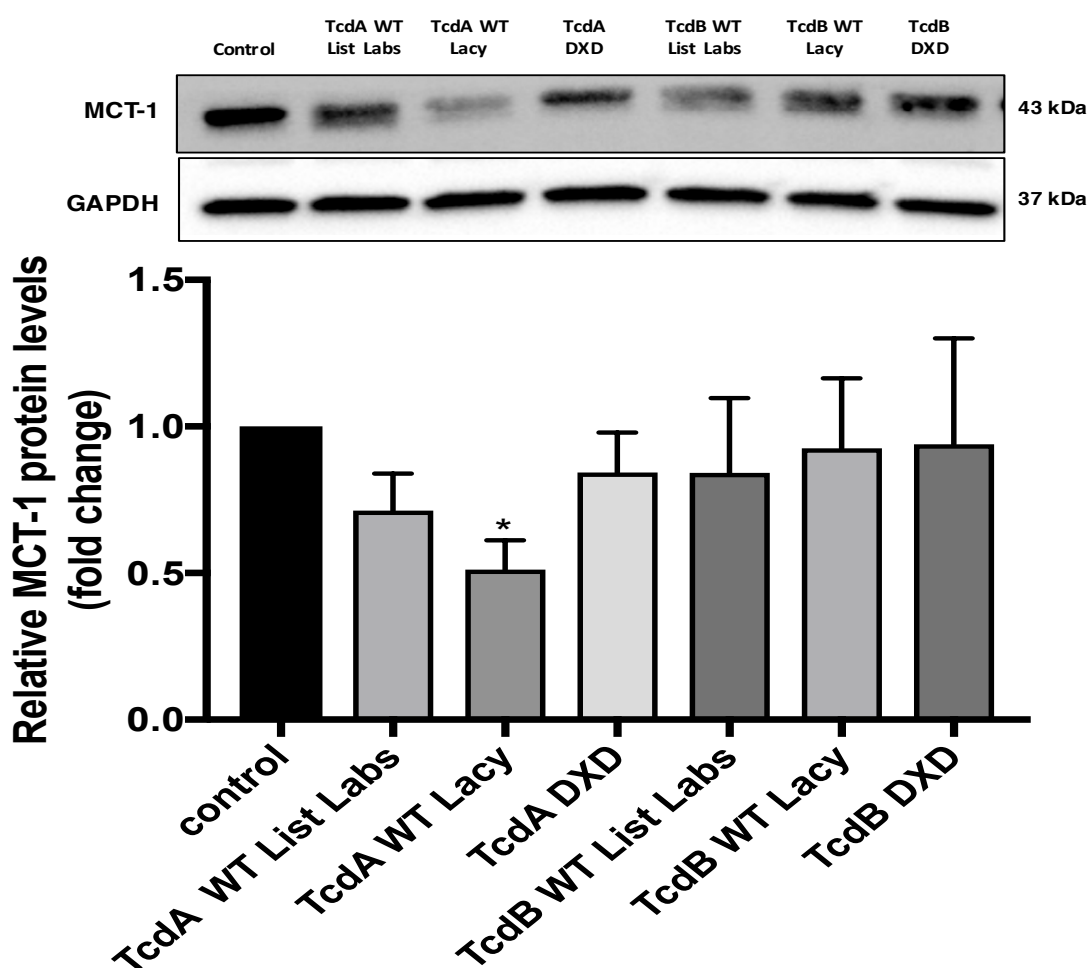
Figure 33: TcdA-mediated decrease in MCT-1 was glucosyltransferase-dependent Immunoblots of MCT-1 levels after 24h treatment with 25 ng/ml TcdA (List Labs, Lacy Lab WT, and TcdA DXD) or 10 ng/ml TcdB (List Labs, Lacy Lab WT, and TcdB DXD). MCT-1 levels were normalized to GAPDH. n=3, asterisks indicate differences between toxin-treated cells and control (*p < 0.05).

3.2.3   Bafilomycin A1 abrogated the toxin-mediated effects on DRA protein *in vitro*

Given that only DRA protein, not mRNA, was reduced in the presence of *C. difficile* toxins, we next examined possible mechanisms of post-transcriptional regulation of DRA protein levels by *C. difficile* toxins. One possible cause of decreased DRA protein levels is increased inducted of protein degradation pathways by toxins. Cellular protein degradation is generally divided into two pathways: the ubiquitin proteasome system (UPS) and the lysosomal pathway (43, 89). The UPS is primarily responsible for the selective degradation of small misfolded cytosolic proteins, and degradation by the 26S proteasome accounts for approximately 80-90% of all eukaryotic protein degradation (93). The other major pathway of protein degradation is the uptake of proteins in intracellular vesicles called lysosomes (43). Lysosomes contain over 60 hydrolytic enzymes to degrade nucleic acids, proteins, and lipids (64). Additionally, lysosomes fuse with autophagosomes to digest larger cellular debris and recycle their contents back into the cytosol during autophagy (43, 96). To investigate the possible role of lysosomal degradation of DRA protein, we utilized Bafilomycin A1, an inhibitor of vacuolar H^+ ATPase (V-ATPase) (167). Bafilomycin A1 has been extensively used to study protein degradation through lysosomes, endosomes, and autophagosomes due to their dependence on V-ATPase for proper acidification and function (112, 167). Bafilomycin A1 is known to inhibit endosomal acidification (via inhibition of V-ATPase) and prevent normal degradation of endosomal contents (139, 167). This is because low intraluminal pH (acidification) is necessary for the function of many lysosomal hydrolases and the maturation and trafficking of endosomes through the lysosomal pathway (64). Moreover, bafilomycin is known to prevent maturation of autophagosomes and fusion of

autophagosomes to lysosomes during autophagy (43, 167). In our studies, Caco2 cells were first treated with 25 ng/ml TcdA or 10 ng/ml TcdB for 1h prior to administration of 100 nM Bafilomycin A1. Pretreatment with TcdA and TcdB was necessary to allow for proper endocytosis and release of the toxins in the cytosol. This process is inhibitied by bafilomycin because the maturation and cleavage of TcdA and TcdB occurs only in acidified endosomes (162). Prior studies have reported that the endocytic uptake and cytosolic release of TcdA and TcdB occurs rapidly in as little as 30 minutes (162). Knowing this, we first administered TcdA and TcdB 1 hour prior to Bafilomycin A1 administration to allow for uptake of toxins into cells. After 1h toxin pretreatment, Caco2 cells were given 100 nM Bafilomycin A1 in the presence or absence (control + Bafilomycin A1) of toxins A or B and harvested after 24h total. As expected, both TcdA and TcdB significantly reduced DRA protein levels compared to control Caco2 cells **(Figure 34).** Control cells treated with Bafilomycin A1 also had slightly elevated DRA protein levels (due to the absence of normal protein degradation), but this did not reach significance. Interestingly, these results also showed that in the presence of Bafilomycin A1, neither TcdA nor TcdB significantly reduced DRA protein levels **(Figure 34)**. This finding illustrated that the toxin-mediated decrease in DRA protein may be occurring through increased protein degradation in the lysosomal/autophagy pathway.
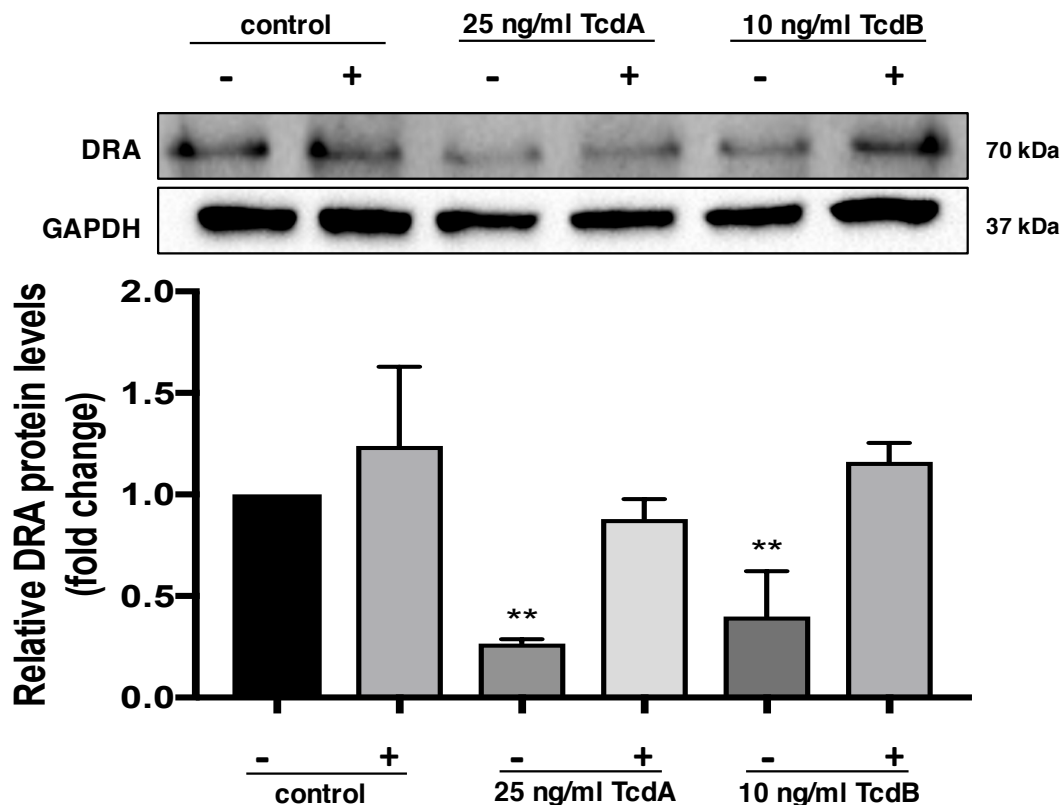
Figure 34: Bafilomycin A1 inhibited the toxin-mediated decrease in DRA protein levels in Caco2 cells. Immunoblots of DRA protein levels after 24h treatment of Caco2 cells (14 days post-plating) with 25 ng/ml TcdA (List Labs, Lacy Lab WT, and TcdA DXD) or 10 ng/mL TcdB (List Labs, Lacy Lab WT, and TcdB DXD) in the presence or absence of 100 nM Bafilomycin A1. n=3, asterisks indicate differences between toxin-treated cells and control (**$p < 0.01$).

3.2.4 *C. difficile* toxins alter protein levels of autophagy-related genes *in vitro*

The vacuolar degradation and recycling of cellular components in lysosomes also occurs through a process called autophagy (43, 167). Autophagy is a precisely regulated cellular process that degrades intracellular cytosolic proteins through fusion with lysosomes **(Figure 15)**. This process plays a pivotal role in cellular homeostasis, stress responses, development, and pathogen defense (9, 93). Consistent with this, studies

have shown that dysregulation of autophagy is implicated in cancers, gastrointestinal disorders, neurodegenerative diseases, and heart conditions (90, 93, 139). Autophagy is comprised of three distinct processes: chaperone mediated autophagy (CMA), microautophagy, and macroautophagy (96). The best characterized autophagic pathway, macroautophagy, degrades the majority of autophagic proteins through the sequestration of cytosolic proteins in autophagosomes, fusion with enzyme-containing lysosomes, and recycling of degraded proteins (9, 96). Autophagy is mediated by autophagy-related genes, collectively known as ATG proteins, which were first isolated in yeast (79). Briefly, the autophagy pathway is separated into four steps: induction/initiation, elongation, substrate targeting, and maturation and fusion with lysosomes (76). A detailed description of key ATG protein complexes and the progression of autophagy is in the introduction and **Figure 15**. One important Atg protein is ATG16L1, which exists in complex with ATG5 and ATG12. The ubiquitin-like ATG5-ATG12-ATG16L1 complex is crucial for the localization of LC3 (microtubule-associated protein light chain 3) to the autophagosome membrane and the progression of late stage autophagy (76, 101). Support for the importance of ATG16L1 is seen in studies showing that loss of ATG16L may contribute to the development of inflammatory bowel diseases like Crohn's disease (55). Additionally, *Atg16L1*-deficient mice have elevated levels of inflammatory cytokines IL-1β and IL-18 after exposure to bacterial toxins (88). These studies contribute to the ever-growing list of autophagy proteins involved in inflammation and infections (72, 109).

While various intestinal pathogens are known to utilize autophagy during infection, little is known about the role of autophagy in *C. difficile* associated diarrhea (59). Furthermore, our studies using Bafilomycin A1 identified the possible role of

lysosomal/autophagic degradation of DRA in response to TcdA and TcdB. Therefore, we next investigated the effects of our purified toxins on expression of key ATG proteins. Using Caco2 cells, we first examined expression of ATG16L1, a key autophagy regulator known to be downregulated in IBD (109, 145). As shown in **Figure 35**, both TcdA and TcdB significantly decreased ATG16L1 expression at 24h. Interestingly, only 25 and 1 ng/ml of TcdA and TcdB, respectively, significantly altered ATG16L1 expression suggesting that the decrease in ATG16L1 protein may occur in a dose-dependent manner.
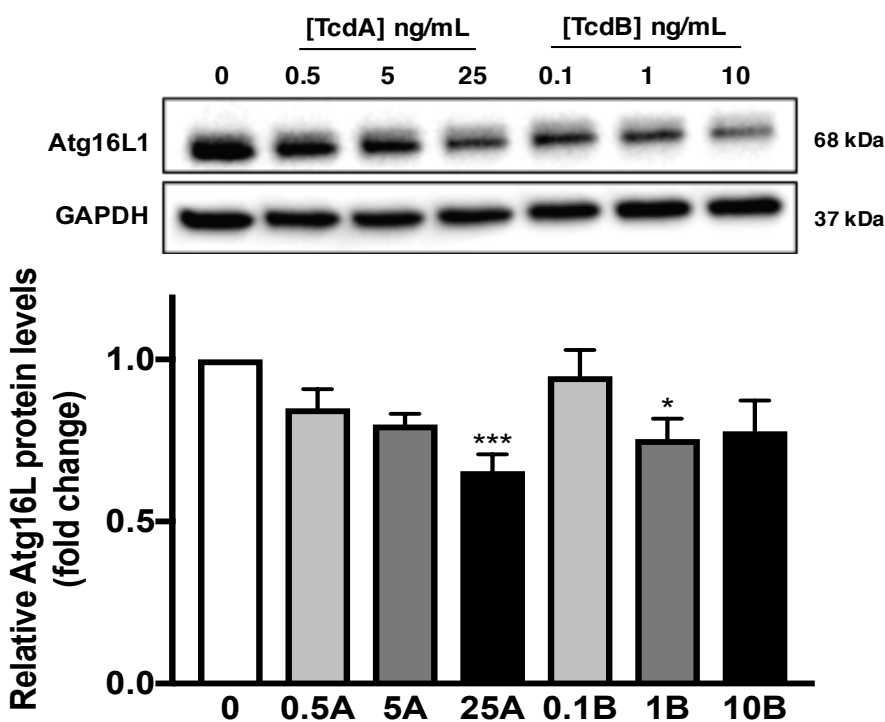
Figure 35: TcdA and TcdB, decreased ATG16L1 protein expression in Caco-2 cells. Confluent Caco-2 cells (14 days post-plating) were treated with purified TcdA or TcdB for 24h. ATG16L1 levels were quantified and normalized to the housekeeping gene GAPDH. n=3, asterisks indicate differences between toxin-treated cells and control (*p < 0.05, ***p<0.001)

After identifying that ATG16L1 protein was decreased in the presence of TcdA and TcdB, we next asked whether the third *C. difficile* toxin, CDT, would elicit similar effects. To our knowledge, the role of CDT in autophagy remains entirely uninvestigated. As mentioned earlier, CDT is an ADP-ribosyltransferase that causes cellular cytoskeletal disruption by destabilizing actin polymers **(Figure 12).** Interest in CDT-focused research has steadily increased in recent years due, in part, to the emergence of epidemic hypervirulent strains of *C. difficile* (33, 49). While the precise contribution of CDT to pathogenesis is not clear, studies suggest that CDT induces microtubule-based protrusions from enterocytes to promote bacterial adhesion (133). Given that CDT is known to induce pathological changes in intestinal epithelial cells, we next examined the effects of CDT on autophagy related genes in Caco2 cells. As shown in **Figure 36**, we found that, similar to TcdA and TcdB, CDT alone decreased ATG16L1 protein expression. Interestingly, treatment of Caco2 cells with both CDT and TcdA resulted in a more significant decrease in ATG16L1 protein than either toxin alone **(Figure 36)**. This may illustrate the possible synergistic effects of *C. difficile* toxins in regulation of cellular autophagy.
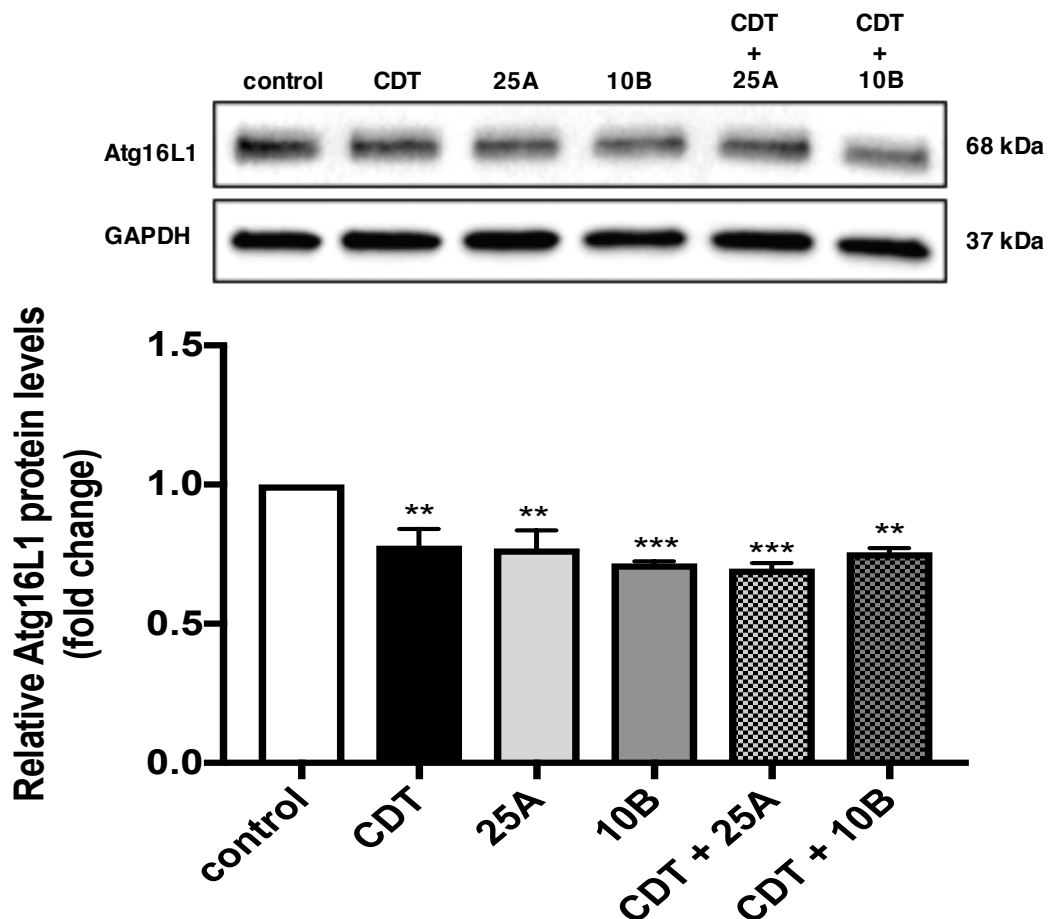
Figure 36: CDT, TcdA, and TcdB, decreased ATG16L1 protein expression in Caco-2 cells. Confluent Caco-2 cells (14 days post-plating) were treated with purified TcdA or TcdB, both alone and in the presence of 100 ng/ml CDTa and 200 ng/ml CDTb for 24h. ATG16L1 levels were quantified and normalized to the housekeeping gene GAPDH. n=3, asterisks indicate differences between toxin-treated cells and control (**p < 0.01, ***p<0.001)

To further investigate the role of autophagy, we next considered the conversion of LC3A to LC3B. The addition of PE to LC3 during the late stages of autophagy marks the conversion of LC3A to L3CB and is a universal hallmark of late stage autophagy induction (43, 59, 65, 167). After 24h treatment, we found that both TcdA and TcdB alone

significantly increased LC3B levels relative to LC3A **(Figure 37)**, thus signaling an increase in autophagosomal accumulation. Additionally, this increase in LC3B was even greater in Caco2 cells given CDT and TcdA or TcdB. Together, these data indicated that both TcdA and TcdB are inducing autophagy and CDT may further contribute to this increase in autophagic flux in intestinal epithelial cells.
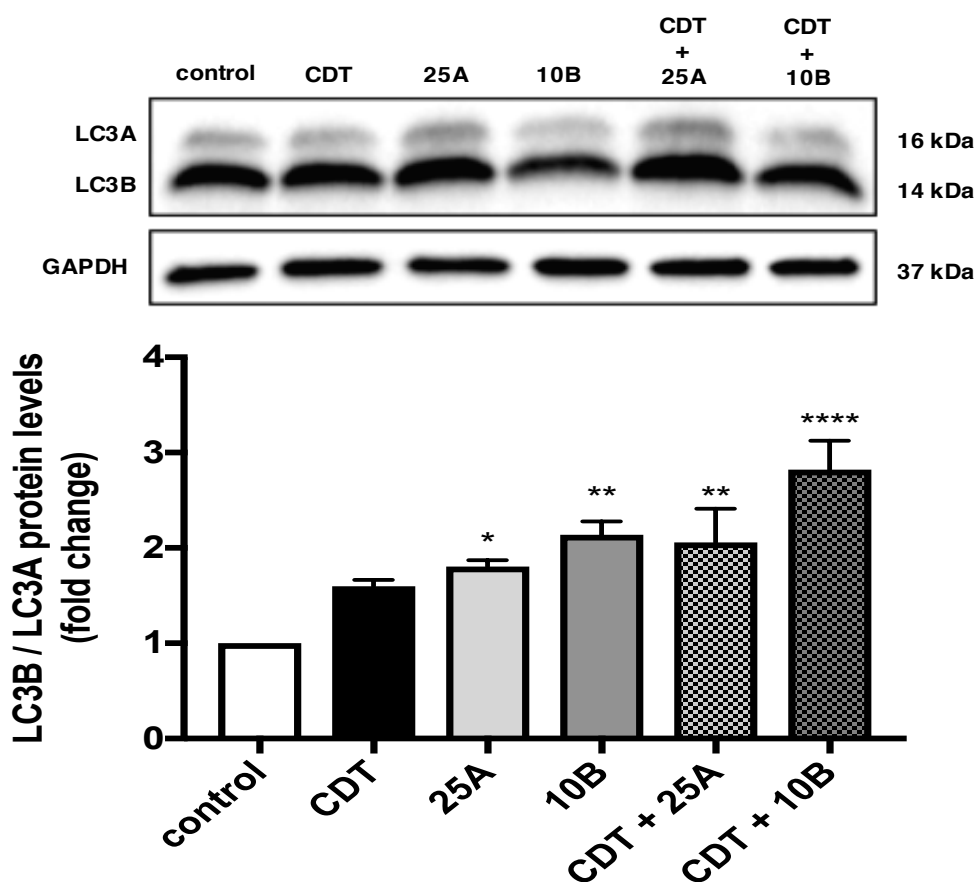
Figure 37: CDT, TcdA, and TcdB induced conversion of LC3A to LC3B in Caco-2 cells. Confluent Caco-2 cells (14 days post-plating) were treated with purified TcdA and TcdB, both alone and in the presence of 100 ng/ml of CDTa and 200 ng/ml of CDTb for 24h. LC3B levels were quantified and normalized to LC3A. n=3, asterisks indicate differences between toxin-treated cells and control (*p < 0.05, **p<0.01, ****p<0.0001)

3.3   Effects of *C. difficile* toxins on DRA expression *in vivo* and in human CDI

3.3.1 Intrarectal administration of TcdA, but not TcdB, induced colonic
       inflammation in a toxigenic mouse model of CDI

While differentiated Caco2 cells are a well-established *in vitro* model for studying the effects of bacterial pathogens (51, 82) and *C. difficile* specifically (56, 86), we next sought an animal model of CDI to investigate how TcdA and TcdB affected DRA expression in a more physiologically relevant model **(Figure 16)**. Using a previously established intrarectal toxigenic mouse model (63), we investigated the direct effects of purified toxins A and B on the colon, the primary target of *C. difficile* colonization and infection (19, 147, 156). Given that CDI is an inflammatory infection (19, 20, 146, 147), we first assessed the inflammatory effects of our purified toxins in the murine colonic mucosa. Consistent with published studies (63), mice administered TcdA alone had significantly higher myeloperoxidase (MPO) levels than control animals or those administered TcdB and TcdA + TcdB **(Figure 38).** Given that MPO release is a well established marker of inflammation and neutrophil infiltration (32, 62, 63), these studies indicated that only TcdA was inducing colonic inflammation in these animals.
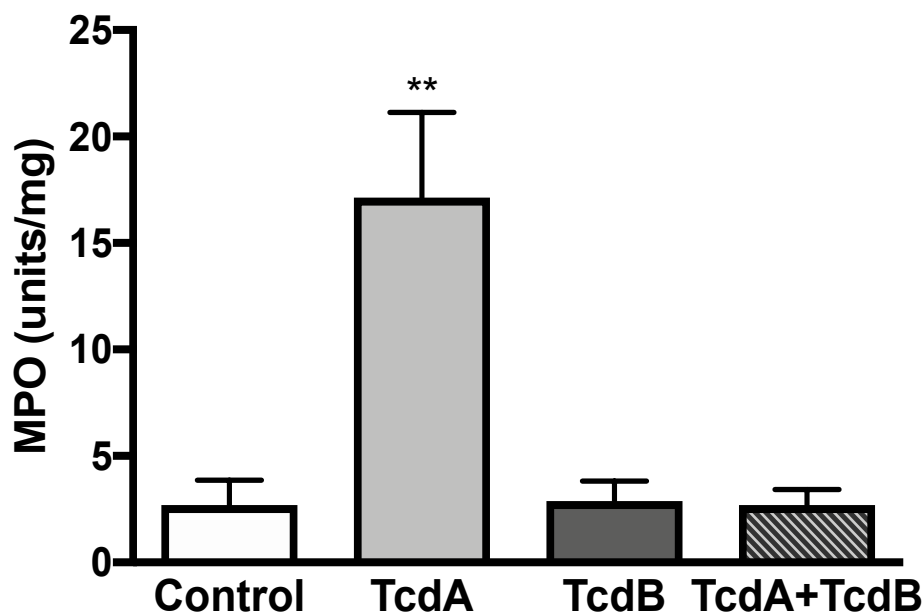
Figure 38: TcdA alone induced colonic inflammation and MPO release in C57BL/6 mice. 10-12 week old female C57BL/6 mice were intrarectally administered purified TcdA (10 µg), TcdB (10 µg), or TcdA+TcdB (5 µg each) in 100 µl PBS. After 4h, mice were sacrificed and the MPO release assay was performed as described in the Methods. MPO release is reported here in units per mg of colonic tissue. n=4, (**p<0.01)

We next investigated markers of inflammation in our toxigenic mouse model using RT-PCR of various inflammatory cytokines associated with intestinal pathogen infection (99, 140, 146). Consistent with our MPO data, we found that mRNA levels of inflammatory cytokines CXCL1, IL-1β, IL-6, and COX2 were significantly increased in the colon of TcdA-treated mice **(Figure 39)**. Interestingly, we also found that IL-10, an anti-inflammatory cytokine implicated in acute bacterial infections (116), was upregulated in mice given TcdA and TcdB **(Figure 40)**.
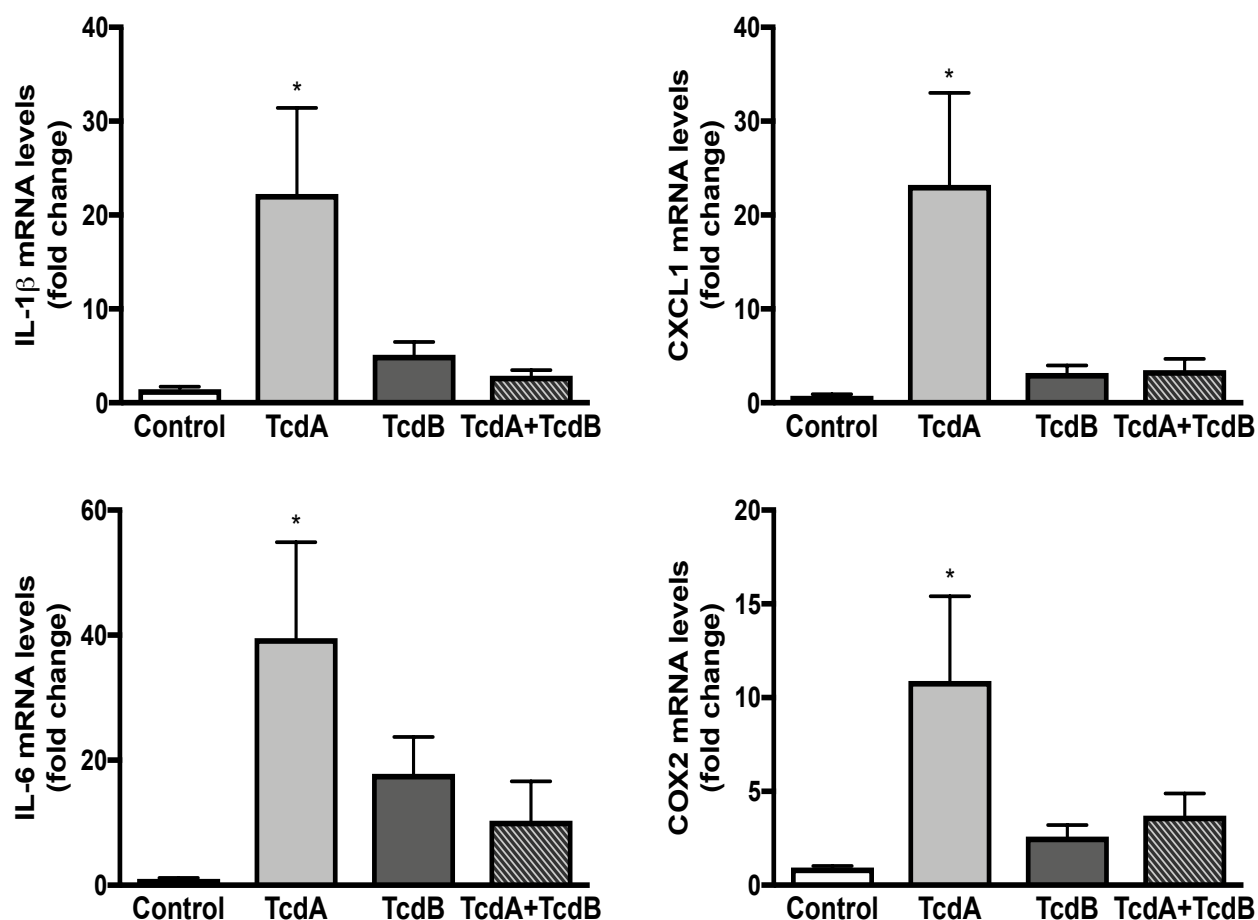
Figure 39: TcdA alone increased mRNA levels of pro-inflammatory cytokines in the colon of C57BL/6 mice. 10-12 week old female C57BL/6 mice were intrarectally administered purified TcdA (10 μg), TcdB (10 μg), or TcdA+TcdB (5 μg each) in 100 μl PBS. After 4h, mice were sacrificed and the colonic mucosa was harvested. Relative mRNA abundance of IL-1β, CXCL1, IL-6, and COX2 in total RNA samples from colonic mucosa was shown via RT-PCR using the gene-specific primers shown in Table 2. Values were normalized to GAPDH as an internal control. n=5, (*p<0.05)
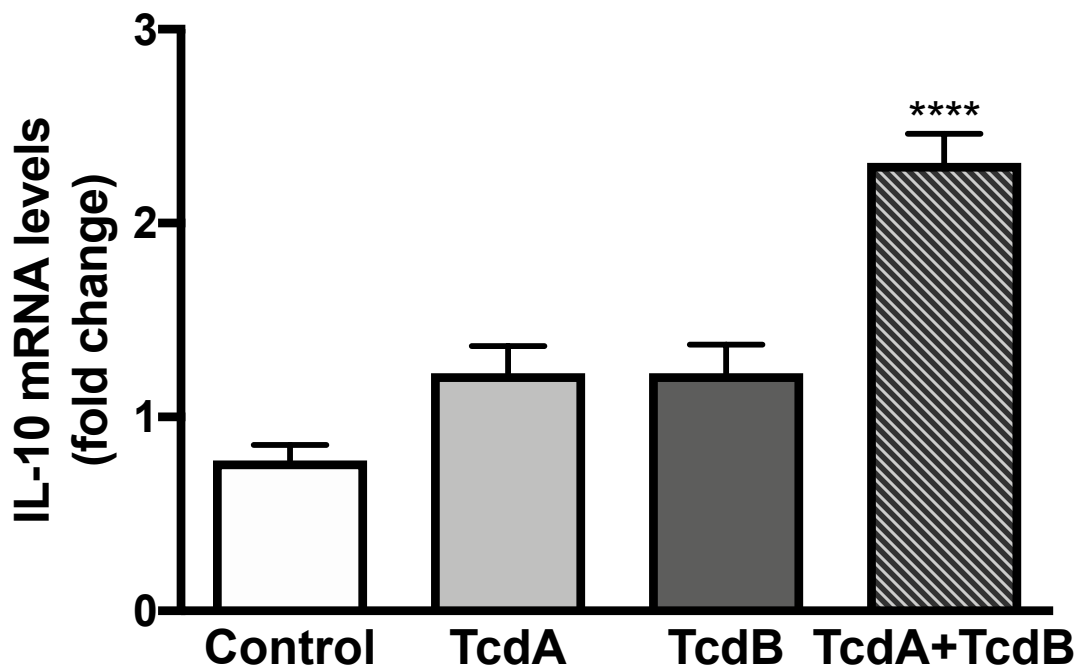
Figure 40: TcdA+TcdB treated mice had significantly higher IL-10 mRNA levels. 10-12 week old female C57BL/6 mice were intrarectally administered purified TcdA (10 µg), TcdB (10 µg), or TcdA+TcdB (5 µg each) in 100 µl PBS. After 4h, mice were sacrificed and the colonic mucosa was harvested. Relative mRNA abundance of IL-10 in total RNA samples from colonic mucosa was shown via RT-PCR using the gene-specific primers shown in Table 2. Values were normalized to GAPDH as an internal control. n=5, (****$p<0.0001$)

To get a better assessment of the inflammation triggered in these toxin-treated mice, we next used paraffin embedded colonic sections and H&E staining to assess overall edema, neutrophil infiltration, and luminal exudate. After H&E staining, sections were scored for inflammation by a blinded pathologist based on the criteria detailed in the Methods section. As shown below, we observed no overt pathological changes in the various toxin-treated mice **(Figure 41,** *left* **)**. Although the score for mice given both TcdA and TcdB was significantly higher than control mice, a total score below 6 was not

considered indicative of inflammation **(Figure 41,** *right)*. Thus, although TcdA is inducing colonic MPO release and cytokine upregulation in these animals, none of the toxins induced the significant architectural changes associated with intestinal inflammation at the 4h time point.
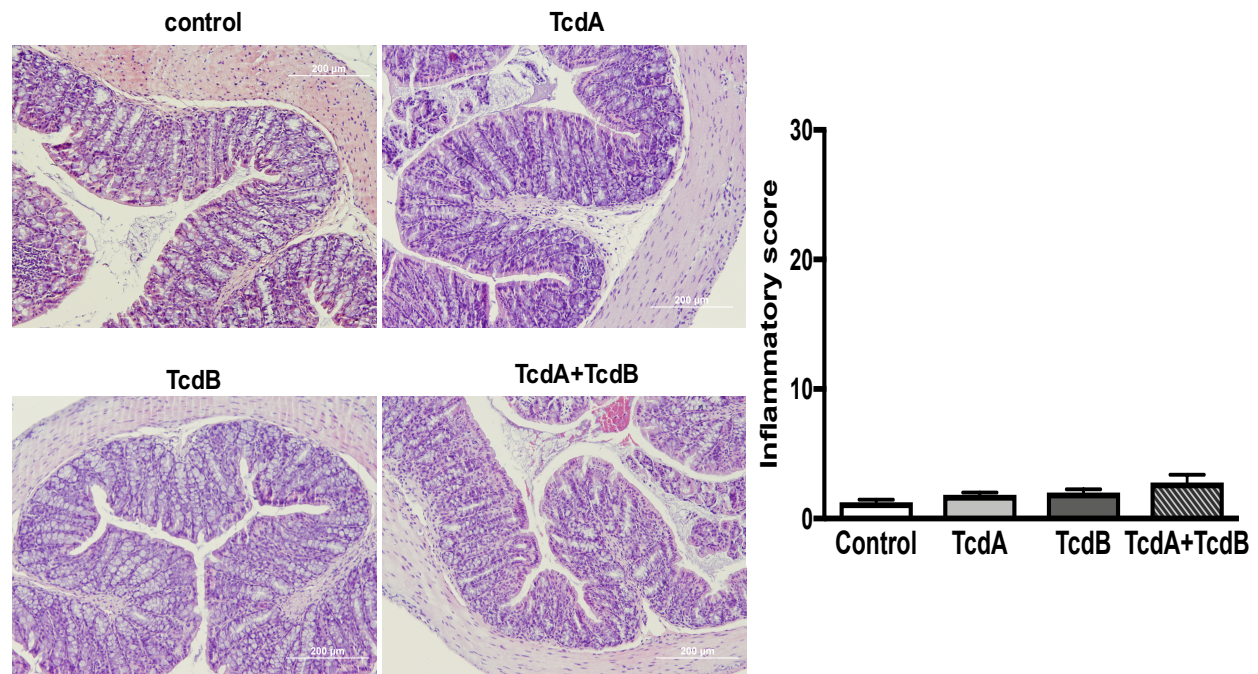
Figure 41: Intrarectal administration of toxins A and B did not cause significant histological changes in the colon of C57BL/6 mice. 10-12 week old female C57BL/6 mice were intrarectally administered purified TcdA (10 µg), TcdB (10 µg), or TcdA+TcdB (5 µg each) in 100 µl PBS. After 4h, mice were sacrificed and distal colonic tissues were embedded in paraffin and stained using H&E as described in the Methods. The left panel shows representative images of the histological changes induced by each toxin. The right panel is a representation of the total inflammatory score in each group (out of 30) described in the methods. n=5

3.3.2 DRA protein, but not mRNA, levels decreased in a toxigenic mouse model of CDI

As mentioned previously, bacterial pathogens like *C. rodentium,* the murine counterpart of EPEC, have been shown to downregulate DRA expression *in vivo* (83). Additionally, our results discussed in chapter 3 show a significant decrease in DRA protein levels after TcdA and TcdB administration **(Figures 18-20)**. Therefore, we also examined DRA protein levels in our toxigenic mouse model of CDI. Consistent with our *in vitro* studies, mice administered TcdA exhibited significantly lower DRA protein levels compared to untreated controls **(Figure 42)**. TcdA + TcdB-treated mice also showed significant loss of colonic DRA protein. This finding was further supported by immunofluorescent staining of DRA showing decreased levels of DRA protein at the apical surface of colonic sections in TcdA- and TcdA + TcdB-treated mice **(Figure 43)** Interestingly, TcdB-treated mice did not exhibit statistically significant changes in DRA protein expression at this dose and time point. To investigate the role of transcriptional modulation of DRA in the toxigenic mouse model, we also examined DRA mRNA levels in the colonic mucosa. Similar to our *in vitro* results shown in **Figure 25**, we found that DRA mRNA levels remained unchanged in the presence of both toxins alone and together **(Figure 42)**. These results illustrated that the toxin-mediated decrease in DRA protein was recapitulated in a toxigenic mouse model of CDI and also likely occurred at the post-transcriptional level.
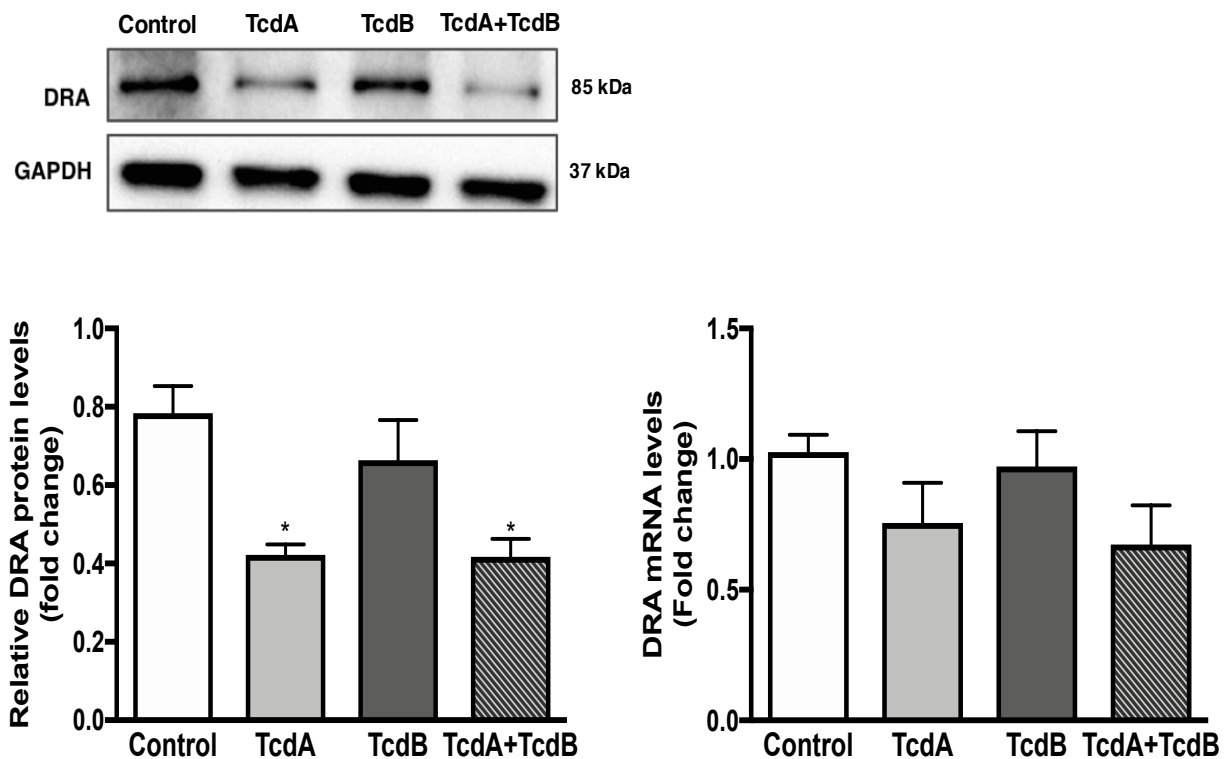
Figure 42: TcdA and TcdA+TcdB decreased DRA protein, but not mRNA, levels in the colon of C57BL/6 mice. 10-12 week old female C57BL/6 mice were intrarectally administered purified TcdA (10 μg), TcdB (10 μg), or TcdA+TcdB (5 μg each) in 100 μl PBS. After 4h, mice were sacrificed and colonic mucosal scrapings were harvested. (*left*) Relative DRA levels (normalized to GAPDH) in total protein extracted from colonic mucosa shown by Western blotting (n=4) (*P < 0.05). (*right*) Relative mRNA abundance of DRA in total RNA samples from colonic mucosa was shown via RT-PCR using the gene-specific primers shown in Table 2. Values were normalized to GAPDH as an internal control (n=4)
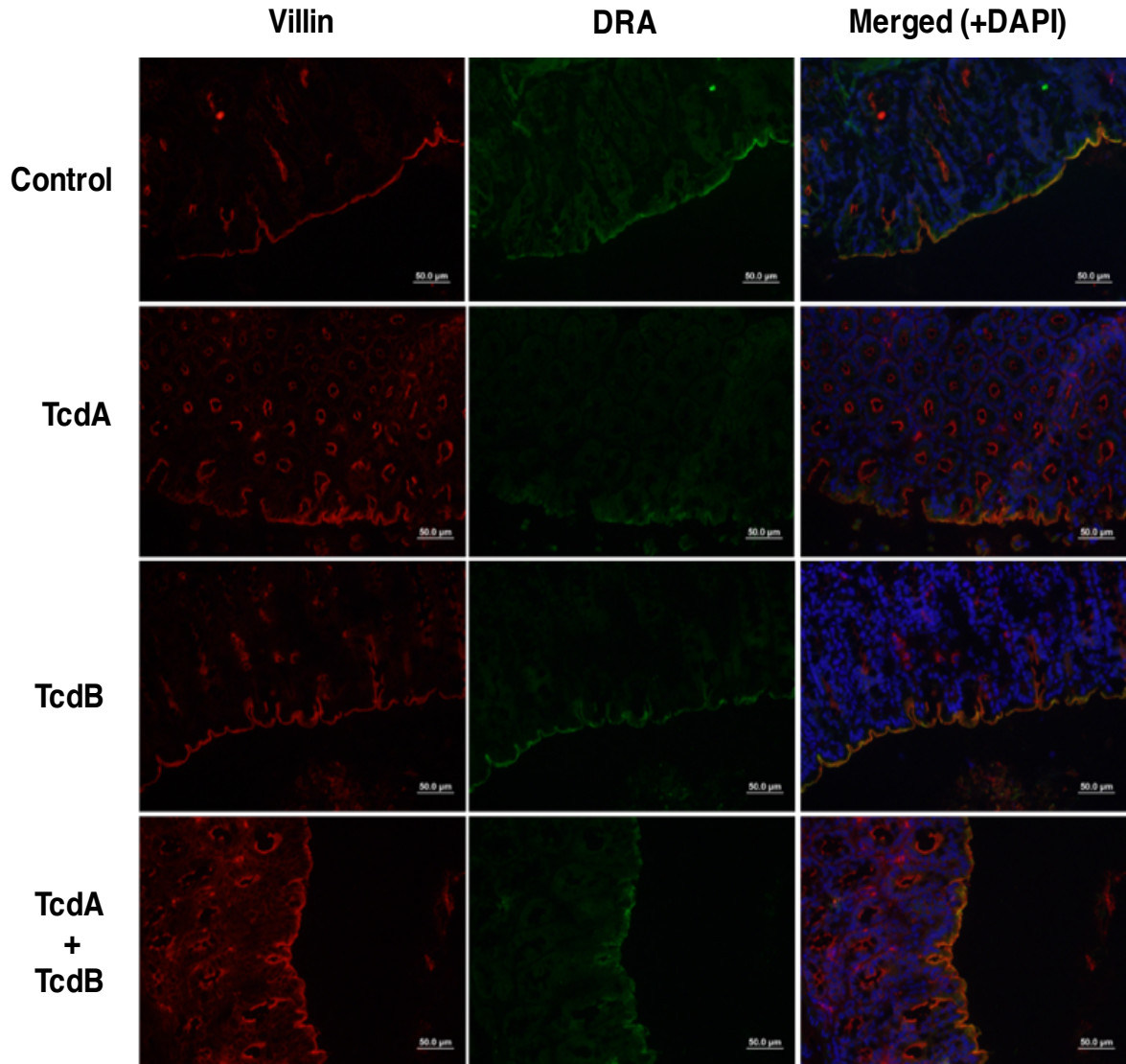
Figure 43: TcdA and TcdA + TcdB decreased DRA protein levels in the colon of C57BL/6 mice. 10-12 week old female C57BL/6 mice were intrarectally administered purified TcdA (10 µg), TcdB (10 µg), or TcdA+TcdB (5 µg each) in 100 µl PBS. After 4h, mice were sacrificed. Distal colonic sections were embedded in OCT and stained for DRA and villin as described in the Methods. Representative image of immumostaining of DRA (green) and villin (red) in distal colonic mucosal sections. n=4

3.3.3   NHE3 protein, but not mRNA, levels decreased in a toxigenic mouse model of CDI

In addition to the role of DRA in our toxigenic mouse model, we also investigated the effect of both toxins A and B on NHE3 expression in C57BL/6 mice. Following the same trend seen with DRA, our results showed that NHE3 protein, but not mRNA, levels were significantly decreased in the presence of TcdA and TcdA + TcdB **(Figure 44)**. Similarly, these results were also observed using immunofluorescent staining of NHE3 **(Figure 45)**.
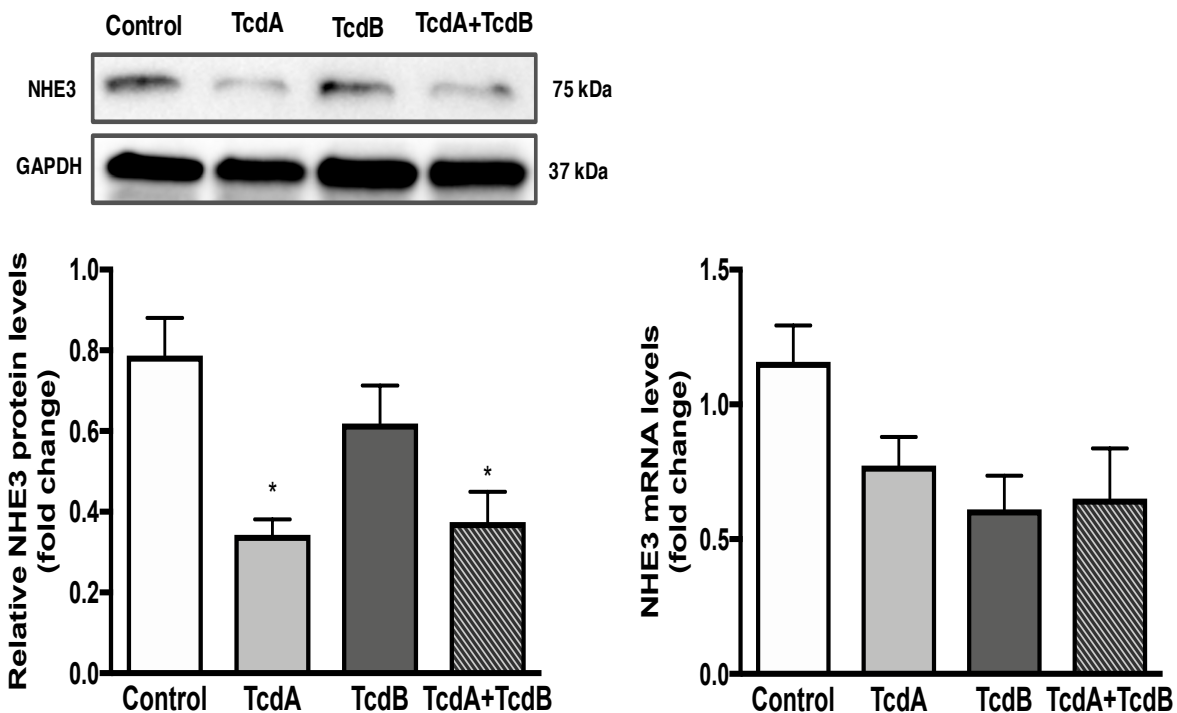
Figure 44: C. difficile toxins decreased NHE3 protein, but not mRNA, levels in the colon of C57BL/6 mice. 10-12 week old female C57BL/6 mice were intrarectally administered purified TcdA (10 µg), TcdB (10 µg), or TcdA/TcdB (5 µg each) in 100 µl PBS. After 4h, mice were sacrificed and colonic mucosal scrapings were harvested.

(*left*) Relative NHE3 levels (normalized to GAPDH) in total protein extracted from colonic mucosa shown by Western blotting (n=4) (*P < 0.05). (*right*) Relative mRNA abundance of NHE3 in total RNA samples from colonic mucosa was shown via RT-PCR using the gene-specific primers shown in Table 2. Values were normalized to GAPDH as an internal control (n=5)
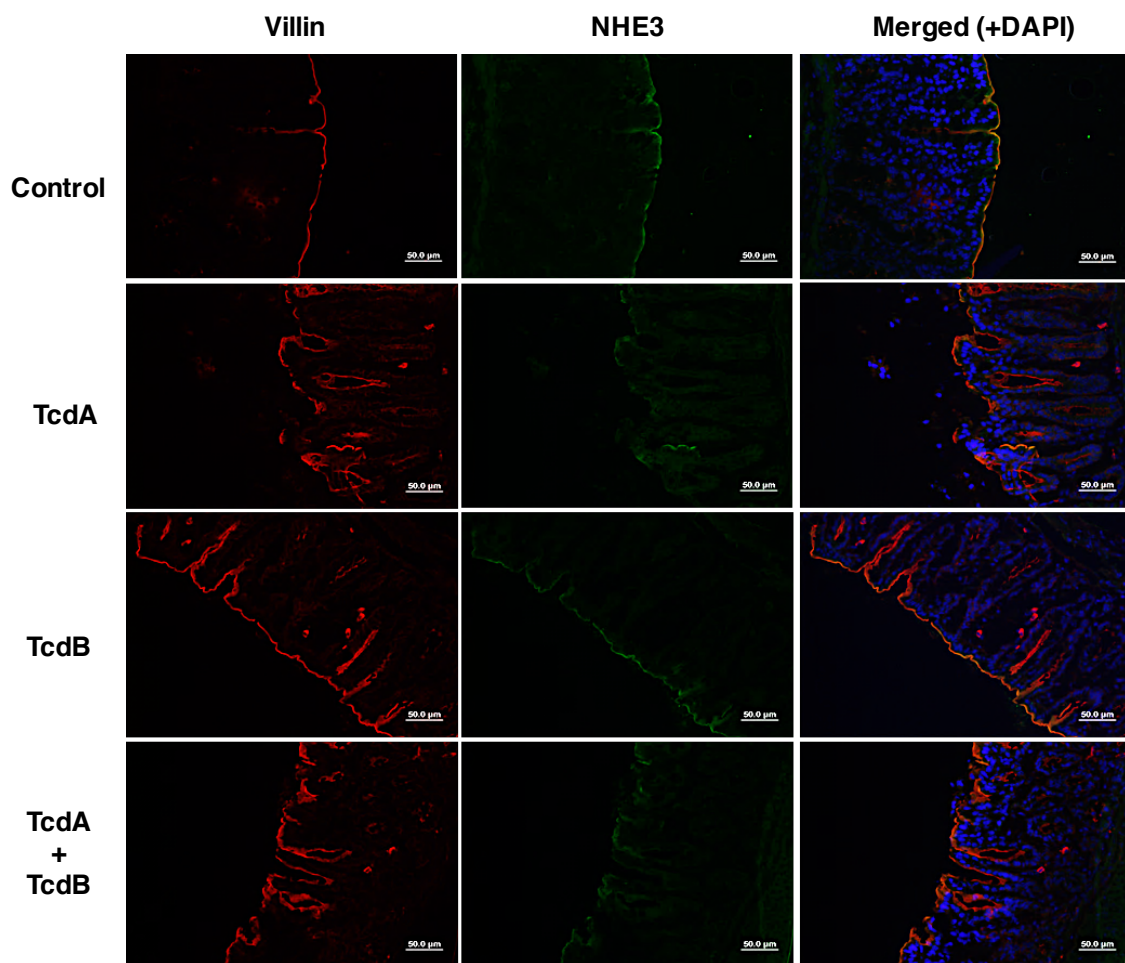
Figure 45: TcdA and TcdA + TcdB decreased NHE3 protein levels in the colon of C57BL/6 mice. 10-12 week old female C57BL/6 mice were intrarectally administered purified TcdA (10 µg), TcdB (10 µg), or TcdA+TcdB (5 µg each) in 100 µl PBS. After 4h, mice were sacrificed. Distal colonic sections were embedded in OCT and stained for NHE3 and villin as described in the Methods. Representative image of immumostaining of NHE3 (green) and villin (red) in distal colonic mucosal sections. n=5

3.3.4 Purified *C. difficile* toxins did not alter mRNA levels of intestinal ion transporters MCT-1, NHE2, CFTR, and PAT-1 *in vivo*

Next, we investigated whether other intestinal ion transporters were altered in our toxigenic mouse model of CDI. Using RT-PCR, we assessed the mRNA levels of MCT-1, NHE2, CFTR, and PAT-1 at 4h post toxin administration. As shown in **Figure 46**, neither TcdA nor TcdB significantly altered the mRNA levels of these transporters. These results, like our *in vitro* studies discussed earlier, illustrated that *C. difficile* toxins A and B did not affect these intestinal ion transporters at the transcriptional level. Moreover, the toxin-mediated alterations in protein levels appeared to be specific to DRA and NHE3 in the toxigenic mouse model. This indicated that TcdA and TcdB primarily target the intestinal transporters involved in electroneutral NaCl absorption and not intestinal ion transport as a whole.
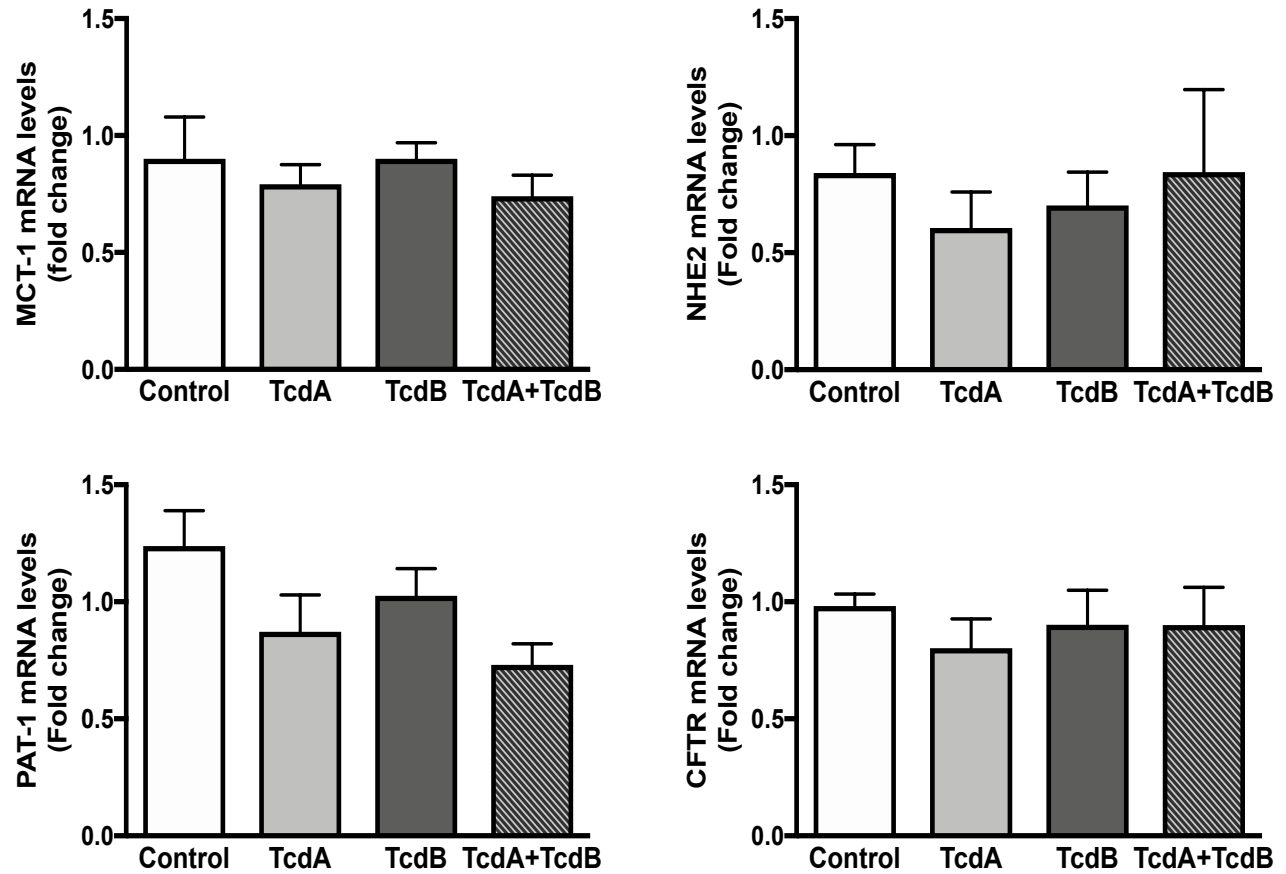
Figure 46: *C. difficile* **toxins did not alter mRNA levels of intestinal ion transporters in a toxigenic mouse model of CDI**. 10-12 week old female C57BL/6 mice were intrarectally administered purified TcdA (10 μg), TcdB (10 μg), or TcdA + TcdB (5 μg each) in 100 μl PBS. After 4h, mice were sacrificed and colonic mucosal scrapings were harvested. Relative mRNA abundance of MCT1, NHE2, PAT1, and CFTR in total RNA samples from colonic mucosa was shown via RT-PCR using the gene-specific primers shown in Table 2. Values were normalized to GAPDH as an internal control (n=5)

3.3.5 <u>The role of autophagy in a toxigenic mouse model of CDI</u>

After identifying that both DRA and NHE3 protein were decreasing in our toxigenic mouse model of CDI, we next asked whether autophagy might play a role in the degradation of these intestinal ion transporters. As shown earlier in **Figures 35-36**, autophagy related protein ATG16L1 was decreased in the presence of TcdA, TcdB, and CDT. Additionally, the loss of ATG16L1 in other infectious mouse models resulted in increased levels of inflammatory cytokines (88). Therefore, we next examined whether ATG16L1 protein levels were downregulated in the presence of *C. difficile* toxins *in vivo.* Our results showed that TcdA alone caused a significant decrease in colonic ATG16L1 protein levels **(Figure 47)**. Interestingly, TcdB-treated mice did not exhibit changes in ATG16L1 protein levels. TcdA + TcdB-treated mice did have a loss of ATG16L1 levels, but this did not reach significance.
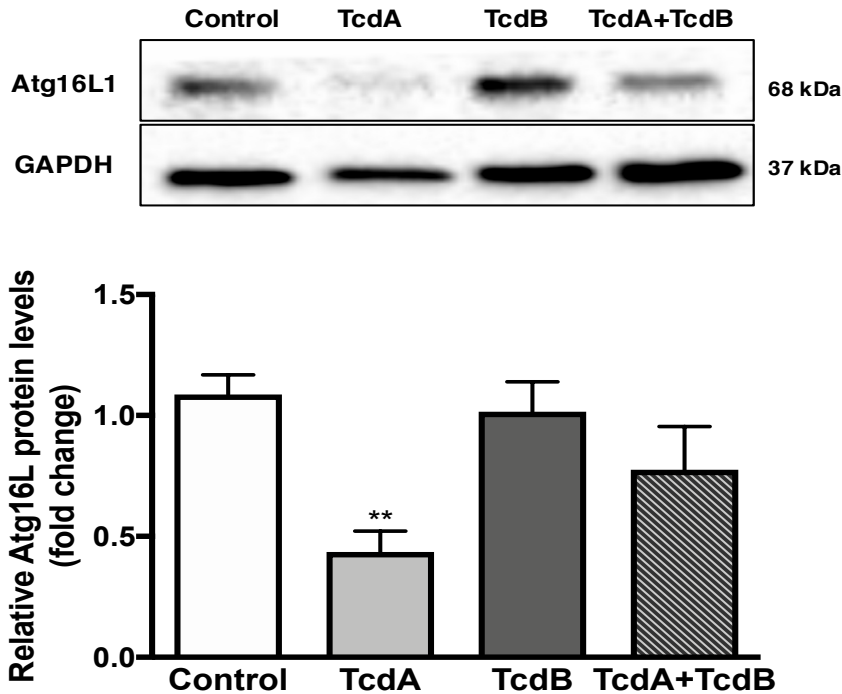
Figure 47: *C. difficile* **TcdA decreased ATG16L1 protein levels in the colon of C57BL/6 mice**. 10-12 week old female C57BL/6 mice were intrarectally administered purified TcdA (10 µg), TcdB (10 µg), or TcdA/TcdB (5 µg each) in 100 µl PBS. After 4h, mice were sacrificed and colonic mucosal scrapings were harvested. Relative ATG16L1 levels (normalized to GAPDH) in total protein extracted from colonic mucosa is shown by Western blotting (n=4) ($**p < 0.01$).

To further investigate the role of autophagy in our toxigenic mouse model, we next examined Beclin-1 levels in the colon of toxin-treated mice. Beclin-1, the mammalian orthologue of yeast ATG6, exists in complex with ATG14L (UVRAG), Vsp34, and PI3KC3 to localize autophagic proteins to the pre-autophagosomal structure (PAS) **(Figure 15)**. Importantly, the Beclin1-PI3K complex functions at a different stage of autophagy compared to the ATG16L1 complex (34, 108). Thus, examination of Beclin-1 levels allowed for the investigation of toxin-induced autophagy regulation at an earlier

autophagic stage. Using our toxigenic mouse model, we found that Beclin-1 protein levels were significantly reduced in mice administered TcdA alone **(Figure 48)**. Similar to our ATG16L1 results, neither TcdB nor TcdA + TcdB caused downregulation of Beclin-1 protein in the colon of C57BL/6 mice.
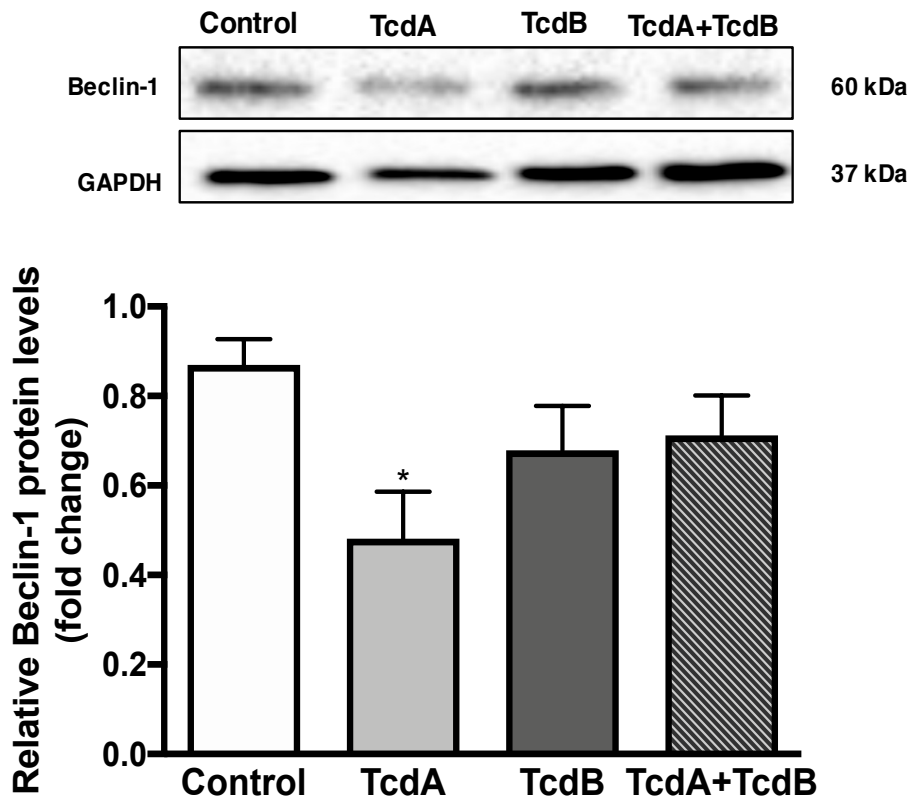
Figure 48: TcdA alone decreased Beclin-1 protein levels in the colon of C57BL/6 mice. 10-12 week old female C57BL/6 mice were intrarectally administered purified TcdA (10 µg), TcdB (10 µg), or TcdA/TcdB (5 µg each) in 100 µl PBS. After 4h, mice were sacrificed and colonic mucosal scrapings were harvested. Relative Beclin-1 levels (normalized to GAPDH) in total protein extracted from colonic mucosa is shown by Western blotting (n=4) (*p < 0.05).

Finally, we investigated whether intrarectal toxin administration induced changes in LC3 lipidation *in vivo.* As mentioned previously, the conversion of LC3A to LC3B through its conjugation to phosphatidylethanolamine (PE) is a trademark step in late stage autophagosomal elongation and expansion (59, 72). Our results showed that only mice administered TcdA had a significant increase in LC3B compared to LC3A levels **(Figure 49)**. While mice given TcdB did have slightly elevated levels of LC3B, this did not reach significance.
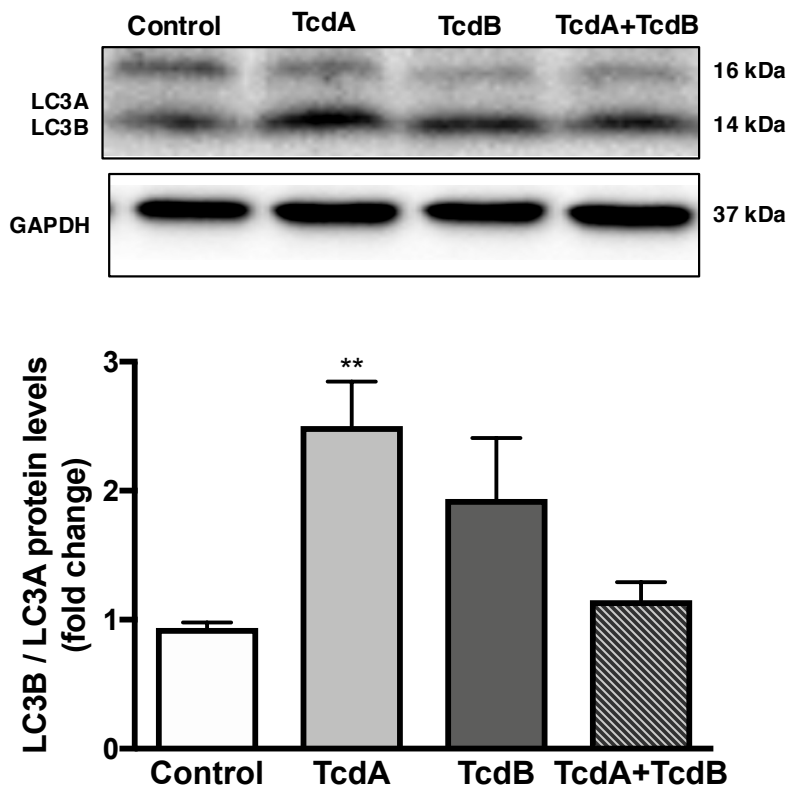
Figure 49: Mice administered TcdA had increased colonic LC3B protein levels. 10-12 week old female C57BL/6 mice were intrarectally administered purified TcdA (10 µg), TcdB (10 µg), or TcdA/TcdB (5 µg each) in 100 µl PBS. After 4h, mice were sacrificed and colonic mucosal scrapings were harvested. Relative LC3B levels (normalized to LC3A) in total protein extracted from colonic mucosa is shown by Western blotting (n=4) (**$p < 0.01$).

3.3.6 DRA protein is significantly decreased in patients with CDI

To further establish the role of DRA in CDI, we obtained slides from sections of transverse colonic biopsies from healthy subjects and patients with recurrent CDI. Using immunofluorescent staining of DRA, we found that CDI patients exhibited a drastic reduction in DRA protein levels compared to healthy subjects **(Figure 50)**. Notably, this decrease in DRA expression appeared to be more robust in the CDI patient biopsies than in our toxigenic mouse model. This marked decrease in CDI patients further confirmed our findings from cell culture and the toxigenic mouse model of CDI.
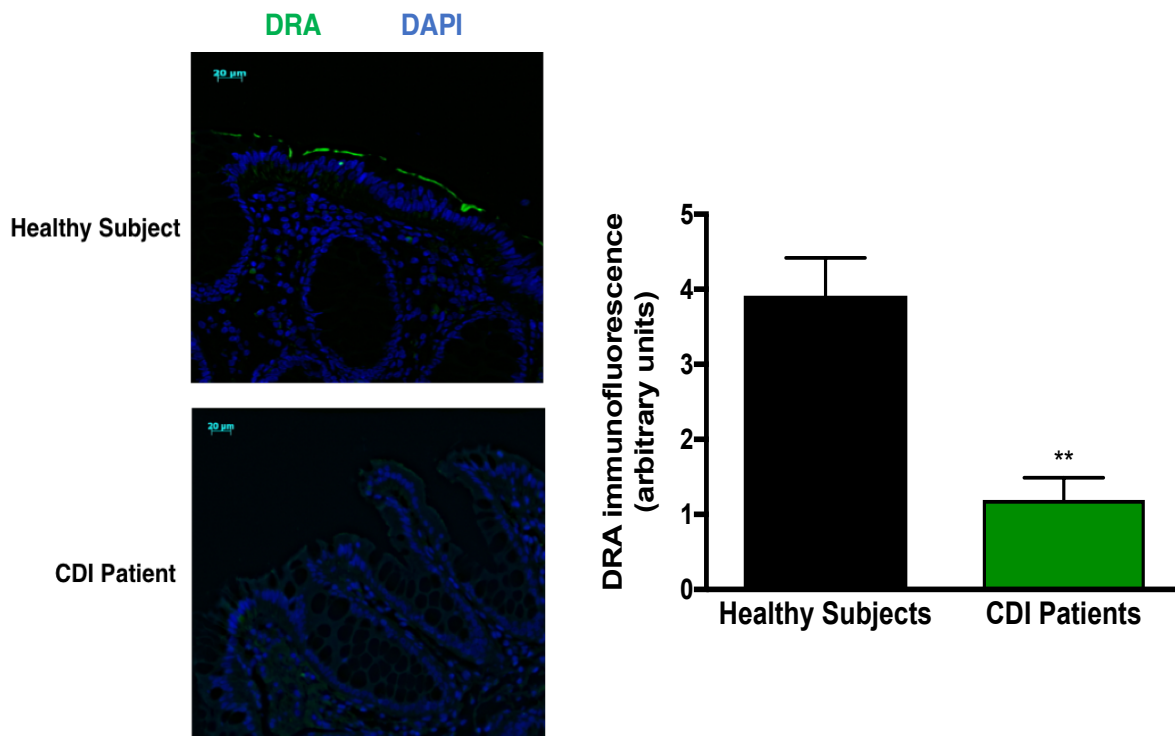
Figure 50: Patients with recurrent *Clostridium difficile* infection exhibited a significant loss in colonic DRA protein. Immunostaining of DRA (green) in transverse colonic biopsies of healthy and CDI patients and semiquantitative analysis of surface DRA expression compared to healthy colon. Representative images from observations seen in n=3 healthy and CDI patients (**$p < 0.01$)

4. DISCUSSION

Clostridium difficile infection is the primary cause of nosocomial diarrhea and hospital acquired infection in the United States (24, 156). In recent years, the emergence of hypervirulent strains and higher recurrence rates have made CDI an increasing health concern worldwide (33, 39, 137). Despite its prevalence and increasing severity, the pathophysiology underlying *C. difficile* associated diarrhea remains poorly understood. In these studies, we have examined the key colonic Cl$^-$ transporter DRA (SLC26A3) and found that purified *C. difficile* toxins TcdA and TcdB significantly reduced DRA protein levels in Caco2 cells, an intestinal epithelial cell line. This downregulation of DRA was not cell-line specific as similar results were obtained in T84 cells (a secretory crypt-like human colonic cell line). Our data also showed that the decrease in DRA in response to toxins was not due to cellular toxicity as no significant change in cell death was observed as assessed by LDH release *in vitro*. These toxin-mediated effects appeared to be specific to DRA as PAT-1 and NHE3 protein and mRNA levels were unaffected by either toxin *in vitro*. Interestingly, treatment with the highest dose of purified TcdA, but not TcdB, resulted in a significant decrease in intestinal SCFA transporter MCT-1 protein levels. Our *in vitro* studies also showed no changes in DRA mRNA levels indicating that the downregulation of DRA by TcdA and TcdB likely occurred at the post-transcriptional level. Likewise, mRNA levels of various other intestinal ion transporters including MCT1, NHE2, PAT-1, CFTR, and SERT also remained unchanged in response to purified *C. difficile* toxins.

Our current studies also investigated the potential role of TcdA and TcdB glucosyltransferase activity on DRA downregulation *in vitro.* Our results showed that the toxin-mediated downregulation of DRA protein was independent of the

glucosyltransferase ability as GTD deficient toxins also significantly decreased DRA protein levels *in vitro.* Given that only DRA protein, but not mRNA, was affected by *C. difficile* toxins, we also investigated the possibility of increased involvement of protein degradation pathways. To that end, we found that co-treatment of Caco2 monolayers with purified toxins and Bafilomycin A1, a known inhibitor of lysosomal and autophagic degradation, abrogated the effects of the toxins on DRA protein expression. These results indicated that *C. difficile* toxins may have induced the increased degradation of DRA protein.

Utilizing a toxigenic intrarectal mouse model of CDI, we also found that TcdA alone and TcdA + TcdB administration significantly reduced colonic DRA protein expression in mice. Similar to our results *in vitro*, this downregulation of DRA protein was not seen at the mRNA level in these mice. Interestingly, mice administered TcdA and TcdA+TcdB also had reduced colonic expression of NHE3 without significant alterations in mRNA levels. Administration of purified TcdA also resulted in an increase in transcript levels of inflammatory cytokines IL-1β, CXCL1, IL-6, and COX2. Furthermore, only TcdA-treated mice had elevated levels of colonic myeloperoxidase (MPO), a neutrophil chemoattractant and marker of inflammation. Finally, our toxigenic mouse model also identified a possible role for autophagy in toxin-mediated CDI as TcdA-treated mice had decreased levels of autophagy related proteins ATG16L1 and Beclin-1. Furthermore, LC3B, a critical component of autophagosome maturation and fusion, was increased in mice administered TcdA.

Lastly, using colonic biopsies from healthy and recurrent CDI patients, we found that patients with recurrent CDI exhibited a drastic loss of colonic DRA protein compared

to healthy controls. Taken together, these studies show, for the first time, that toxin-mediated downregulation of Cl^-/HCO_3^- exchanger DRA may play a key role in decreasing intestinal epithelial electrolyte absorption in CDI and hence may contribute to CDI associated diarrhea.

4.1   Downregulation of DRA by *C. difficile* toxins

The functional coupling of Na^+/H^+ and Cl^-/HCO_3^- exchangers is the predominant route for electroneutral NaCl absorption in the human intestine. SLC26A3 (DRA) is a Cl^-/HCO_3^- exchanger expressed throughout the mammalian intestine with the highest expression seen in the colon (50, 119). Intestinal luminal chloride absorption through DRA has a well-established role in diarrheal diseases (15, 135, 136, 164). A loss of function mutation in DRA causes congenital chloride diarrhea (CLD), a disease characterized by profuse, watery diarrhea, high fecal Cl^- content, and metabolic alkalosis (161). Likewise, DRA knockout mice exhibit reduced chloride absorption and have a severe diarrheal phenotype similar to that of CLD patients (136, 164). DRA dysfunction has also been tied to cases of infectious diarrhea as well (51, 82). Studies have shown that EPEC-infected intestinal epithelial cells have decreased levels of apical DRA due to increased endocytic and decreased exocytic trafficking to the plasma membrane (54). Similarly, mice infected with *C. rodentium*, the murine counterpart of EPEC, also have decreased DRA mRNA and protein levels in the distal colon (83). Taken together, these reports illustrate the critical role for DRA in mediating intestinal luminal chloride absorption in inflammatory and infectious diarrhea.

We first investigated the effects of purified *C. difficile* toxins on total DRA expression *in vitro*. In intestinal epithelial cells, our results showed a significant decrease in DRA protein, but not mRNA levels, in response to TcdA and TcdB. We also examined colonic DRA expression using a previously established toxigenic mouse model of CDI (63). Our results showed that mice administered purified TcdA alone and TcdA + TcdB had a significant loss in DRA protein levels. Interestingly, DRA protein levels remained unaffected in mice administered TcdB alone, a finding different from our *in vitro* studies. Given that the efficacy of TcdA or TcdB in various models of CDI has been heavily debated (19, 95), it is possible that TcdA is more potent in this animal model of CDI. Thus, future mechanistic studies of TcdA-specific downregulation of DRA protein in the toxigenic mouse model will significantly aid in the understanding of *C. difficile* infection *in vivo*. Similar to our results *in vitro*, DRA mRNA levels were unaffected by both toxins *in vivo*. Given our *in vitro* and *in vivo* results, we then hypothesized that toxin-mediated downregulation of DRA protein occurred at the post-transcriptional level. Considering this, we examined the possible mechanisms of toxin-mediated DRA protein downregulation, which are discussed in detail in the following sections.

4.1.1 Role of Rho GTPase inactivation in toxin-mediated downregulation of DRA

Symptoms associated with *C. difficile* infection (diarrhea, pseudomembranous colitis, disruption of the intestinal barrier) are primarily associated with two major cytotoxins, TcdA and TcdB (24, 147). Both TcdA and TcdB are large glucosylating enterotoxins that irreversibly glycosylate Rho family GTPases (Rac1, Cdc42, Rho) at Thr-35 or Thr-37 (103, 147). The inactivation of Rho GTPases elicits cytoskeletal changes,

disrupts tight junctions, induces inflammatory cascades, and causes cell death by both apoptotic and necrotic mechanisms (12, 24, 70, 86, 160). While many of the cytotoxic and cytopathic effects of TcdA and TcdB are attributed to the glucosyltransferase activity of the toxins, recent reports have shown glucosyltransferase-independent effects as well (24, 117). To investigate the contribution of the GTD domain to the toxin-mediated decrease in DRA protein, we utilized glucosyltransferase mutant TcdA (TcdA DXD) and TcdB (TcdB DXD). The DXD mutant toxins were obtained through our collaboration with Dr. Borden Lacy's laboratory at Vanderbilt. These DXD mutants have double point mutations in their GTD domains thus removing their glucosyltransferase activity (23, 24). The mutant toxins were well-validated for their lack of glucosyltransferase activity by the Lacy laboratory (23, 24). Additionally, the DXD mutants were validated for efficacy in Caco2 cells as evidenced by their inability to glycosylate Rac1 (compared to wild type toxins). Our studies showed that DRA protein was downregulated in the presence of both *C. difficile* toxins regardless of GTD function. This finding indicated that *C. difficile* toxins decreased DRA protein in a Rho GTPase independent manner.

In addition to the GTD domain, TcdA and TcdB have three other functional domains including the CROPs region used in receptor binding, the autoprocessing region, and the delivery domain (2, 41). The autoprocessing domain possesses a cysteine protease domain (CPD) responsible for toxin maturation and release of the GTD domain into the host cell cytosol (1, 147). Using autoprocessing and GTD mutant toxins, Chumbler et al reported that TcdB-induced necrosis of intestinal epithelial cells was independent of both the autoprocessing and GTD toxin domains (23). In future studies,

the use of autoprocessing mutant toxins may help elucidate the role of the precise toxin region responsible for DRA downregulation *in vitro.*

4.1.2 Effect of *C. difficile* toxins on the cellular cytoskeleton

Previous studies have shown that dysregulation of cytoskeletal proteins can affect the expression and/or function of intestinal ion transporters (54, 92, 144). For example, Asghar et al showed that keratin-8 (an intermediate filament component) deficient mice exhibited decreased DRA protein and mRNA levels. Additionally, silencing of K8 in Caco2 cells resulted in decreased DRA protein levels (6). Studies from our lab have also identified a role of cytoskeletal components in the modulation of DRA apical membrane levels in response to EPEC infection (51, 54). Treatment of intestinal epithelial cells with EPEC induced an increase in clathrin-independent endocytosis of DRA from the apical membrane (54). Additionally, these studies showed that DRA was redistributed from its normal association in the plasma membrane with lipid rafts to detergent soluble membrane fractions (54). The loss of DRA protein, however, was only seen in membrane associated DRA with total DRA protein levels remaining unchanged (54). Likewise, another recent study has reported that DRA expression and function were drastically reduced in intestinal epithelial cells lacking actin motor myosin 5b (Myo5b), a cytoskeletal component important in plasma membrane recycling (80). Loss of function mutations in Myo5b are known to cause microvillus inclusion disease (MVID), a disease characterized by secretory diarrhea, villus atrophy, and brush border membrane defects (80). Taken together, these studies highlight the pivotal role of the cellular cytoskeleton in maintaining normal DRA protein expression and localization in intestinal epithelial cells.

In this regard, TcdA and TcdB are also known to alter barrier function in Caco2 cells through the reorganization of actin filaments and tight junction proteins such as ZO-1, occludin, and claudin (117). Thus, future studies may examine the relationship between cytoskeletal reorganization and DRA down-regulation by *C. difficile* toxins. However, it should be noted that cytoskeletal changes by TcdA and TcdB are widely considered secondary to glucosyltransferase activity of the toxins (35, 146, 147). Therefore, it is unlikely that DRA expression changes are due to cytoskeletal disruptions as DRA protein levels decreased regardless of a functional toxin GTD domain. Additionally, some strains of *C. difficile,* including recent hypervirulent NAPI/027 strains, also produce a third toxin, binary toxin or *C. difficile* transferase (CDT). CDT is known to cause microtubule-based protrusions and F-actin depolymerization via ADP-ribosylation of actin at arginine 177 (49, 133). Preliminary studies in our lab found that total DRA protein expression was unchanged after CDT toxin treatment (data not shown). Given that EPEC-induced endocytosis of apical DRA was microtubule-dependent, future detailed studies should focus on the possible effect of CDT on DRA apical membrane localization and function.

4.1.3 Role of inflammatory cascades in DRA downregulation

One of the most commonly used *in vivo* models of CDI is the small animal ileal loop method, a surgical procedure involving ligation of the terminal ileum after injection with *C. difficile* toxins (32, 62). While this method is a mainstay of CDI animal models, it is not without its drawbacks. In addition to the risks associated with small animal surgery, the primary target of human CDI is the colon, not the ileum. Therefore, our studies utilized

a toxigenic intrarectal mouse model developed by Hirota *et al.* (63). In contrast to previous methodologies (22, 153), this mouse model requires no prior antibiotic treatment and allows direct intrarectal instillation of *C. difficile* toxins into the colon. As mentioned earlier, we found that mice administered TcdA or TcdA + TcdB exhibited significantly lower colonic DRA protein levels. Mice administered TcdB alone, however, exhibited no changes in DRA protein levels. Since DRA protein levels were significantly lower in mice administered *C. difficile* toxins, we wanted to evaluate the potential role of intestinal inflammation in downregulation of DRA in this mouse model. In this context, the establishment of this intrarectal model by Hirota et al showed that only TcdA was capable of inducing colonic tissue damage and intestinal inflammation (63). Similarly, our results showed that only TcdA alone caused a significant increase in colonic myeloperoxidase (MPO) levels, a key marker of neutrophil recruitment and intestinal inflammation. TcdA also induced a significant increase in mRNA levels of pro-inflammatory cytokines commonly associated with human CDI, specifically IL-1β, IL-6, CXCL1, and COX2 (14, 23, 35, 147). Although markers of inflammation (cytokine mRNA levels and MPO activity) were elevated in TcdA-treated mice, no toxin treated mice exhibited histological colonic defects as shown by H&E staining and inflammatory scoring by a blinded pathologist (Dr. Christine Salibay, UIC). Interestingly, mice administered TcdA + TcdB did show a relatively higher inflammatory score (compared to control), however, a total inflammatory score under 6 was not considered significant indicating that overall inflammation was quite mild. Furthermore, TcdA + TcdB-treated mice did not exhibit elevated cytokine mRNA levels or an increase in MPO activity. This is noteworthy as it indicated that the inflammation seen in this toxigenic mouse model is not only TcdA-dependent, but dose-

dependent as TcdA + TcdB-treated mice were administered only 5 μg of TcdA. Thus, while both TcdA and TcdA + TcdB -treated mice had significant loss of DRA protein, only TcdA-treated mice exhibited colonic inflammation. These results indicated that the toxin-mediated decrease in DRA protein was likely independent of inflammation *in vivo*. Further supporting this notion, previous studies have shown that the decrease in DRA protein by inflammatory mediators is also seen at the transcriptional level (6, 83, 129, 168). For example, downregulation of DRA is known to occur at the post-transcriptional level after IFNγ treatment *in vitro* (129). Additionally, the downregulation of DRA mRNA and protein levels in patients with UC was shown to occur downstream of intestinal inflammation (168).

4.1.4 Role of protein degradation pathways

Modulation of intestinal ion exchangers NHE3 and DRA has been implicated in a variety of inflammatory and infectious models of diarrhea (6, 51, 83, 119). Consistent with these studies, TcdA and TcdB caused a significant decrease in DRA protein levels *in vitro*. However, our current studies did not show alterations in DRA mRNA, an observation frequently seen in other models of diarrhea (141, 168). For example, patients with IBD have decreased expression of DRA protein and mRNA levels (168). Additionally, studies have shown that probiotics like *Lactobacillus* attenuate the downregulation of DRA induced in inflammatory models of diarrhea (141). Thus, in contrast to the downregulation of DRA seen during inflammation, our results indicated that the toxin-mediated alterations in DRA protein likely occurred post-transcriptionally. One possible mechanism by which *C. difficile* toxins may have decreased DRA protein *in vitro* is by increasing cellular

degradation of DRA protein. Protein degradation is divided into two major pathways, the ubiquitin-proteasome system (UPS) and the lysosomal/autophagy pathway, described below.

One pathway regulating cellular protein degradation is the degradation of large misfolded or damaged proteins in lysosomes. Lysosomes are heterogenous membrane-bound organelles containing over 60 hydrolytic enzymes to aid in protein degradation (96, 167). Lysosomes receive their intracellular substrates from endocytosis, phagocytosis, and autophagy (43, 65). Lysosomal degradation of substrates from these pathways occurs via lysosomal fusion with endosomes, phagosomes and autophagosomes and subsequent degradation of the engulfed contents. Lysosomal digestion of extracellular material occurs through endocytosis and phagocytosis while intracellular proteins are degraded through autophagy (43).

Autophagy is the degradation of proteins through fusion with lysosomes after the *de novo* formation of double membrane vacuoles called autophagosomes. Autophagy dysregulation has been implicated in a variety of diseases including cancers, neurodegenerative disorders, and infections (10). Autophagy is a precisely regulated cellular process mediated by key autophagy related proteins (ATGs) (43). Many studies have reported the modulation of ATG proteins by pathogenic bacteria to exploit cellular autophagy and promote bacterial survival (65, 76, 101). For example, *M. tuberculosis* has been shown to inhibit ROS-induced autophagy induction and block Rab7-mediated fusion with lysosomes, effectively inhibiting autophagy at two steps (76). Additionally, *S. typhyimurium* has been shown to utilize autophagy machinery to repair its vacuolar membrane and promote intracellular survival (72). Interestingly, while the exploitation of

autophagy by many intracellular pathogens is well-characterized, the role of autophagy in *C. difficile* infection remains poorly understood.

Recently, a study published by He et al reported the effects of *C. difficile* TcdB on autophagy and cell growth arrest (58). To our knowledge, this was the first article published on *C. difficile* toxins and autophagy. In these studies, He et al utilized immunofluorescent imaging and autophagy-deficient cell lines to examine the effects of TcdB on autophagy and the inhibition of cellular proliferation. They reported that 5 ng/ml of TcdB resulted in increased accumulation of LC3 puncta and autophagosome accumulation (58). Furthermore, they found that this induction of autophagy by TcdB was dependent on the glucosyltransferase activity of the toxin (58). In addition to examining LC3-positive autophagosomes, this study also investigated how this increase in autophagy would affect cell proliferation and cell rounding in response to TcdB. Using ATG7- deficient HeLa cells, they found that the TcdB-induced inhibition of cell proliferation was facilitated by autophagy (58). Furthermore, this TcdB-mediated autophagy induction utilized the mTOR pathway and PI3K complex, although the mechanism remained unclear. Overall, this study concluded that TcdB-mediated autophagy induction inhibited host cell proliferation. Furthermore, the glucosyltransferase activity of TcdB was necessary for autophagy induction and the subsequent autophagy-mediated cell growth arrest. Finally, while the GTD activity of TcdB is related to both cell rounding and autophagy, the two processes occurred independently (58).

For our current studies on autophagy, we first identified the role of lysosomal degradation in DRA downregulation through use of bafilomycin A1 treatment along with *C. difficile* toxins. Bafilomycin prevents endosomal/lysosomal acidification through its

inhibition of vacuolar H$^+$ ATPase (167). This inhibition also prevents the maturation and fusion of autophagomes with lysosomes and as such, was utilized to block protein degradation through lysosomes. Our results showed that the toxin-mediated decrease in DRA protein levels was inhibited by co-treatment with bafilomycin.This indicated that *C. difficile* toxins were likely increasing DRA protein degradation through degradation in lysosomes. Since bafilomycin A1 not only inhibits lysosomal degradation but also autophagy, further studies were needed to identify whether DRA downregulation in lysosomes might be occurring specifically through autophagy.

Given that the study by He et al was not yet published, we first examined the effects of *C. difficile* toxins on various autophagy related proteins. One autophagy protein of interest in our studies was ATG16L1 due to its association with inflammatory disorders and infections specifically in the GI tract (88, 101). ATG16L1 has been implicated specifically in GI diseases as a mutation in ATG16L1 is associated with an increased risk of IBD (88). Additionally, loss of ATG16L1 in mice infected with uropathogenic *E. coli* (UPEC) have higher levels of IL-1β production from macrophages and increased inflammation. Likewise, adherent and invasive *E. coli* (AIEC) infection in intestinal epithelial cells causes an upregulation of microRNAs that reduce ATG16L1 levels and inhibit autophagy (65). Given this, our studies first investigated how *C. difficile* toxins affected ATG16L1 protein levels. Our results showed that ATG16L1 protein was significantly decreased in Caco2 cells treated with TcdA or TcdB. Additionally, ATG16L1 protein was also decreased in the presence of CDT. To our knowledge, this was the first insight into the effect of CDT binary toxin on host cell autophagy. Further supporting our results *in vitro,* results from our toxigenic mouse model showed that TcdA-treated mice

had significant loss of ATG16L1 protein. Together, these results indicated that purified *C. difficile* toxins reduced protein levels of ATG16L1 and appeared to inhibit host cell autophagy. The study published by He et al did not specifically look at the downregulation of autophagy related proteins in response to toxins, but rather utilized ATG7 deficient cell lines to examine the effects of TcdB. In light of this, future studies may examine whether ATG7 is knocked down in response to either TcdA or TcdB. Additionally, *in vitro* studies utilizing ATG16L1 knockdown may help in further elucidating the effect of the toxin-mediated downregulation of ATG16L1.

We next investigated whether *C. difficile* toxins would affect other stages of autophagy. To that end, we examined Beclin-1 protein levels both *in vitro* and *in vivo*. Beclin-1 is part of the ATG14L-Vsp34 complex that regulates initiation of autophagy at the forming phagophore (43, 79). While less is known about interplay between Beclin-1 and bacterial pathogens, one study reported that mice lacking Beclin-1 are more resistant to *A. phagocytophilum* infection and proposed that the bacteria utilizes autophagic machinery for replication (76). Similar to our results seen with ATG16L1, Beclin-1 protein levels were also decreased in mice administered TcdA. Beclin-1 levels were not assessed *in vitro,* and this should be examined in future studies. This result, along with those seen in ATG16L1, appears to show a decrease in host cell autophagy in response to *C. difficile* toxins. It is worth noting that Beclin-1 levels, like ATG16L1 levels, have not been previously investigated in the context of CDI and this finding warrants further investigation. One possible way that purified toxins may decrease Beclin-1 or ATG16L1 protein is through direct interaction with the autophagy machinery, and as such, co-

immunoprecipitation assays with TcdA or TcdB and autophagy related proteins would be worthwhile in future experiments.

The final autophagy related protein we examined was LC3B. LC3B, also called LC3II, is the PE-conjugated form of LC3A (43, 76). LC3B accumulation is one of the most common markers of autophagy as LC3B levels will remain high until autophagosomal degradation (43, 79). Interestingly, we found that in Caco2 cells treated with TcdA and TcdB, LC3B levels were significantly increased. Additionally, mice administered TcdA alone had increased LC3B levels whereas TcdB-treated mice did not. Initially, our results with these different autophagy related proteins appeared contradictory. The toxin-induced decrease in ATG16L1 and Beclin-1 appeared to indicate that autophagy was being inhibited while an increase in LC3B suggested an induction of autophagy. One possible explanation for this lies in the interpretation of autophagy data. Historically, electron micrographs visualizing the double-membrane autophagosomes were key for the identification of autophagy induction (76). More recently, calculation of the ratio of lipidated LC3B (compared to unlipidated LC3A) either by immnoblotting or GFP-LC3B has become the newer standard for autophagy approaches. A common misconception, however, in interpreting LC3 data is that accumulation of LC3B always means an increase in autophagy. In reality, LC3B accumulation can indicate increased LC3B formation (autophagosome biogenesis) or decreased autophagosomal degradation (79). Given this, it is possible that the increase in LC3B seen *in vitro* and *in vivo* is not due to the induction of autophagy, but rather the absence of normal autophagosomeal degradation. In this case, our results with ATG16L1, Beclin-1, and LC3B may indicate that purified *C.*

difficile toxins are inhibiting host cell autophagy at three different stages in the autophagy pathway.

As mentioned previously, the study by He et al reported that purified TcdB induces host cell autophagy in a glucosyltranserase-dependent manner. These studies showed that even at a 5 ng/ml dose of TcdB, there was an increased number of LC3$^+$ autophagosomes in both HeLa and HT29 cells (58). These results are in agreement with our current studies that showed an increase in LC3B levels after toxin treatment. To further investigate autophagic flux in these cell types, He et al also utilized the lysosomal inhibitor chloroquine in addition to TcdB. Chloroquine is used in autophagy studies to specifically block autophagosomal degradation. In this way, chloroquine treatment can be used to distinguish between increased autophagosome accumulation (induction of autophagy) and decreased autophagosome degradation (58, 79). He et al reported that chloroquine treatment further increased the TcdB-mediated autophagosomal accumulation in HeLa cells thus indicating that TcdB was, in fact, inducing autophagy and not inhibiting degradation of autophagosomes (58). While our current studies share similar results with those of He et al, our studies also showed that other ATG proteins are decreasing in the presence of both TcdA and TcdB. Thus, future studies may benefit from co-administration of toxins with chloroquine to identify whether autophagy is truly induced. Additionally, since TcdB is reportedly inducing autophagy in a glucosyltransferase-dependent manner, future studies may also investigate the expression of ATG proteins after treatment with DXD mutant toxins. Finally, it is worth noting that the studies by He et al exclusively reported the effects of low dose TcdB on autophagy (58). In fact, TcdA only increased LC3B levels at a concentration of 250 ng/ml, a dose too high to be

considered physiologically relevant (23). Our current studies, however, found that low doses of both TcdA and TcdB are capable of increasing LC3B levels *in vitro* and only TcdA alone increased LC3B protein levels in our toxigenic mouse model. Given these conflicting results, a more in depth analysis should be conducted to identify the mechanism underlying the interaction of *C. difficile* toxins with host cell autophagy.

In examining autophagy regulation by both toxins A and B, these studies were aimed at identifying the location of DRA protein degradation in lysosomes. Interestingly, autophagy may be inhibited in the presence of TcdA and TcdB and therefore, autophagy dysregulation appears to be independent of the toxin-mediated decrease in DRA protein levels. Additional studies utilizing lysosomal-associated membrane proteins, LAMP1 and LAMP2, as lysosomal markers may provide additional insight as to the localization of DRA after toxin treatment. Furthermore, staining of DRA and LC3 *in vitro* may definitively identify if DRA is targeted to developing autophagosomes in response to toxins.

Another possible mechanism for the reduction in DRA after toxin administration may be due to increased protein degradation through the ubiquitin/proteasomal pathway (UPS). Premature protein degradation of cytosolic proteins by bacterial toxins has been shown in a variety of bacterial infections including *L. monocytogenes* and enteropathogenic *E. coli (*EPEC) (123, 149). These bacteria utilize post-translational modifications of ubiquitin and ubiquitin-like proteins, such as SUMO and Nedd8, to covalently attach ubiquitin to lysine residues of proteins thus targeting them for degradation (91). Thus, future studies may examine the potential interplay between toxin-

mediated reduction in DRA protein levels and the ubiquitin/proteasomal pathway of protein degradation.

4.2   Downregulation of NHE3 by *C. difficile* toxins

Electroneutral NaCl absorption is primarily mediated through the coupling of Na$^+$/H$^+$ exchanger 3 (NHE3) and the Cl$^-$/HCO$_3^-$ exchanger (DRA) (119). Previous work has shown that TcdB causes internalization of NHE3 from the apical surface of renal and placental cell lines (57). This mislocalization of NHE3 was suggested to have caused an inhibition of NHE3 during CDI. However, when using a human intestinal organoid (HIO) model system, Engevik et al showed that NHE3 levels were reduced at both the mRNA and protein levels when HIOs were infected with toxin-producing *C. difficile* (42)*.* Interestingly, our current studies did not find alterations in NHE3 protein or mRNA levels in Caco2 cells. This may have been due to use of different model systems and/or cell types used in addition to the different effects commonly seen in different strains of *C. difficile* and varying concentrations of toxins (70, 95, 100). Additionally, since Caco2 cells are transformed human colonic cells, it is possible that some components of the regulatory machinery for NHE3 down regulation by *C. difficile* toxins were absent.

The results published by Hayashi et al exclusively reported the effects of TcdB on NHE3 localization and activity. Their studies showed that the redistribution of NHE3 was due to the dephosphorylation of ezrin, a member of the ERM protein family that mediates interactions between the actin cytoskeleton and the plasma membrane. Ezrin is known to play key roles in cell adhesion, migration, and cytoskeletal organization (57). By decreasing the stability of ezrin, Hayashi et al hypothesized that apical NHE3 was

increasingly endocytosed thus causing a decrease in surface level NHE3 activity (57). Importantly, total protein levels of NHE3 remained unchanged in these studies. It should be noted that the studies conducted by Hayashi et al used only renal and placental cell lines, not intestinal epithelial cells. Therefore, while their findings on NHE3 were novel, the effects of *C. difficile* toxins on intestine-specific NHE3 were still unknown.

Given the limitations of prior studies, Engevik et al further investigated the modulation of NHE3 in CDI using human intestinal organoids (HIOs) and CDI patient biopsies (42). Use of HIOs has become increasingly popular as they more closely resemble native intestine compared to classical cell culture systems. Intestinal organoids contain all intestinal cell lineages, have secretory and absorptive cell functions, secrete mucus, and exhibit cellular architecture akin to the mammalian intestine (42, 84). In these studies, HIOs were microinjected with either toxin-producing *C. difficile* NAP1/027 cultures or stool supernatants of CDI patients and examined for NHE3 function and expression. Additionally, transverse colonic biopsies of patients with recurrent CDI were examined for loss of apical NHE3 expression. In contrast to the work of Hayashi et al, these studies found that NHE3 protein and mRNA expression was downregulated in HIOs microinjected with *C. difficile* or CDI stool supernatants. Furthermore, patients with recurrent CDI had significant loss of NHE3 protein levels at the apical surface of colonic enterocytes (42). The conflicting results shown by Hayashi and Engevik in renal/placental epithelial cells and human colonic biopsies, respectively, may have been partly due to key differences between *in vitro* models and human CDI. Additionally, the use of HIOs in Engevik's studies represented a superior model system and allowed for examination of NHE3 expression in all intestinal cell lineages.

One important factor in the comparison of these results is the concentration of toxins used. Hayashi et al administered TcdB at a concentration of 1 μg/ml, whereas our current studies used no more than 10 ng/ml for either toxin. Thus, it is possible that a high concentration of TcdB elicits different effects than the lower doses utilized in these studies. This notion is supported by the numerous studies reporting differential effects of both TcdA and TcdB depending on the concentrations used (23, 24, 103, 111). Importantly, clinical reports of TcdB concentration in CDI patient stool has been estimated at 5 pM to 413 pM (23). The maximum toxin concentration used in our *in vitro* studies was approximately 19 pM TcdA and 32 pM TcdB. Hayashi et al, on the other hand, used approximately 4 nM TcdB (57). Thus, our studies on NHE3 in Caco2 cells utilized more physiologically relevant concentrations of *C. difficile* toxins than previously published reports.

Another important component to consider is the strain of *C. difficile* utilized in the studies of Engevik et al (42), as different strains of *C. difficile* are known to have varying disease severities (146, 153). Also, respective roles of TcdA and TcdB in CDI pathogenesis have been shown to be different across various model systems (20, 24, 95). For example, TcdA was historically considered more damaging in small animal ileal loop models (32, 153), while TcdB has been considered to be a more potent cytotoxin (32, 95, 143). In our intrarectal toxigenic mouse model, we found that TcdA alone and TcdA + TcdB significantly reduced total NHE3 protein levels without changing mRNA levels. This finding may illustrate an emerging role for TcdA in NHE3 dysregulation as purified TcdB alone did not induce changes in NHE3 expression *in vitro* or *in vivo.* Interestingly, the *C. difficile* strain utilized by Engevik et al belonged to the epidemic

hypervirulent NAP1/027 strain, which not only produces high levels of TcdA and TcdB, but is also CDT (binary toxin) positive (42, 49, 121, 156). Therefore, another possible confounding factor in deciphering the dysregulation of NHE3 by *C. difficile* may be the addition of binary toxin. To our knowledge, no studies have been done on the effects of CDT on NHE3 expression and function. Thus, in future studies it would be of interest to examine the contribution, if any, of CDT to NHE3 dysregulation in response to *C. difficile* toxins A and B.

4.3   Effects of *C. difficile* toxins on PAT-1 expression *in vitro* and *in vivo*

The functional coupling of DRA and NHE3 is the predominant route for electroneutral NaCl absorption in the mammalian intestine (50, 136, 164). In addition to DRA, some studies have reported the functional coupling of NHE3 with another Cl^-/HCO_3^- exchanger, PAT-1 or SLC26A6 in the small intestine (3, 158). PAT-1, like DRA, is an intestinal luminal Cl^-/HCO_3^- exchanger found predominantly in the duodenum, jejunum, and ileum with mRNA transcripts also seen in the heart, kidneys and pancreas (74). Although both PAT-1 and DRA facilitate intestinal luminal Cl^- absorption, only DRA is predominantly expressed in the colon (100, 119), the primary site of *C. difficile* colonization and infection (156). In contrast, almost no PAT-1 is expressed in the colon (158, 159). Furthermore, DRA, but not PAT-1, knockout mice exhibit a diarrheal phenotype similar to that seen in Congenital Chloride Diarrhea (CLD) (75). Our current studies found no changes in PAT-1 mRNA *in vitro* or *in vivo.* Additionally, PAT-1 protein expression was unchanged after toxin administration to Caco2 monolayers. It should be noted that PAT-1 protein levels were not examined *in vivo* because the murine colon has

almost negligible PAT-1 expression (3). These findings illustrate that the effects of TcdA and TcdB were specific to DRA rather than affecting other Cl^-/HCO_3^- exchangers in general. Also, our results further support previous studies that reported the dysregulation of DRA in infectious models of diarrhea (51, 82, 83).

4.4   Purified TcdA increased MDR1 mRNA levels *in vitro*

Multi-drug resistance 1 (MDR1) or P-glycoprotein (Pgp) is an ATP-dependent efflux pump important in intestinal epithelial cell defense against microbial toxins and xenobiotics (13, 127, 128). MDR1 dysfunction has been implicated in the pathophysiology underlying IBD as MDR1 expression is reportedly reduced in patients with ulcerative colitis (UC) and Crohn's disease (13). Likewise, *MDR1* knockout mice develop spontaneous colitis similar to that of humans with UC (113). IL-10 knockout mice have also been shown to have decreased MDR1 expression (17). Thus, MDR1 has emerged as a potential target for therapeutic intervention in cases of intestinal inflammation.

Studies from our lab have shown that administration of probiotic *L acidophilus* significantly decreased the attenuation of MDR1 expression in intestinal epithelial cells and in DSS-colitis mice (127). Recently, this upregulation of MDR1 function and expression was shown to occur through transcriptional regulation of the MDR1 promoter via the Erk 1/2 MAPK pathway, specifically through indution of c-Fos and c-Jun transcription factors (118).

Given the emerging role for MDR1 in intestinal inflammation, our current studies also examined the effects of *C. difficile* toxins on MDR1 expression. Interestingly, only

treatment of Caco2 monolayers with TcdA caused increased expression of MDR1 mRNA while MDR1 mRNA levels were unchanged in the presence of TcdB. These results were surprising considering that MDR1 is historically downregulated over the course of inflammation (13, 17, 113). It is important to note that the upregulation of MDR1 mRNA occurred only after 24h treatment with the highest dose of TcdA (10 ng/ml). MDR1 mRNA levels were unaffected by either toxin A or toxin B at the 6h time point. This differed from the drastic decrease in DRA protein seen in response to *C. difficile* toxins as early as 6h post-treatment and with as little as 1 ng/ml dose. It is possible that this upregulation of MDR1 occurred as a compensatory mechanism for toxin efflux employed by intestinal epithelial cells at later time points. In future studies, it would be of interest to examine the effects of *C. difficile* toxins on MDR1 protein levels and the mechanisms underlying these effects.

4.5   Effect of purified toxins on MCT-1 expression *in vitro*

Mono-carboxylate transporter MCT-1 is an intestinal epithelial short chain fatty acid transporter that mediates the H^+-linked transport of SCFAs like butyrate, lactate, acetate, and pyruvate (16, 53). Butyrate transport via MCT-1 plays a pivotal role in intestinal epithelial cell homeostasis and cell differentiation (82). Furthermore, MCT-1 dysfunction has been implicated in various diarrheal diseases including IBD, colorectal cancer, and EPEC infection (16, 53, 82, 155). In our current studies, we showed that MCT-1 protein levels were decreased in the presence of 25 ng/ml TcdA *in vitro.* In contrast, MCT-1 protein remained unaffected by any dose of TcdB. We next investigated whether the TcdA-mediated decrease in MCT-1 was dependent on the glucosyltransferase activity of

TcdA. Utilizing the DXD mutants described earlier, our results showed that MCT-1 downregulation only occurred after Caco2 treatment with wild type TcdA. This result indicated that MCT-1 protein levels, unlike DRA, were decreased due to the GTD domain of TcdA. Thus, it is unlikely that the downregulation of MCT-1 by TcdA occurred by the same toxin-mediated mechanism used to reduce DRA protein levels. Furthermore, this change in MCT-1 was not seen at the mRNA level. Thus, future studies should also investigate the possible role of protein degradation pathways in the TcdA-mediated decrease in MCT-1 protein.

4.6 Downregulation of DRA in human CDI

Given that *C. difficile* infection is the primary cause of nosocomial diarrhea and represents a significant burden to human health, we also examined the levels of DRA in transverse colonic biopsies of CDI patients. In the current studies, we found that patients with recurrent CDI had a drastic reduction in colonic DRA protein expression compared to healthy subjects. This reduction in DRA levels was similar to the findings of Engevik et al who observed that CDI patients had reduced expression of NHE3 in the transverse colon (42). Together with our results *in vitro* and *in vivo*, this finding indicated that the toxin-mediated decrease in DRA protein is a phenomenon recapitulated in multiple models of CDI, and a coupled decrease in NHE3 and DRA could contribute to CDI associated diarrhea.

5. CONCLUSION

In recent years, *Clostridium difficile* infection (CDI) has emerged as the predominant cause of hospital acquired infection and antibiotic associated diarrhea (33). CDI causes a spectrum of gastrointestinal symptoms ranging from self-limiting diarrhea to severe diarrhea and in extreme cases, pseudomembranous colitis, sepsis, and death (2, 35). The symptoms of CDI are primarily mediated through the release of two major exotoxins, TcdA and TcdB with some hypervirulent strains producing a third toxin, CDT or binary toxin (49, 156). Although many of the symptoms associated with CDI are caused by TcdA and TcdB, the pathophysiology underlying CDI associated diarrhea remains poorly understood.

Generally, diarrhea is a multifactorial disorder caused by increased secretion and/or decreased absorption in the gastrointestinal tract. The coupled operation of luminal membrane Na^+/H^+ and Cl^-/HCO_3^- exchangers is the predominant route for electroneutral NaCl absorption in the human ileum and colon (38). SLC9A3 (NHE3) is the key transporter involved in Na^+ absorption in the ileum and colon. Two members of the SLC26 gene family, SLC26A3 and SLC26A6 (DRA and PAT-1, respectively) have been implicated in intestinal luminal Cl^-/HCO_3^- exchange process, however, DRA is considered the critical transporter given its role in congenital chloride diarrhea (CLD), a genetic disorder characterized by profuse chloride-rich diarrhea and metabolic alkalosis (50, 120). Moreover, knock-down of DRA is known to induce a diarrheal phenotype, similar to CLD, in mice whereas knock-down of PAT-1 does not (161). Furthermore, DRA expression is significantly reduced in animal models of inflammatory and infectious diarrhea and in patients with inflammatory bowel disease (164, 168). Thus, electroneutral electrolyte absorption by NHE3 and DRA represents a therapeutic target for diarrheal diseases.

Previous studies have shown that purified TcdB causes internalization of NHE3 from the apical surface in various cell lines (57). Additionally, decreased NHE3 expression and function were also shown in patients with CDI. Prior to these studies, however, how *C. difficile* toxins affect DRA had not been investigated.

Our current studies demonstrated, for the first time, that *C. difficile* toxins reduced DRA protein, but not mRNA, levels in intestinal epithelial cells and, in the case of TcdA and TcdA + TcdB, in a toxigenic mouse model of CDI. Additionally, patients with recurrent CDI also showed significantly lower levels of colonic DRA protein than healthy patients. Given the critical role of DRA in intestinal NaCl absorption and its implications in infectious and inflammatory diarrhea, these findings indicate that a downregulation of DRA may be a critical factor in CDI associated diarrhea. These findings agree with earlier studies showing the inhibition of NHE3 during *C. difficile* infection (42, 57). Taken together, these studies show a direct targeting of intestinal ion transporters by *C. difficile* toxins and highlight a potentially novel target for therapeutic intervention in CDI associated diarrhea.

Given the previous reports on NHE3 dysregulation in CDI and our current studies on DRA, one exciting therapeutic option in treating CDI may be through use of probiotics. Treatment with probiotics like *L. acidophilus* and *Bifidobacteria* has been shown to counteract bacterial inhibition of DRA (83, 85, 141). Additionally, *L. acidophilus* has been shown to upregulate NHE3 expression in intestinal epithelial cells (83). Therefore, treatment of CDI patients with probiotics may prove beneficial in decreasing diarrheal symptoms due to loss of NHE3 and DRA function and expression. The addition of beneficial intestinal microbes is also the basic principal underlying fecal microbiota transplant (FMT), which is the administration of healthy donor's stool to CDI patients (33).

The use of FMT has gained popularity in recent years due to the high recurrence rate of CDI and the increasing co-morbidities associated with hypervirulent strains of *C. difficile.* It is plausible, then, that the reconstitution of the normal gut microflora allows for upregulation of intestinal ion transporters DRA and NHE3 thus alleviating the diarrheal phenotype associated with CDI. It is our hope that these current studies contribute to a better understanding of the pathophysiology of CDI associated diarrhea and how current CDI therapies may specifically target key intestinal ion transporters.

CITED LITERATURE

1.	**Abt MC**, **McKenney PT**, **Pamer EG**. Clostridium difficile colitis: pathogenesis and host defence. *Nat Rev Microbiol* 14: 609–620, 2016.

2.	**Aktories K**, **Schwan C**, **Jank T**. Clostridium difficile Toxin Biology. *Annu Rev Microbiol* 71: 281–307, 2017.

3.	**Alper SL**, **Sharma AK**. The SLC26 gene family of anion transporters and channels. *Mol Aspects Med* 34: 494–515, 2013.

4.	**Amin MR**, **Malakooti J**, **Sandoval R**, **Dudeja PK**, **Ramaswamy K**. IFN-gamma and TNF-alpha regulate human NHE3 gene expression by modulating the Sp family transcription factors in human intestinal epithelial cell line C2BBe1. *Am J Physiol, Cell Physiol* 291: C887–96, 2006.

5.	**Anbazhagan AN**, **Thaqi M**, **Priyamvada S**, **Jayawardena D**, **Kumar A**, **Gujral T**, **Chatterjee I**, **Mugarza E**, **Saksena S**, **Onyuksel H**, **Dudeja PK**. GLP-1 nanomedicine alleviates gut inflammation. *Nanomedicine* 13: 659–665, 2017.

6.	**Asghar MN**, **Priyamvada S**, **Nyström JH**, **Anbazhagan AN**, **Dudeja PK**, **Toivola DM**. Keratin 8 knockdown leads to loss of the chloride transporter DRA in the colon. *Am J Physiol Gastrointest Liver Physiol* 310: G1147–54, 2016.

7.	**Bachmann O**, **Riederer B**, **Rossmann H**, **Groos S**, **Schultheis PJ**, **Shull GE**, **Gregor M**, **Manns MP**, **Seidler U**. The Na+/H+ exchanger isoform 2 is the predominant NHE isoform in murine colonic crypts and its lack causes NHE3 upregulation. *Am J Physiol Gastrointest Liver Physiol* 287: G125–33, 2004.

8.	**Barrett KE**, **Keely SJ**. Chloride secretion by the intestinal epithelium: molecular basis and regulatory aspects. *Annu Rev Physiol* 62: 535–572, 2000.

9.	**Bejarano E**, **Cuervo AM**. Chaperone-mediated autophagy. *Proc Am Thorac Soc* 7: 29–39, 2010.

10.	**Bento CF**, **Renna M**, **Ghislat G**, **Puri C**, **Ashkenazi A**, **Vicinanza M**, **Menzies FM**, **Rubinsztein DC**. Mammalian Autophagy: How Does It Work? *Annu Rev Biochem* 85: 685–713, 2016.

11.	**Berdiev BK**, **Qadri YJ**, **Benos DJ**. Assessment of the CFTR and ENaC association. *Mol Biosyst* 5: 123–127, 2009.

12.	**Bezerra Lima B**, **Faria Fonseca B**, **da Graça Amado N**, **Moreira Lima D**, **Albuquerque Ribeiro R**, **Garcia Abreu J**, **de Castro Brito GA**. Clostridium difficile toxin A attenuates Wnt/β-catenin signaling in intestinal epithelial cells. *Infect Immun* 82: 2680–2687, 2014.

13.	**Blokzijl H**, **Borght SV**, **Bok LIH**, **Libbrecht L**, **Geuken M**, **van den Heuvel FAJ**, **Dijkstra G**, **Roskams TAD**, **Moshage H**, **Jansen PLM**, **Faber KN**. Decreased P-glycoprotein (P-gp/MDR1) expression in inflamed human intestinal

epithelium is independent of PXR protein levels. *Inflamm Bowel Dis* 13: 710–720, 2007.

14. **Bobo LD**, **Feghaly El RE**, **Chen Y-S**, **Dubberke ER**, **Han Z**, **Baker AH**, **Li J**, **Burnham C-AD**, **Haslam DB**. MAPK-activated protein kinase 2 contributes to Clostridium difficile-associated inflammation. *Infect Immun* 81: 713–722, 2013.

15. **Borenshtein D**, **Schlieper KA**, **Rickman BH**, **Chapman JM**, **Schweinfest CW**, **Fox JG**, **Schauer DB**. Decreased expression of colonic Slc26a3 and carbonic anhydrase iv as a cause of fatal infectious diarrhea in mice. *Infect Immun* 77: 3639–3650, 2009.

16. **Borthakur A**, **Gill RK**, **Hodges K**, **Ramaswamy K**, **Hecht G**, **Dudeja PK**. Enteropathogenic Escherichia coli inhibits butyrate uptake in Caco-2 cells by altering the apical membrane MCT1 level. *Am J Physiol Gastrointest Liver Physiol* 290: G30–5, 2006.

17. **Buyse M**, **Radeva G**, **Bado A**, **Farinotti R**. Intestinal inflammation induces adaptation of P-glycoprotein expression and activity. *Biochem Pharmacol* 69: 1745–1754, 2005.

18. **Cant N**, **Pollock N**, **Ford RC**. CFTR structure and cystic fibrosis. *Int J Biochem Cell Biol* 52: 15–25, 2014.

19. **Carter GP**, **Chakravorty A**, **Pham Nguyen TA**, **Mileto S**, **Schreiber F**, **Li L**, **Howarth P**, **Clare S**, **Cunningham B**, **Sambol SP**, **Cheknis A**, **Figueroa I**, **Johnson S**, **Gerding D**, **Rood JI**, **Dougan G**, **Lawley TD**, **Lyras D**. Defining the Roles of TcdA and TcdB in Localized Gastrointestinal Disease, Systemic Organ Damage, and the Host Response during Clostridium difficile Infections. *MBio* 6: e00551, 2015.

20. **Carter GP**, **Rood JI**, **Lyras D**. The role of toxin A and toxin B in the virulence of Clostridium difficile. *Trends Microbiol* 20: 21–29, 2012.

21. **Chen S**, **Sun C**, **Wang H**, **Wang J**. The Role of Rho GTPases in Toxicity of Clostridium difficile Toxins. *Toxins (Basel)* 7: 5254–5267, 2015.

22. **Chen X**, **Katchar K**, **Goldsmith JD**, **Nanthakumar N**, **Cheknis A**, **Gerding DN**, **Kelly CP**. A mouse model of Clostridium difficile-associated disease. *Gastroenterology* 135: 1984–1992, 2008.

23. **Chumbler NM**, **Farrow MA**, **Lapierre LA**, **Franklin JL**, **Haslam DB**, **Haslam D**, **Goldenring JR**, **Lacy DB**. Clostridium difficile Toxin B causes epithelial cell necrosis through an autoprocessing-independent mechanism. *PLoS Pathog* 8: e1003072, 2012.

24. **Chumbler NM**, **Farrow MA**, **Lapierre LA**, **Franklin JL**, **Lacy DB**. Clostridium difficile Toxins TcdA and TcdB Cause Colonic Tissue Damage by Distinct

Mechanisms. *Infect Immun* 84: 2871–2877, 2016.

25.   **Chumbler NM**, **Rutherford SA**, **Zhang Z**, **Farrow MA**, **Lisher JP**, **Farquhar E**, **Giedroc DP**, **Spiller BW**, **Melnyk RA**, **Lacy DB**. Crystal structure of Clostridium difficile toxin A. *Nat Microbiol* 1: 15002, 2016.

26.   **Citalán-Madrid AF**, **García-Ponce A**, **Vargas-Robles H**, **Betanzos A**, **Schnoor M**. Small GTPases of the Ras superfamily regulate intestinal epithelial homeostasis and barrier function via common and unique mechanisms. *Tissue Barriers* 1: e26938, 2013.

27.   **Clayburgh DR**, **Musch MW**, **Leitges M**, **Fu Y-X**, **Turner JR**. Coordinated epithelial NHE3 inhibition and barrier dysfunction are required for TNF-mediated diarrhea in vivo. *J Clin Invest* 116: 2682–2694, 2006.

28.   **Coates MD**, **Mahoney CR**, **Linden DR**, **Sampson JE**, **Chen J**, **Blaszyk H**, **Crowell MD**, **Sharkey KA**, **Gershon MD**, **Mawe GM**, **Moses PL**. Molecular defects in mucosal serotonin content and decreased serotonin reuptake transporter in ulcerative colitis and irritable bowel syndrome. *Gastroenterology* 126: 1657–1664, 2004.

29.   **Daig R**. Human intestinal epithelial cells secrete interleukin-1 receptor antagonist and interleukin-8 but not interleukin-1 or interleukin-6. *Gut* 46: 350–358, 2000.

30.   **Das JK**, **Salam RA**, **Bhutta ZA**. Global burden of childhood diarrhea and interventions. *Curr Opin Infect Dis* 27: 451–458, 2014.

31.   **Das JK**, **Salam RA**, **Bhutta ZA**. Global burden of childhood diarrhea and interventions. *Curr Opin Infect Dis* 27: 451–458, 2014.

32.   **de Araújo Junqueira AFT**, **Dias AAM**, **Vale ML**, **Spilborghs GMGT**, **Bossa AS**, **Lima BB**, **Carvalho AF**, **Guerrant RL**, **Ribeiro RA**, **Brito GA**. Adenosine deaminase inhibition prevents Clostridium difficile toxin A-induced enteritis in mice. *Infect Immun* 79: 653–662, 2011.

33.   **Depestel DD**, **Aronoff DM**. Epidemiology of Clostridium difficile infection. *J Pharm Pract* 26: 464–475, 2013.

34.   **Deretic V**, **Kimura T**, **Timmins G**, **Moseley P**, **Chauhan S**, **Mandell M**. Immunologic manifestations of autophagy. *J Clin Invest* 125: 75–84, 2015.

35.   **Di Bella S**, **Ascenzi P**, **Siarakas S**, **Petrosillo N**, **di Masi A**. Clostridium difficile Toxins A and B: Insights into Pathogenic Properties and Extraintestinal Effects. *Toxins (Basel)* 8: 134, 2016.

36.   **Donohoe DR**, **Garge N**, **Zhang X**, **Sun W**, **O'Connell TM**, **Bunger MK**, **Bultman SJ**. The microbiome and butyrate regulate energy metabolism and

autophagy in the mammalian colon. *Cell Metab* 13: 517–526, 2011.

37. **Donowitz M**, **Ming Tse C**, **Fuster D**. SLC9/NHE gene family, a plasma membrane and organellar family of Na⁺/H⁺ exchangers. *Mol Aspects Med* 34: 236–251, 2013.

38. **Donowitz M**, **Mohan S**, **Zhu CX**, **Chen T-E**, **Lin R**, **Cha B**, **Zachos NC**, **Murtazina R**, **Sarker R**, **Li X**. NHE3 regulatory complexes. *J Exp Biol* 212: 1638–1646, 2009.

39. **Dubberke ER**, **Olsen MA**. Burden of Clostridium difficile on the healthcare system. *Clin Infect Dis* 55 Suppl 2: S88–92, 2012.

40. **Dudeja PK**, **Rao DD**, **Syed I**, **Joshi V**, **Dahdal RY**, **Gardner C**, **Risk MC**, **Schmidt L**, **Bavishi D**, **Kim KE**, **Harig JM**, **Goldstein JL**, **Layden TJ**, **Ramaswamy K**. Intestinal distribution of human Na+/H+ exchanger isoforms NHE-1, NHE-2, and NHE-3 mRNA. *Am J Physiol* 271: G483–93, 1996.

41. **Egerer M**, **Giesemann T**, **Herrmann C**, **Aktories K**. Autocatalytic processing of Clostridium difficile toxin B. Binding of inositol hexakisphosphate. *J Biol Chem* 284: 3389–3395, 2009.

42. **Engevik MA**, **Engevik KA**, **Yacyshyn MB**, **Wang J**, **Hassett DJ**, **Darien B**, **Yacyshyn BR**, **Worrell RT**. Human Clostridium difficile infection: inhibition of NHE3 and microbiota profile. *Am J Physiol Gastrointest Liver Physiol* 308: G497–509, 2015.

43. **Eskelinen E-L**, **Saftig P**. Autophagy: a lysosomal degradation pathway with a central role in health and disease. *Biochim Biophys Acta* 1793: 664–673, 2009.

44. **Farkas K**, **Yeruva S**, **Rakonczay Z**, **Ludolph L**, **Molnár T**, **Nagy F**, **Szepes Z**, **Schnúr A**, **Wittmann T**, **Hubricht J**, **RIEDERER B**, **Venglovecz V**, **Lázár G**, **Király M**, **Zsembery Á**, **Varga G**, **SEIDLER U**, **Hegyi P**. New therapeutic targets in ulcerative colitis: the importance of ion transporters in the human colon. *Inflamm Bowel Dis* 17: 884–898, 2011.

45. **Feng Y**, **Cohen SN**. Upregulation of the host SLC11A1 gene by Clostridium difficile toxin B facilitates glucosylation of Rho GTPases and enhances toxin lethality. *Infect Immun* 81: 2724–2732, 2013.

46. **Field M**. Intestinal ion transport and the pathophysiology of diarrhea. *J Clin Invest* 111: 931–943, 2003.

47. **Field M**. Intestinal ion transport and the pathophysiology of diarrhea. *J Clin Invest* 111: 931–943, 2003.

48. **Genth H**, **Huelsenbeck J**, **Hartmann B**, **Hofmann F**, **Just I**, **Gerhard R**. Cellular stability of Rho-GTPases glucosylated by Clostridium difficile toxin B.

FEBS Lett 580: 3565–3569, 2006.

49. **Gerding DN**, **Johnson S**, **Rupnik M**, **Aktories K**. Clostridium difficile binary toxin CDT: mechanism, epidemiology, and potential clinical importance. *Gut Microbes* 5: 15–27, 2014.

50. **Gill RK**, **Alrefai WA**, **Borthakur A**, **Dudeja PK**. Intestinal Anion Absorption. In: *Physiology of the Gastrointestinal Tract*. Elsevier, 2012, p. 1819–1847.

51. **Gill RK**, **Borthakur A**, **Hodges K**, **Turner JR**, **Clayburgh DR**, **Saksena S**, **Zaheer A**, **Ramaswamy K**, **Hecht G**, **Dudeja PK**. Mechanism underlying inhibition of intestinal apical Cl/OH exchange following infection with enteropathogenic E. coli. *J Clin Invest* 117: 428–437, 2007.

52. **Goldenberg SD**, **French GL**. Lack of association of tcdC type and binary toxin status with disease severity and outcome in toxigenic Clostridium difficile. *J Infect* 62: 355–362, 2011.

53. **Gonçalves P**, **Martel F**. Butyrate and colorectal cancer: the role of butyrate transport. *Curr Drug Metab* 14: 994–1008, 2013.

54. **Gujral T**, **Kumar A**, **Priyamvada S**, **Saksena S**, **Gill RK**, **Hodges K**, **Alrefai WA**, **Hecht GA**, **Dudeja PK**. Mechanisms of DRA recycling in intestinal epithelial cells: effect of enteropathogenic E. coli. *Am J Physiol, Cell Physiol* 309: C835–46, 2015.

55. **Hampe J**, **Franke A**, **Rosenstiel P**, **Till A**, **Teuber M**, **Huse K**, **Albrecht M**, **Mayr G**, **La Vega De FM**, **Briggs J**, **Günther S**, **Prescott NJ**, **Onnie CM**, **Häsler R**, **Sipos B**, **Fölsch UR**, **Lengauer T**, **Platzer M**, **Mathew CG**, **Krawczak M**, **Schreiber S**. A genome-wide association scan of nonsynonymous SNPs identifies a susceptibility variant for Crohn disease in ATG16L1. *Nat Genet* 39: 207–211, 2007.

56. **Hansen A**, **Alston L**, **Tulk SE**, **Schenck LP**, **Grassie ME**, **Alhassan BF**, **Veermalla AT**, **Al-Bashir S**, **Gendron F-P**, **Altier C**, **MacDonald JA**, **Beck PL**, **Hirota SA**. The P2Y6 receptor mediates Clostridium difficile toxin-induced CXCL8/IL-8 production and intestinal epithelial barrier dysfunction. *PLoS ONE* 8: e81491, 2013.

57. **Hayashi H**, **Szászi K**, **Coady-Osberg N**, **Furuya W**, **Bretscher AP**, **Orlowski J**, **Grinstein S**. Inhibition and redistribution of NHE3, the apical Na+/H+ exchanger, by Clostridium difficile toxin B. *J Gen Physiol* 123: 491–504, 2004.

58. **He R**, **Peng J**, **Yuan P**, **Yang J**, **Wu X**, **Wang Y**, **Wei W**. Glucosyltransferase Activity of Clostridium difficile Toxin B Triggers Autophagy-mediated Cell Growth Arrest. *Sci Rep* 7: 10532, 2017.

59. **He R**, **Peng J**, **Yuan P**, **Yang J**, **Wu X**, **Wang Y**, **Wei W**. Glucosyltransferase

Activity of Clostridium difficile Toxin B Triggers Autophagy-mediated Cell Growth Arrest. *Sci Rep* 7: 10532, 2017.

60.   **Hecht G**, **Hodges K**, **Gill RK**, **Kear F**, **Tyagi S**, **Malakooti J**, **Ramaswamy K**, **Dudeja PK**. Differential regulation of Na+/H+ exchange isoform activities by enteropathogenic E. coli in human intestinal epithelial cells. *Am J Physiol Gastrointest Liver Physiol* 287: G370–8, 2004.

61.   **Hecht G**, **Hodges K**, **Gill RK**, **Kear F**, **Tyagi S**, **Malakooti J**, **Ramaswamy K**, **Dudeja PK**. Differential regulation of Na+/H+ exchange isoform activities by enteropathogenic E. coli in human intestinal epithelial cells. *Am J Physiol Gastrointest Liver Physiol* 287: G370–8, 2004.

62.   **Hirota SA**, **Fines K**, **Ng J**, **Traboulsi D**, **Lee J**, **Ihara E**, **Li Y**, **Willmore WG**, **Chung D**, **Scully MM**, **Louie T**, **Medlicott S**, **Lejeune M**, **Chadee K**, **Armstrong G**, **Colgan SP**, **Muruve DA**, **MacDonald JA**, **Beck PL**. Hypoxia-inducible factor signaling provides protection in Clostridium difficile-induced intestinal injury. *Gastroenterology* 139: 259–69.e3, 2010.

63.   **Hirota SA**, **Iablokov V**, **Tulk SE**, **Schenck LP**, **Becker H**, **Nguyen J**, **Al-Bashir S**, **Dingle TC**, **Laing A**, **Liu J**, **Li Y**, **Bolstad J**, **Mulvey GL**, **Armstrong GD**, **MacNaughton WK**, **Muruve DA**, **MacDonald JA**, **Beck PL**. Intrarectal instillation of Clostridium difficile toxin A triggers colonic inflammation and tissue damage: development of a novel and efficient mouse model of Clostridium difficile toxin exposure. *Infect Immun* 80: 4474–4484, 2012.

64.   **Hu Y-B**, **Dammer EB**, **Ren R-J**, **Wang G**. The endosomal-lysosomal system: from acidification and cargo sorting to neurodegeneration. *Translational Neurodegeneration* 4: 869, 2015.

65.   **Huang J**, **Brumell JH**. Bacteria-autophagy interplay: a battle for survival. *Nat Rev Microbiol* 12: 101–114, 2014.

66.   **Jakab RL**, **Collaco AM**, **Ameen NA**. Characterization of CFTR High Expresser cells in the intestine. *Am J Physiol Gastrointest Liver Physiol* 305: G453–65, 2013.

67.   **Janecke AR**, **Heinz-Erian P**, **Müller T**. Congenital Sodium Diarrhea: A Form of Intractable Diarrhea, With a Link to Inflammatory Bowel Disease. *J Pediatr Gastroenterol Nutr* 63: 170–176, 2016.

68.   **Jank T**, **Giesemann T**, **Aktories K**. Clostridium difficileGlucosyltransferase Toxin B-essential Amino Acids for Substrate Binding. *J Biol Chem* 282: 35222–35231, 2007.

69.   **Jiang Z**, **Asplin JR**, **Evan AP**, **Rajendran VM**, **Velazquez H**, **Nottoli TP**, **Binder HJ**, **Aronson PS**. Calcium oxalate urolithiasis in mice lacking anion transporter Slc26a6. *Nat Genet* 38: 474–478, 2006.

70. **Johal SS**, **Solomon K**, **Dodson S**, **Borriello SP**, **Mahida YR**. Differential effects of varying concentrations of clostridium difficile toxin A on epithelial barrier function and expression of cytokines. *J Infect Dis* 189: 2110–2119, 2004.

71. **Johal SS**, **Solomon K**, **Dodson S**, **Borriello SP**, **Mahida YR**. Differential effects of varying concentrations of clostridium difficile toxin A on epithelial barrier function and expression of cytokines. *J Infect Dis* 189: 2110–2119, 2004.

72. **Kageyama S**, **Omori H**, **Saitoh T**, **Sone T**, **Guan J-L**, **Akira S**, **Imamoto F**, **Noda T**, **Yoshimori T**. The LC3 recruitment mechanism is separate from Atg9L1-dependent membrane formation in the autophagic response against Salmonella. *Mol Biol Cell* 22: 2290–2300, 2011.

73. **Kato A**, **Romero MF**. Regulation of electroneutral NaCl absorption by the small intestine. *Annu Rev Physiol* 73: 261–281, 2011.

74. **Kato A**, **Romero MF**. Regulation of electroneutral NaCl absorption by the small intestine. *Annu Rev Physiol* 73: 261–281, 2011.

75. **Kim KH**, **Shcheynikov N**, **Wang Y**, **Muallem S**. SLC26A7 is a Cl- channel regulated by intracellular pH. *J Biol Chem* 280: 6463–6470, 2005.

76. **Kimmey JM**, **Stallings CL**. Bacterial Pathogens versus Autophagy: Implications for Therapeutic Interventions. *Trends Mol Med* 22: 1060–1076, 2016.

77. **Kinross JM**, **Darzi AW**, **Nicholson JK**. Gut microbiome-host interactions in health and disease. *Genome Medicine* 3: 14, 2011.

78. **Klaus A**, **Birchmeier W**. Wnt signalling and its impact on development and cancer. *Nat Rev Cancer* 8: 387–398, 2008.

79. **Klionsky DJ**, **Abeliovich H**, **Agostinis P**, **Agrawal DK**, **Aliev G**, **Askew DS**, **Baba M**, **Baehrecke EH**, **Bahr BA**, **Ballabio A**, **Bamber BA**, **Bassham DC**, **Bergamini E**, **Bi X**, **Biard-Piechaczyk M**, **Blum JS**, **Bredesen DE**, **Brodsky JL**, **Brumell JH**, **Brunk UT**, **Bursch W**, **Camougrand N**, **Cebollero E**, **Cecconi F**, **Chen Y**, **Chin L-S**, **Choi A**, **Chu CT**, **Chung J**, **Clarke PGH**, **Clark RSB**, **Clarke SG**, **Clavé C**, **Cleveland JL**, **Codogno P**, **Colombo MI**, **Coto-Montes A**, **Cregg JM**, **Cuervo AM**, **Debnath J**, **Demarchi F**, **Dennis PB**, **Dennis PA**, **Deretic V**, **Devenish RJ**, **Di Sano F**, **Dice JF**, **Difiglia M**, **Dinesh-Kumar S**, **Distelhorst CW**, **Djavaheri-Mergny M**, **Dorsey FC**, **Dröge W**, **Dron M**, **Dunn WA**, **Duszenko M**, **Eissa NT**, **Elazar Z**, **Esclatine A**, **Eskelinen E-L**, **Fésüs L**, **Finley KD**, **Fuentes JM**, **Fueyo J**, **Fujisaki K**, **Galliot B**, **Gao F-B**, **Gewirtz DA**, **Gibson SB**, **Gohla A**, **Goldberg AL**, **Gonzalez R**, **González-Estévez C**, **Gorski S**, **Gottlieb RA**, **Häussinger D**, **He Y-W**, **Heidenreich K**, **Hill JA**, **Høyer-Hansen M**, **Hu X**, **Huang W-P**, **Iwasaki A**, **Jäättelä M**, **Jackson WT**, **Jiang X**, **Jin S**, **Johansen T**, **Jung JU**, **Kadowaki M**, **Kang C**, **Kelekar A**, **Kessel DH**, **Kiel JAKW**, **Kim HP**, **Kimchi A**, **Kinsella TJ**, **Kiselyov K**, **Kitamoto K**, **Knecht E**, **Komatsu M**, **Kominami E**, **Kondo S**, **Kovács AL**,

Kroemer G, **Kuan C-Y**, **Kumar R**, **Kundu M**, **Landry J**, **Laporte M**, **Le W**, **Lei H-Y**, **Lenardo MJ**, **Levine B**, **Lieberman A**, **Lim K-L**, **Lin F-C**, **Liou W**, **Liu LF**, **Lopez-Berestein G**, **López-Otín C**, **Lu B**, **Macleod KF**, **Malorni W**, **Martinet W**, **Matsuoka K**, **Mautner J**, **Meijer AJ**, **Meléndez A**, **Michels P**, **Miotto G**, **Mistiaen WP**, **Mizushima N**, **Mograbi B**, **Monastyrska I**, **Moore MN**, **Moreira PI**, **Moriyasu Y**, **Motyl T**, **Münz C**, **Murphy LO**, **Naqvi NI**, **Neufeld TP**, **Nishino I**, **Nixon RA**, **Noda T**, **Nürnberg B**, **Ogawa M**, **Oleinick NL**, **Olsen LJ**, **Ozpolat B**, **Paglin S**, **Palmer GE**, **Papassideri I**, **Parkes M**, **Perlmutter DH**, **Perry G**, **Piacentini M**, **Pinkas-Kramarski R**, **Prescott M**, **Proikas-Cezanne T**, **Raben N**, **Rami A**, **Reggiori F**, **Rohrer B**, **Rubinsztein DC**, **Ryan KM**, **Sadoshima J**, **Sakagami H**, **Sakai Y**, **Sandri M**, **Sasakawa C**, **Sass M**, **Schneider C**, **Seglen PO**, **Seleverstov O**, **Settleman J**, **Shacka JJ**, **Shapiro IM**, **Sibirny A**, **Silva-Zacarin ECM**, **Simon H-U**, **Simone C**, **Simonsen A**, **Smith MA**, **Spanel-Borowski K**, **Srinivas V**, **Steeves M**, **Stenmark H**, **Stromhaug PE**, **Subauste CS**, **Sugimoto S**, **Sulzer D**, **Suzuki T**, **Swanson MS**, **Tabas I**, **Takeshita F**, **Talbot NJ**, **Tallóczy Z**, **Tanaka K**, **Tanaka K**, **Tanida I**, **Taylor GS**, **Taylor JP**, **Terman A**, **Tettamanti G**, **Thompson CB**, **Thumm M**, **Tolkovsky AM**, **Tooze SA**, **Truant R**, **Tumanovska LV**, **Uchiyama Y**, **Ueno T**, **Uzcátegui NL**, **van der Klei I**, **Vaquero EC**, **Vellai T**, **Vogel MW**, **Wang H-G**, **Webster P**, **Wiley JW**, **Xi Z**, **Xiao G**, **Yahalom J**, **Yang J-M**, **Yap G**, **Yin X-M**, **Yoshimori T**, **Yu L**, **Yue Z**, **Yuzaki M**, **Zabirnyk O**, **Zheng X**, **Zhu X**, **Deter RL**. Guidelines for the use and interpretation of assays for monitoring autophagy in higher eukaryotes. *Autophagy* 4: 151–175, 2008.

80. **Kravtsov DV**, **Ahsan MK**, **Kumari V**, **van Ijzendoorn SCD**, **Reyes-Mugica M**, **Kumar A**, **Gujral T**, **Dudeja PK**, **Ameen NA**. Identification of intestinal ion transport defects in microvillus inclusion disease. *Am J Physiol Gastrointest Liver Physiol* 311: G142–55, 2016.

81. **Krawisz JE**, **Sharon P**, **Stenson WF**. Quantitative assay for acute intestinal inflammation based on myeloperoxidase activity. Assessment of inflammation in rat and hamster models. *Gastroenterology* 87: 1344–1350, 1984.

82. **Kumar A**, **Alrefai WA**, **Borthakur A**, **Dudeja PK**. Lactobacillus acidophilus counteracts enteropathogenic E. coli-induced inhibition of butyrate uptake in intestinal epithelial cells. *Am J Physiol Gastrointest Liver Physiol* 309: G602–7, 2015.

83. **Kumar A**, **Anbazhagan AN**, **Coffing H**, **Chatterjee I**, **Priyamvada S**, **Gujral T**, **Saksena S**, **Gill RK**, **Alrefai WA**, **Borthakur A**, **Dudeja PK**. Lactobacillus acidophilus counteracts inhibition of NHE3 and DRA expression and alleviates diarrheal phenotype in mice infected with Citrobacter rodentium. *Am J Physiol Gastrointest Liver Physiol* 311: G817–G826, 2016.

84. **Kumar A**, **Chatterjee I**, **Gujral T**, **Alakkam A**, **Coffing H**, **Anbazhagan AN**, **Borthakur A**, **Saksena S**, **Gill RK**, **Alrefai WA**, **Dudeja PK**. Activation of Nuclear Factor-κB by Tumor Necrosis Factor in Intestinal Epithelial Cells and

Mouse Intestinal Epithelia Reduces Expression of the Chloride Transporter SLC26A3. *Gastroenterology* 153: 1338–1350.e3, 2017.

85. **Kumar A**, **Hecht C**, **Priyamvada S**, **Anbazhagan AN**, **Alakkam A**, **Borthakur A**, **Alrefai WA**, **Gill RK**, **Dudeja PK**. Probiotic Bifidobacterium species stimulate human SLC26A3 gene function and expression in intestinal epithelial cells. *Am J Physiol, Cell Physiol* 307: C1084–92, 2014.

86. **LaFrance ME**, **Farrow MA**, **Chandrasekaran R**, **Sheng J**, **Rubin DH**, **Lacy DB**. Identification of an epithelial cell receptor responsible for Clostridium difficile TcdB-induced cytotoxicity. *Proc Natl Acad Sci USA* 112: 7073–7078, 2015.

87. **Lamprecht G**, **Baisch S**, **Schoenleber E**, **Gregor M**. Transport properties of the human intestinal anion exchanger DRA (down-regulated in adenoma) in transfected HEK293 cells. *Pflugers Arch* 449: 479–490, 2005.

88. **Lassen KG**, **Kuballa P**, **Conway KL**, **Patel KK**, **Becker CE**, **Peloquin JM**, **Villablanca EJ**, **Norman JM**, **Liu T-C**, **Heath RJ**, **Becker ML**, **Fagbami L**, **Horn H**, **Mercer J**, **Yilmaz OH**, **Jaffe JD**, **Shamji AF**, **Bhan AK**, **Carr SA**, **Daly MJ**, **Virgin HW**, **Schreiber SL**, **Stappenbeck TS**, **Xavier RJ**. Atg16L1 T300A variant decreases selective autophagy resulting in altered cytokine signaling and decreased antibacterial defense. *Proc Natl Acad Sci USA* 111: 7741–7746, 2014.

89. **Lecker SH**, **Goldberg AL**, **Mitch WE**. Protein degradation by the ubiquitin-proteasome pathway in normal and disease states. *J Am Soc Nephrol* 17: 1807–1819, 2006.

90. **Lee MJ**, **Lee JH**, **Rubinsztein DC**. Tau degradation: The ubiquitin–proteasome system versus the autophagy-lysosome system. *Progress in Neurobiology* 105: 49–59, 2013.

91. **Lemichez E**, **Barbieri JT**. General aspects and recent advances on bacterial protein toxins. *Cold Spring Harb Perspect Med* 3: a013573–a013573, 2013.

92. **LENZEN H**, **Lünnemann M**, **BLEICH A**, **Manns MP**, **SEIDLER U**, **Jörns A**. Downregulation of the NHE3-binding PDZ-adaptor protein PDZK1 expression during cytokine-induced inflammation in interleukin-10-deficient mice. *PLoS ONE* 7: e40657, 2012.

93. **Lilienbaum A**. Relationship between the proteasomal system and autophagy. *Int J Biochem Mol Biol* 4: 1–26, 2013.

94. **Lord MS**, **Day AJ**, **Youssef P**, **Zhuo L**, **Watanabe H**, **Caterson B**, **Whitelock JM**. Sulfation of the bikunin chondroitin sulfate chain determines heavy chain·hyaluronan complex formation. *J Biol Chem* 288: 22930–22941, 2013.

95. **Lyras D**, **O'Connor JR**, **Howarth PM**, **Sambol SP**, **Carter GP**, **Phumoonna T**,

Poon R, **Adams V**, **Vedantam G**, **Johnson S**, **Gerding DN**, **Rood JI**. Toxin B is essential for virulence of Clostridium difficile. *Nature* 458: 1176–1179, 2009.

96.   **Ma Y**, **Galluzzi L**, **Zitvogel L**, **Kroemer G**. Autophagy and cellular immune responses. *Immunity* 39: 211–227, 2013.

97.   **Magalhães D**, **Cabral JM**, **Soares-da-Silva P**, **Magro F**. Role of epithelial ion transports in inflammatory bowel disease. *Am J Physiol Gastrointest Liver Physiol* 310: G460–76, 2016.

98.   **Mahida YR**, **Makh S**, **Hyde S**, **Gray T**, **Borriello SP**. Effect of Clostridium difficile toxin A on human intestinal epithelial cells: induction of interleukin 8 production and apoptosis after cell detachment. *Gut* 38: 337–347, 1996.

99.   **Mahida YR**, **Makh S**, **Hyde S**, **Gray T**, **Borriello SP**. Effect of Clostridium difficile toxin A on human intestinal epithelial cells: induction of interleukin 8 production and apoptosis after cell detachment. *Gut* 38: 337–347, 1996.

100. **Malakooti J**, **Saksena S**, **Gill RK**, **Dudeja PK**. Transcriptional regulation of the intestinal luminal Na$^+$ and Cl$^-$ transporters. *Biochem J* 435: 313–325, 2011.

101. **Marchiando AM**, **Ramanan D**, **Ding Y**, **Gomez LE**, **Hubbard-Lucey VM**, **Maurer K**, **Wang C**, **Ziel JW**, **van Rooijen N**, **Nuñez G**, **Finlay BB**, **Mysorekar IU**, **Cadwell K**. A deficiency in the autophagy gene Atg16L1 enhances resistance to enteric bacterial infection. *Cell Host Microbe* 14: 216–224, 2013.

102. **Masuda S**, **Oda Y**, **Sasaki H**, **Ikenouchi J**, **Higashi T**, **Akashi M**, **Nishi E**, **Furuse M**. LSR defines cell corners for tricellular tight junction formation in epithelial cells. *Journal of Cell Science* 124: 548–555, 2011.

103. **May M**, **Wang T**, **Müller M**, **Genth H**. Difference in F-actin depolymerization induced by toxin B from the Clostridium difficile strain VPI 10463 and toxin B from the variant Clostridium difficile serotype F strain 1470. *Toxins (Basel)* 5: 106–119, 2013.

104. **Melmed GY**, **Kaplan GG**, **Sparrow MP**, **Velayos FS**, **Baidoo L**, **Bressler B**, **Cheifetz AS**, **Devlin SM**, **Irving PM**, **Jones J**, **Kozuch PL**, **Raffals LE**, **Siegel CA**. Appropriateness of Combination Therapy in Inflammatory Bowel Disease: One Size Still Does Not Fit All. *Clin. Gastroenterol. Hepatol.* (March 2, 2018). doi: 10.1016/j.cgh.2018.02.036.

105. **Mount DB**, **Romero MF**. The SLC26 gene family of multifunctional anion exchangers. *Pflugers Arch* 447: 710–721, 2004.

106. **Murek M**, **Kopic S**, **Geibel J**. Evidence for intestinal chloride secretion. *Exp Physiol* 95: 471–478, 2010.

107. **Na X**, **Kim H**, **Moyer MP**, **Pothoulakis C**, **LaMont JT**. gp96 is a human

colonocyte plasma membrane binding protein for Clostridium difficile toxin A. *Infect Immun* 76: 2862–2871, 2008.

108. **Nam T**, **Han JH**, **Devkota S**, **Lee H-W**. Emerging Paradigm of Crosstalk between Autophagy and the Ubiquitin-Proteasome System. *Mol Cells* 40: 897–905, 2017.

109. **Naser SA**, **Arce M**, **Khaja A**, **Fernandez M**, **Naser N**, **Elwasila S**, **Thanigachalam S**. Role of ATG16L, NOD2 and IL23R in Crohn's disease pathogenesis. *World J Gastroenterol* 18: 412–424, 2012.

110. **Nicholas A**, **Jeon H**, **Selasi GN**, **Na SH**, **Kwon HI**, **Kim YJ**, **Choi CW**, **Kim SI**, **Lee JC**. Clostridium difficile-derived membrane vesicles induce the expression of pro-inflammatory cytokine genes and cytotoxicity in colonic epithelial cells in vitro. *Microb Pathog* 107: 6–11, 2017.

111. **Nusrat A**, **Eichel-Streiber von C**, **Turner JR**, **Verkade P**, **Madara JL**, **Parkos CA**. Clostridium difficile toxins disrupt epithelial barrier function by altering membrane microdomain localization of tight junction proteins. *Infect Immun* 69: 1329–1336, 2001.

112. **Ohta T**, **Arakawa H**, **Futagami F**, **Fushida S**, **Kitagawa H**, **Kayahara M**, **Nagakawa T**, **Miwa K**, **Kurashima K**, **Numata M**, **Kitamura Y**, **Terada T**, **Ohkuma S**. Bafilomycin A1 induces apoptosis in the human pancreatic cancer cell line Capan-1. *The Journal of Pathology* 185: 324–330, 1998.

113. **Panwala CM**, **Jones JC**, **Viney JL**. A novel model of inflammatory bowel disease: mice deficient for the multiple drug resistance gene, mdr1a, spontaneously develop colitis. *J Immunol* 161: 5733–5744, 1998.

114. **Papatheodorou P**, **Carette JE**, **Bell GW**, **Schwan C**, **Guttenberg G**, **Brummelkamp TR**, **Aktories K**. Lipolysis-stimulated lipoprotein receptor (LSR) is the host receptor for the binary toxin Clostridium difficile transferase (CDT). *Proc Natl Acad Sci USA* 108: 16422–16427, 2011.

115. **Peng L**, **Li Z-R**, **Green RS**, **Holzman IR**, **Lin J**. Butyrate enhances the intestinal barrier by facilitating tight junction assembly via activation of AMP-activated protein kinase in Caco-2 cell monolayers. *J Nutr* 139: 1619–1625, 2009.

116. **Peñaloza HF**, **Schultz BM**, **Nieto PA**, **Salazar GA**, **Suazo I**, **Gonzalez PA**, **Riedel CA**, **Alvarez-Lobos MM**, **Kalergis AM**, **Bueno SM**. Opposing roles of IL-10 in acute bacterial infection. *Cytokine Growth Factor Rev* 32: 17–30, 2016.

117. **Popoff MR**, **Geny B**. Rho/Ras-GTPase-dependent and -independent activity of clostridial glucosylating toxins. *J Med Microbiol* 60: 1057–1069, 2011.

118. **Priyamvada S**, **Anbazhagan AN**, **Kumar A**, **Soni V**, **Alrefai WA**, **Gill RK**, **Dudeja PK**, **Saksena S**. Lactobacillus acidophilus stimulates intestinal P-

glycoprotein expression via a c-Fos/c-Jun-dependent mechanism in intestinal epithelial cells. *Am J Physiol Gastrointest Liver Physiol* 310: G599–608, 2016.

119. **Priyamvada S**, **Gomes R**, **Gill RK**, **Saksena S**, **Alrefai WA**, **Dudeja PK**. Mechanisms Underlying Dysregulation of Electrolyte Absorption in Inflammatory Bowel Disease-Associated Diarrhea. *Inflamm Bowel Dis* 21: 2926–2935, 2015.

120. **Priyamvada S**, **Gomes R**, **Gill RK**, **Saksena S**, **Alrefai WA**, **Dudeja PK**. Mechanisms Underlying Dysregulation of Electrolyte Absorption in Inflammatory Bowel Disease-Associated Diarrhea. *Inflamm Bowel Dis* 21: 2926–2935, 2015.

121. **Quesada-Gómez C**, **López-Ureña D**, **Chumbler N**, **Kroh HK**, **Castro-Peña C**, **Rodríguez C**, **Orozco-Aguilar J**, **González-Camacho S**, **Rucavado A**, **Guzmán-Verri C**, **Lawley TD**, **Lacy DB**, **Chaves-Olarte E**. Analysis of TcdB Proteins within the Hypervirulent Clade 2 Reveals an Impact of RhoA Glucosylation on Clostridium difficile Proinflammatory Activities. *Infect Immun* 84: 856–865, 2016.

122. **Rahimi N**. The ubiquitin-proteasome system meets angiogenesis. *Mol Cancer Ther* 11: 538–548, 2012.

123. **Ribet D**, **Hamon M**, **Gouin E**, **Nahori M-A**, **Impens F**, **Neyret-Kahn H**, **Gevaert K**, **Vandekerckhove J**, **Dejean A**, **Cossart P**. Listeria monocytogenes impairs SUMOylation for efficient infection. *Nature* 464: 1192–1195, 2010.

124. **Ritzhaupt A**, **Wood IS**, **Ellis A**, **Hosie KB**, **Shirazi-Beechey SP**. Identification and characterization of a monocarboxylate transporter (MCT1) in pig and human colon: its potential to transport L-lactate as well as butyrate. *The Journal of Physiology* 513 (Pt 3): 719–732, 1998.

125. **Rocha F**, **Musch MW**, **Lishanskiy L**, **Bookstein C**, **Sugi K**, **Xie Y**, **Chang EB**. IFN-gamma downregulates expression of Na(+)/H(+) exchangers NHE2 and NHE3 in rat intestine and human Caco-2/bbe cells. *Am J Physiol, Cell Physiol* 280: C1224–32, 2001.

126. **Roth DM**, **Balch WE**. Modeling general proteostasis: proteome balance in health and disease. *Curr Opin Cell Biol* 23: 126–134, 2011.

127. **Saksena S**, **Goyal S**, **Raheja G**, **Singh V**, **Akhtar M**, **Nazir TM**, **Alrefai WA**, **Gill RK**, **Dudeja PK**. Upregulation of P-glycoprotein by probiotics in intestinal epithelial cells and in the dextran sulfate sodium model of colitis in mice. *Am J Physiol Gastrointest Liver Physiol* 300: G1115–23, 2011.

128. **Saksena S**, **Priyamvada S**, **Kumar A**, **Akhtar M**, **Soni V**, **Anbazhagan AN**, **Alakkam A**, **Alrefai WA**, **Dudeja PK**, **Gill RK**. Keratinocyte growth factor-2 stimulates P-glycoprotein expression and function in intestinal epithelial cells. *Am J Physiol Gastrointest Liver Physiol* 304: G615–22, 2013.

129. **Saksena S**, **Singla A**, **Goyal S**, **Katyal S**, **Bansal N**, **Gill RK**, **Alrefai WA**, **Ramaswamy K**, **Dudeja PK**. Mechanisms of transcriptional modulation of the human anion exchanger SLC26A3 gene expression by IFN-{gamma}. *Am J Physiol Gastrointest Liver Physiol* 298: G159–66, 2010.

130. **Sandle GI**. Salt and water absorption in the human colon: a modern appraisal. *Gut* 43: 294–299, 1998.

131. **Savidge TC**, **Pan W-H**, **Newman P**, **O'brien M**, **Anton PM**, **Pothoulakis C**. Clostridium difficile toxin B is an inflammatory enterotoxin in human intestine. *Gastroenterology* 125: 413–420, 2003.

132. **Schmittgen TD**, **Livak KJ**. Analyzing real-time PCR data by the comparative C(T) method. *Nat Protoc* 3: 1101–1108, 2008.

133. **Schwan C**, **Kruppke AS**, **Nölke T**, **Schumacher L**, **Koch-Nolte F**, **Kudryashev M**, **Stahlberg H**, **Aktories K**. Clostridium difficile toxin CDT hijacks microtubule organization and reroutes vesicle traffic to increase pathogen adherence. *Proc Natl Acad Sci USA* 111: 2313–2318, 2014.

134. **Schwan C**, **Stecher B**, **Tzivelekidis T**, **van Ham M**, **Rohde M**, **Hardt W-D**, **Wehland J**, **Aktories K**. Clostridium difficile toxin CDT induces formation of microtubule-based protrusions and increases adherence of bacteria. *PLoS Pathog* 5: e1000626, 2009.

135. **Schweinfest CW**, **Henderson KW**, **Suster S**, **Kondoh N**, **Papas TS**. Identification of a colon mucosa gene that is down-regulated in colon adenomas and adenocarcinomas. *Proc Natl Acad Sci USA* 90: 4166–4170, 1993.

136. **Schweinfest CW**, **Spyropoulos DD**, **Henderson KW**, **Kim J-H**, **Chapman JM**, **Barone S**, **Worrell RT**, **Wang Z**, **Soleimani M**. slc26a3 (dra)-deficient mice display chloride-losing diarrhea, enhanced colonic proliferation, and distinct up-regulation of ion transporters in the colon. *J Biol Chem* 281: 37962–37971, 2006.

137. **Seekatz AM**, **Young VB**. Clostridium difficile and the microbiota. *J Clin Invest* 124: 4182–4189, 2014.

138. **SEIDLER U**, **LENZEN H**, **CINAR A**, **TESSEMA T**, **BLEICH A**, **RIEDERER B**. Molecular Mechanisms of Disturbed Electrolyte Transport in Intestinal Inflammation. *Annals of the New York Academy of Sciences* 1072: 262–275, 2006.

139. **Shacka JJ**. The autophagy-lysosomal degradation pathway: role in neurodegenerative disease and therapy. *Frontiers in Bioscience* 13: 718, 2008.

140. **Shen A**. Clostridium difficile toxins: mediators of inflammation. *J Innate Immun* 4: 149–158, 2012.

141. **Singh V**, **Kumar A**, **Raheja G**, **Anbazhagan AN**, **Priyamvada S**, **Saksena S**, **Jhandier MN**, **Gill RK**, **Alrefai WA**, **Borthakur A**, **Dudeja PK**. Lactobacillus acidophilus attenuates downregulation of DRA function and expression in inflammatory models. *Am J Physiol Gastrointest Liver Physiol* 307: G623–31, 2014.

142. **Singhal M**, **Manzella C**, **Soni V**, **Alrefai WA**, **Saksena S**, **Hecht GA**, **Dudeja PK**, **Gill RK**. Role of SHP2 protein tyrosine phosphatase in SERT inhibition by enteropathogenicE. coli(EPEC). *Am J Physiol Gastrointest Liver Physiol* 312: G443–G449, 2017.

143. **Smits WK**, **Lyras D**, **Lacy DB**, **Wilcox MH**, **Kuijper EJ**. Clostridium difficile infection. *Nat Rev Dis Primers* 2: 16020, 2016.

144. **Sullivan S**, **Alex P**, **Dassopoulos T**, **Zachos NC**, **Iacobuzio-Donahue C**, **Donowitz M**, **Brant SR**, **Cuffari C**, **Harris ML**, **Datta LW**, **Conklin L**, **Chen Y**, **Li X**. Downregulation of sodium transporters and NHERF proteins in IBD patients and mouse colitis models: Potential contributors to IBD-associated diarrhea. *Inflamm Bowel Dis* 15: 261–274, 2009.

145. **Sun J**. VDR/vitamin D receptor regulates autophagic activity through ATG16L1. *Autophagy* 12: 1057–1058, 2016.

146. **Sun X**, **Hirota SA**. The roles of host and pathogen factors and the innate immune response in the pathogenesis of Clostridium difficile infection. *Mol Immunol* 63: 193–202, 2015.

147. **Sun X**, **Savidge T**, **Feng H**. The enterotoxicity of Clostridium difficile toxins. *Toxins (Basel)* 2: 1848–1880, 2010.

148. **Tai H-C**, **Schuman EM**. Ubiquitin, the proteasome and protein degradation in neuronal function and dysfunction. *Nature Reviews Neuroscience* 9: 826–838, 2008.

149. **Taieb F**, **Nougayrède J-P**, **Oswald E**. Cycle inhibiting factors (cifs): cyclomodulins that usurp the ubiquitin-dependent degradation pathway of host cells. *Toxins (Basel)* 3: 356–368, 2011.

150. **Tan J**, **McKenzie C**, **Potamitis M**, **Thorburn AN**, **Mackay CR**, **Macia L**. The role of short-chain fatty acids in health and disease. *Adv Immunol* 121: 91–119, 2014.

151. **Tao L**, **Zhang J**, **Meraner P**, **Tovaglieri A**, **Wu X**, **Gerhard R**, **Zhang X**, **Stallcup WB**, **Miao J**, **He X**, **Hurdle JG**, **Breault DT**, **Brass AL**, **Dong M**. Frizzled proteins are colonic epithelial receptors for C. difficile toxin B. *Nature* 538: 350–355, 2016.

152. **Tao L**, **Zhang J**, **Meraner P**, **Tovaglieri A**, **Wu X**, **Gerhard R**, **Zhang X**,

Stallcup WB, **Miao J**, **He X**, **Hurdle JG**, **Breault DT**, **Brass AL**, **Dong M**. Frizzled proteins are colonic epithelial receptors for C. difficile toxin B. *Nature* 538: 350–355, 2016.

153. **Theriot CM**, **Koumpouras CC**, **Carlson PE**, **Bergin II**, **Aronoff DM**, **Young VB**. Cefoperazone-treated mice as an experimental platform to assess differential virulence of Clostridium difficile strains. *Gut Microbes* 2: 326–334, 2011.

154. **Thiagarajah JR**, **Donowitz M**, **Verkman AS**. Secretory diarrhoea: mechanisms and emerging therapies. *Nat Rev Gastroenterol Hepatol* 12: 446–457, 2015.

155. **Thibault R**, **De Coppet P**, **Daly K**, **Bourreille A**, **Cuff M**, **Bonnet C**, **Mosnier J-F**, **Galmiche J-P**, **Shirazi-Beechey S**, **Segain J-P**. Down-regulation of the monocarboxylate transporter 1 is involved in butyrate deficiency during intestinal inflammation. *Gastroenterology* 133: 1916–1927, 2007.

156. **Vedantam G**, **Clark A**, **Chu M**, **McQuade R**, **Mallozzi M**, **Viswanathan VK**. Clostridium difficile infection: toxins and non-toxin virulence factors, and their contributions to disease establishment and host response. *Gut Microbes* 3: 121–134, 2012.

157. **Walker NM**, **Simpson JE**, **Brazill JM**, **Gill RK**, **Dudeja PK**, **Schweinfest CW**, **Clarke LL**. Role of down-regulated in adenoma anion exchanger in HCO3-secretion across murine duodenum. *Gastroenterology* 136: 893–901, 2009.

158. **Wang Z**, **Petrovic S**, **Mann E**, **Soleimani M**. Identification of an apical Cl(-)/HCO3(-) exchanger in the small intestine. *Am J Physiol Gastrointest Liver Physiol* 282: G573–9, 2002.

159. **Wang Z**, **Wang T**, **Petrovic S**, **Tuo B**, **RIEDERER B**, **Barone S**, **Lorenz JN**, **SEIDLER U**, **Aronson PS**, **Soleimani M**. Renal and intestinal transport defects in Slc26a6-null mice. *Am J Physiol, Cell Physiol* 288: C957–65, 2005.

160. **Warny M**, **Keates AC**, **Keates S**, **Castagliuolo I**, **Zacks JK**, **Aboudola S**, **Qamar A**, **Pothoulakis C**, **LaMont JT**, **Kelly CP**. p38 MAP kinase activation by Clostridium difficile toxin A mediates monocyte necrosis, IL-8 production, and enteritis. *J Clin Invest* 105: 1147–1156, 2000.

161. **Wedenoja S**, **Höglund P**, **Holmberg C**. Review article: the clinical management of congenital chloride diarrhoea. *Aliment Pharmacol Ther* 31: 477–485, 2010.

162. **Wohlan K**, **Goy S**, **Olling A**, **Srivaratharajan S**, **Tatge H**, **Genth H**, **Gerhard R**. Pyknotic cell death induced by Clostridium difficile TcdB: chromatin condensation and nuclear blister are induced independently of the glucosyltransferase activity. *Cell Microbiol* 16: 1678–1692, 2014.

163. **Woo AL**, **Gildea LA**, **Tack LM**, **Miller ML**, **Spicer Z**, **Millhorn DE**, **Finkelman**

FD, **Hassett DJ**, **Shull GE**. In vivo evidence for interferon-gamma-mediated homeostatic mechanisms in small intestine of the NHE3 Na+/H+ exchanger knockout model of congenital diarrhea. *J Biol Chem* 277: 49036–49046, 2002.

164. **Xiao F**, **Yu Q**, **Li J**, **Johansson MEV**, **Singh AK**, **Xia W**, **Riederer B**, **Engelhardt R**, **Montrose M**, **Soleimani M**, **Tian DA**, **Xu G**, **Hansson GC**, **Seidler U**. Slc26a3 deficiency is associated with loss of colonic HCO3 (-) secretion, absence of a firm mucus layer and barrier impairment in mice. *Acta Physiol (Oxf)* 211: 161–175, 2014.

165. **Xu H**, **Chen H**, **Dong J**, **Lynch R**, **Ghishan FK**. Gastrointestinal Distribution and Kinetic Characterization of the Sodium-Hydrogen Exchanger Isoform 8 (NHE8). *CPB* 21: 109–116, 2008.

166. **Xue L**, **Aihara E**, **Wang TC**, **Montrose MH**. Trefoil factor 2 requires Na/H exchanger 2 activity to enhance mouse gastric epithelial repair. *J Biol Chem* 286: 38375–38382, 2011.

167. **Yamamoto A**, **Tagawa Y**, **Yoshimori T**, **Moriyama Y**, **Masaki R**, **Tashiro Y**. Bafilomycin A1 prevents maturation of autophagic vacuoles by inhibiting fusion between autophagosomes and lysosomes in rat hepatoma cell line, H-4-II-E cells. *Cell Struct Funct* 23: 33–42, 1998.

168. **Yang H**, **Jiang W**, **Furth EE**, **Wen X**, **Katz JP**, **Sellon RK**, **Silberg DG**, **Antalis TM**, **Schweinfest CW**, **Wu GD**. Intestinal inflammation reduces expression of DRA, a transporter responsible for congenital chloride diarrhea. *Am J Physiol* 275: G1445–53, 1998.

169. **Yen FT**, **Mann CJ**, **Guermani LM**, **Hannouche NF**, **Hubert N**, **Hornick CA**, **Bordeau VN**, **Agnani G**, **Bihain BE**. Identification of a lipolysis-stimulated receptor that is distinct from the LDL receptor and the LDL receptor-related protein. *Biochemistry* 33: 1172–1180, 1994.

170. **Yuan P**, **Zhang H**, **Cai C**, **Zhu S**, **Zhou Y**, **Yang X**, **He R**, **Li C**, **Guo S**, **Li S**, **Huang T**, **Perez-Cordon G**, **Feng H**, **Wei W**. Chondroitin sulfate proteoglycan 4 functions as the cellular receptor for Clostridium difficile toxin B. *Cell Res* 25: 157–168, 2015.

171. **Zachos NC**, **Tse M**, **Donowitz M**. Molecular physiology of intestinal Na+/H+ exchange. *Annu Rev Physiol* 67: 411–443, 2005.

172. **Zdebik AA**, **Cuffe JE**, **Bertog M**, **Korbmacher C**, **Jentsch TJ**. Additional disruption of the ClC-2 Cl(-) channel does not exacerbate the cystic fibrosis phenotype of cystic fibrosis transmembrane conductance regulator mouse models. *J Biol Chem* 279: 22276–22283, 2004.

APPENDIX

American Society for Clinical Investigation LICENSE
TERMS AND CONDITIONS
Mar 22, 2018

This is a License Agreement between University of Illinois at Chicago -- Hayley Coffing ("You") and American Society for Clinical Investigation ("American Society for Clinical Investigation") provided by Copyright Clearance Center ("CCC"). The license consists of your order details, the terms and conditions provided by American Society for Clinical Investigation, and the payment terms and conditions.

All payments must be made in full to CCC. For payment instructions, please see information listed at the bottom of this form.

License Number	4293651081111
License date	Feb 13, 2018
Licensed content publisher	American Society for Clinical Investigation
Licensed content title	JOURNAL OF CLINICAL INVESTIGATION. ONLINE
Licensed content date	Dec 31, 1969
Type of Use	Thesis/Dissertation
Requestor type	Academic institution
Format	Print, Electronic
Portion	cartoon
Number of cartoons	1
The requesting person/organization is:	Hayley Coffing / University of Illinois at Chicaglo
Title or numeric reference of the portion(s)	Figure 1: CDI Pathogenesis
Title of the article or chapter the portion is from	Clostridium difficile and the microbiota
Editor of portion(s)	N/A
Author of portion(s)	Anna M. Seekatz and Vincent B. Young
Volume of serial or monograph.	124
Issue, if republishing an article from a serial	10
Page range of the portion	4183
Publication date of portion	July 18, 2014
Rights for	Main product

Duration of use	Current edition and up to 5 years
Creation of copies for the disabled	no
With minor editing privileges	no
For distribution to	United States
In the following language(s)	Original language of publication
With incidental promotional use	no
The lifetime unit quantity of new product	Up to 499
Title	The role of SLC26A3 in toxin-mediated Clostridium difficile infection
Instructor name	n/a
Institution name	n/a
Expected presentation date	Mar 2018
Billing Type	Invoice
Billing Address	University of Illinois at Chicago 820 South Damen Ave #7221 MIDWEST, IL 60612 United States Attn: Seema Saksena
Total (may include CCC user fee)	0.00 USD
Terms and Conditions	

TERMS AND CONDITIONS

SPRINGER NATURE LICENSE
TERMS AND CONDITIONS
Mar 22, 2018

_____

This Agreement between University of Illinois at Chicago -- Hayley Coffing ("You") and Springer Nature ("Springer Nature") consists of your license details and the terms and conditions provided by Springer Nature and Copyright Clearance Center.

License Number	4291531193391
License date	Feb 17, 2018
Licensed Content Publisher	Springer Nature
Licensed Content Publication	Nature Reviews Microbiology
Licensed Content Title	Clostridium difficile colitis: pathogenesis and host defence
Licensed Content Author	Michael C. Abt, Peter T. McKenney, Eric G. Pamer
Licensed Content Date	Aug 30, 2016
Licensed Content Volume	14
Licensed Content Issue	10
Type of Use	Thesis/Dissertation
Requestor type	academic/university or research institute
Format	print and electronic
Portion	figures/tables/illustrations
Number of figures/tables/illustrations	1
High-res required	no
Will you be translating?	no
Circulation/distribution	<501
Author of this Springer Nature content	no
Title	The role of SLC26A3 in toxin-mediated Clostridium difficile infection
Instructor name	n/a
Institution name	n/a
Expected presentation date	Mar 2018

Portions	Figure 2b - Mechanism of action of C. difficile toxins in epithelial cells. page 614
Requestor Location	University of Illinois at Chicago 820 South Damen Ave #7221 MIDWEST, IL 60612 United States Attn: Seema Saksena
Billing Type	Invoice
Billing Address	University of Illinois at Chicago 820 South Damen Ave #7221 MIDWEST, IL 60612 United States Attn: Seema Saksena
Total	0.00 USD
Terms and Conditions	

SPRINGER NATURE LICENSE
TERMS AND CONDITIONS
Mar 22, 2018

This Agreement between University of Illinois at Chicago -- Hayley Coffing ("You") and Springer Nature ("Springer Nature") consists of your license details and the terms and conditions provided by Springer Nature and Copyright Clearance Center.

License Number	4292731059514
License date	Feb 19, 2018
Licensed Content Publisher	Springer Nature
Licensed Content Publication	Nature Reviews Microbiology
Licensed Content Title	Bacteria–autophagy interplay: a battle for survival
Licensed Content Author	Ju Huang, John H. Brumell
Licensed Content Date	Jan 2, 2014
Licensed Content Volume	12
Licensed Content Issue	2
Type of Use	Thesis/Dissertation
Requestor type	academic/university or research institute
Format	print and electronic
Portion	figures/tables/illustrations
Number of figures/tables/illustrations	1
High-res required	no
Will you be translating?	no
Circulation/distribution	<501
Author of this Springer Nature content	no
Title	The role of SLC26A3 in toxin-mediated Clostridium difficile infection
Instructor name	n/a
Institution name	n/a
Expected presentation date	Mar 2018

Portions	Figure 1: A diagram of the autophagy pathway. page 10:
Requestor Location	University of Illinois at Chicago 820 South Damen Ave #7221 MIDWEST, IL 60612 United States Attn: Seema Saksena
Billing Type	Invoice
Billing Address	University of Illinois at Chicago 820 South Damen Ave #7221 MIDWEST, IL 60612 United States Attn: Seema Saksena
Total	0.00 USD
Terms and Conditions	

SPRINGER NATURE LICENSE
TERMS AND CONDITIONS
Mar 22, 2018

This Agreement between University of Illinois at Chicago -- Hayley Coffing ("You") and Springer Nature ("Springer Nature") consists of your license details and the terms and conditions provided by Springer Nature and Copyright Clearance Center.

License Number	4295660706260
License date	Feb 24, 2018
Licensed Content Publisher	Springer Nature
Licensed Content Publication	Nature Reviews Neuroscience
Licensed Content Title	Ubiquitin, the proteasome and protein degradation in neuronal function and dysfunction
Licensed Content Author	Hwan-Ching Tai, Erin M. Schuman
Licensed Content Date	Nov 1, 2008
Licensed Content Volume	9
Licensed Content Issue	11
Type of Use	Thesis/Dissertation
Requestor type	academic/university or research institute
Format	print and electronic
Portion	figures/tables/illustrations
Number of figures/tables/illustrations	2
High-res required	no
Will you be translating?	no
Circulation/distribution	<501
Author of this Springer Nature content	no
Title	The role of SLC26A3 in toxin-mediated Clostridium difficile infection
Instructor name	n/a
Institution name	n/a
Expected presentation date	Mar 2018

Portions	Figures 1 and 2
Requestor Location	University of Illinois at Chicago 820 South Damen Ave #7221 MIDWEST, IL 60612 United States Attn: Seema Saksena
Billing Type	Invoice
Billing Address	University of Illinois at Chicago 820 South Damen Ave #7221 MIDWEST, IL 60612 United States Attn: Seema Saksena
Total	0.00 USD
Terms and Conditions	

Copyright
Clearance
Center

Welcome, Hayley
Not you?

Log out | 🛒 Cart (0) | Manage Account | Feedback | Help | ❤ Live Help

Get Permission / Find Title

Publication Title or ISBN/ISSN | Go

Advanced Search Options

⚠ **Note:** Copyright.com supplies permissions but not the copyrighted content itself.

1	2	3
PAYMENT	REVIEW	CONFIRMATION

Step 3: Order Confirmation

Start new search ▹   View your Order History ▹

🖨 Print order information: includes order confirmation, terms and conditions, and citation information (What's this?)

Thank you for your order! A confirmation for your order will be sent to your account email address. If you have questions about your order, you can call us 24 hrs/day, M-F at +1.855.239.3415 Toll Free, or write to us at info@copyright.com. This is not an invoice.

Confirmation Number: 11706621
Order Date: 03/22/2018

If you paid by credit card, your order will be finalized and your card will be charged within 24 hours. If you choose to be invoiced, you can change or cancel your order until the invoice is generated.

Payment Information

Hayley Coffing
University of Illinois at Chicago
coffing1@uic.edu
+1 (708) 218-8164
Payment Method: n/a

Order Details

Annual review of microbiology

Order detail ID:	71078892
Order License Id:	4314371010388
ISSN:	1545-3251
Publication Type:	e-Journal
Volume:	
Issue:	
Start page:	
Publisher:	ANNUAL REVIEWS

Permission Status: ✅ Granted

Permission type: Republish or display content
Type of use: Thesis/Dissertation

⊞ View details

Note: This item will be invoiced or charged separately through CCC's **RightsLink** service. More info

$ 0.00

UIC UNIVERSITY OF ILLINOIS
AT CHICAGO

Office of Animal Care and Institutional
Biosafety Committee (OACIB) (M/C 672)
Office of the Vice Chancellor for Research
206 Administrative Office Building
1737 West Polk Street
Chicago, Illinois 60612

9/15/2017

Pradeep K. Dudeja
Medicine/Gastroenterology and Hepatology
JAVAMC, R&D, MP-151
820 S. Damen, Suite 6215
Chicago, IL 60612

Dear Dr. Dudeja:

The protocol indicated below was reviewed in accordance with the Animal Care Policies and Procedures of the University of Illinois at Chicago and **renewed on 9/15/2017.**

Title of Application:	Ion Transporter Mechanisms in Infectious Diarrhea
ACC NO:	15-185
Original Protocol Approval:	10/5/2015 **(3 year approval with annual continuation required).**
Current Approval Period:	9/15/2017 **to** 9/15/2018

Funding: *Portions of this protocol are supported by the funding sources indicated in the table below.*
Number of funding sources: 1

Funding Agency	Funding Title			Portion of Funding Matched
NIH	*Transporter Trafficking Mechanisms In Infectious Diarrhea*			*All matched*
Funding Number	**Current Status**	**UIC PAF NO.**	**Performance Site**	**Funding PI**
RO1 DK09211 (original yrs 1-4)	*Funded*	*2011-01559*	*JBVAMC*	*Pradeep Dudeja*

This institution has Animal Welfare Assurance Number A3460.01 on file with the Office of Laboratory Animal Welfare, NIH. **This letter may only be provided as proof of IACUC approval for those specific funding sources listed above in which all portions of the grant are matched to this ACC protocol.**

Thank you for complying with the Animal Care Policies and Procedures of the UIC.

Sincerely,

John P. O'Bryan, PhD
Chair, Animal Care Committee
JPO/*kg*
cc: BRL, ACC File, Seema Saksena

**Department of
Veterans Affairs**

Memorandum

Date: March 9, 2016

From: Rhonda Kineman Chairman
        R&D Institutional Animal Care and Use Committee (IACUC) (537/151)

To: Dr. Pradeep K Dudeja
        Protocol Entitled: "Ion Transporter Mechanisms in Infectious Diarrhea",
        IACUC # 15-22.02

RE: Animal Care and Use Approval

On **March 8, 2016** your modification request (#**2**- *request to add personnel,* **Hayley Coffing,** *to this referenced animal protocol.)* entitled: **"Ion Transporter Mechanisms in Infectious Diarrhea"** IACUC# 15-22 (Mice) received **Administrative Approval as of March 9, 2016.**

Please note: this approval is valid only for animals that are housed at **Jesse Brown VAVMU.**

Additionally, you may not initiate your research at JBVAMC until after written approval from the R&D ACOS is obtained. Please contact the JBVAMC R&D Office for further information at 312-569-7440.

Should it become necessary to make any additional changes in this protocol, you must submit a modification request for approval prior to initiating changes. Failure to comply with these provisions can result in a suspension of the research.

If you have any questions, or need further assistance, please contact Robin McWherter, IACUC Administrator at Robin.McWherter@va.gov and Tyler Ridgeway, IACUC Coordinator, at Tyler.Ridgeway@va.gov.

Sincerely,

Rhonda Kineman, Ph.D.
Co-Chair IACUC

**Department of
Veterans Affairs**

Memorandum

Date: February 5, 2016

From: Rhonda Kineman, Ph.D, Chairman
R&D Institutional Animal Care and Use Committee (IACUC) (537/151)

To: Dr. Pradeep Dudeja
Protocol Entitled: "Ion Transporter Mechanisms in Infectious Diarrhea"
IACUC #15-22 (Mice)

RE: Animal Care and Use Approval

At the **January 13, 2016** meeting of the IACUC, your protocol entitled: **"Ion Transporter Mechanisms in Infectious Diarrhea" (Mice) IACUC #15-22** was brought before the IACUC and received **Full Approval** **(With the exception of the closed loop experiments using modified bacteria (BSL-2) and radioactive tracers to assess ion flux, Experiment 8g.)** on **February 5, 2016**. The Project Personnel listed are: **Dudeja, Saksena, Borthakur, Tyagi, Anbazhagan, Kumar, Priyamavada, and Chaterjee.** The funding source is: **NIH**.

Please note: this approval is valid only for animals that are housed at **JBVAMC VMU**.

Additionally, you may not initiate your research at JBVAMC until after written approval from the R&D ACOS is obtained. Please contact the JBVAMC R&D Office for further information at 312-569-7440.

Please verify the information below. If corrections are required please notify Robin McWherter, IACUC Administrator, at Robin.McWherter@va.gov and Tyler Ridgeway, IACUC Coordinator, at Tyler.Ridgeway@va.gov.

a.   USDA Category: C (1,220), & D (1,130)
b.   Species: Mice , Please see main body of ACORP for animal strains
c.   # of Animals Approved: 2,350 Total
d.   Approval Date: February 5, 2016
e.   Approval Termination: February 4, 2019
f.   IACUC #**15-22**

Should it become necessary to make any additional changes in this protocol, you must submit a modification request for approval prior to initiating changes. In the case in which animal work is being done at an affiliate institute, you must obtain approval from both the affiliate and the JBVAMC prior to initiation. Failure to comply with these provisions can result in a suspension of the research.

If you have any questions, or need further assistance, please contact Robin McWherter, IACUC Administrator, at Robin.McWherter@va.gov and Tyler Ridgeway, IACUC Coordinator, at Tyler.Ridgeway@va.gov.

Sincerely,

Rhonda Kineman, Ph.D.
Chair, IACUC

UIC | UNIVERSITY OF ILLINOIS
AT CHICAGO

September 21, 2014

Pradeep Dudeja
Medicine/Digestive Diseases & Nutrition
Jesse Brown VA Medical Center, R&D
820 S. Damen Avenue, MP151
Chicago IL 60612-

Office of Animal Care and
Institutional Biosafety Committees (MC 672)
Office of the Vice Chancellor for Research
206 Administrative Office Building
1737 West Polk Street
Chicago, Illinois 60612-7227

Dear Dr. Dudeja:

The protocol indicated below has been reviewed in accordance with the Institutional Biosafety Committee Policies of the University of Illinois at Chicago on 8/13/2014. *The protocol was not initiated until final clarifications were reviewed and approved on 9/19/2014. Protocol expires 3 years from the date of review (8/13/2017). This protocol replaces protocol 11-042 which has been terminated.*

Title of Application: Transporter Trafficking Mechanisms in Infectious Diarrhea

IBC Number: 14-042

Highest Biosafety Level: 2

Condition of Approval: The enclosed report indicates the training status for bloodborne pathogen (BBP) training. Only those personnel who have been trained and whose training has not expired are approved for work that may involve exposure to bloodborne pathogens. Please note that federal regulations require yearly training for BBP.

You may forward this letter of acceptable IBC verification of your research protocol to the funding agency considering this proposal. **Please be advised that investigators must report significant changes in their research protocol to the IBC office via a letter addressed to the IBC chair prior to initiation of the change. If a protocol changes in such a manner as to require IBC approval, the change may not be initiated without IBC approval being granted.**

Thank you for complying with the UIC's Policies and Procedures.

Sincerely,

[signature]

Randal C. Jaffe, Ph.D.
Chair, Institutional Biosafety Committee

RCJ/*mbb*

Enclosures

Cc: IBC file, Seema Saksena, Alip Borthakur

VITA

VITA

NAME Hayley Coffing

EDUCATION

B.S., Science Pre-Professional, University of Notre Dame, 2012

Ph.D., Department of Microbiology and Immunology, University of Illinois at Chicago (UIC), Concentration: Intestinal ion transport physiology

PROFESSIONAL EXPERIENCE

Pre-doctoral Research, 2013- Present
Dr. Pradeep K. Dudeja, Department of Medicine, University of Illinois at Chicago
- Dissertation research primarily investigated the effects of *Clostridium difficile* infection (CDI) on intestinal ion transport, specifically electroneutral sodium chloride absorption
- Overall focus of lab is to elucidate mechanisms underlying intestinal epithelial ion transport (sodium, chloride, short chain fatty acids) during inflammatory and infectious diarrheal diseases

Undergraduate Research Assistant, 2009-2012
Dr. Peter Burns, Department of Chemistry and Biochemistry, Energy Frontier Research Center, University of Notre Dame
- Assisted post-doctoral fellows with experiments at the Materials Science of Actinides Center, a Department of Energy-funded EFRC
- The experiments at the Notre Dame EFRC sought to better understand actinide-containing materials to discover more advanced ways to utilize energy while minimizing nuclear waste

PUBLICATIONS

1. **Coffing H,** Tyagi S, Saksena S, Gill R, Alrefai W, Dudeja PK. *Clostridium difficile* Toxins A and B Decrease SLC26A3 Protein Expression in Human Intestinal Epithelial Cells *(Manuscript submitted to AJP)*

2. Kumar A, Malhotra P, **Coffing H,** Priyamvada S, Anbazhagan AN, Krishnan H, Gill R, Alrefai W, Gavin D, Pandey S, Dudeja PK, Saksena S. Epigenetic Modulation of Intestinal Na^+/H^+ Exchanger-3 Expression. <u>Am J Physiol Gastrointest Liver Physiol</u>, 2017 Nov 22; epub ahead of print

3. Kumar A, Chatterjee I, Gujral T, Alakkam A, **Coffing H**, Anbazhagan AN, Borthakur A, Saksena S, Gill RK, Alrefai WA, Dudeja PK. Activation of Nuclear Factor-κB by Tumor Necrosis Factor in Intestinal Epithelial Cells and Mouse Intestinal Epithelia Reduces Expression of the Chloride Transporter SLC26A3. Gastroenterology, 2017 Nov;153(5):1338-1350

4. Kumar A, Anbazhagan AN, **Coffing H**, Chatterjee I, Priyamvada S, Gujral T, Saksena S, Gill RK, Alrefai WA, Borthakur A, Dudeja PK. Lactobacillus acidophilus counteracts inhibition of NHE3 and DRA expression and alleviates diarrheal phenotype in mice infected with Citrobacter rodentium. Am J Physiol Gastrointest Liver Physiol, 2016 Nov 1;311(5):G817-G826

5. Namachivayam K, **Coffing H,** Sankaranarayanan NV, Jin Y, MohanKumar K, Frost BL, Blanco CL, Patel AL, Meier PP, Garzon SA, Desai UR, Maheshwari A. Transforming growth factor-β2 is sequestered in preterm human milk by chondroitin sulfate proteoglycans. Am J Physiol Gastrointest Liver Physiol, 2015 Aug 1;309(3):G171-80

AWARDS AND HONORS

- Early Career Scientist Award, Digestive Diseases Week (DDW), 2017
- UIC College of Medicine Scholar, 2015 -2016
- DDW Poster of Distinction, DDW 2015
- Notre Dame Glynn Family Honors Program Scholar, 2008-2012
- Notre Dame College of Science Summer Research Grant, 2011